STEADY FLOW AND PULSED PERFORMANCE TRENDS OF HIGH CONCENTRATION DMFCS

A Thesis
Presented to
The Academic Faculty

by

Larry K. McCarthy

In Partial Fulfillment
of the Requirements for the Degree
Master of Science in Mechanical Engineering

Georgia Institute of Technology

May 2006

STEADY FLOW AND PULSED PERFORMANCE TRENDS OF HIGH CONCENTRATION DMFCS

Approved by:

Dr. William J. Wepfer, Co-Advisor
School of Mechanical Engineering
Georgia Institute of Technology

Dr. Comas L. Haynes, Co-Advisor
Center for Innovative Fuel Cell and Battery Technologies
Georgia Tech Research Institute

Dr. Samuel Shelton
School of Mechanical Engineering
Georgia Institute of Technology

Date Approved: December 18, 2005

ACKNOWLEDGEMENT

I would like to particularly thank my co-advisor, Dr. Comas Haynes, whose valuable support, guidance, and encouragement helped me complete this research and thesis. I would also like to extend my gratitude to Dr. William Wepfer and Dr. Sam Shelton for their support as committee members. I am thankful to the personnel of the Georgia Tech Research Institute that helped in more than one way by answering many questions and providing useful insights and suggestions. Finally, but not least, I would like to thank Scott Leahy who helped me greatly during my apprenticeship at the GTRI laboratory.

TABLE OF CONTENTS

LIST OF TABLES

Table

LIST OF FIGURES

Figure

LIST OF SYMBOLS

a	fuel supply time
b	fuel discontinuation time
C	methanol concentration
DC	duty cycle
e^-	electron
E_{ideal}	ideal potential
F	Faraday's constant
G	Gibbs free energy
H	enthalpy
i	current
i_l	limiting current
i_o	reaction exchange current
j	current density
M	molarity
m_{soln}	reactant concentration
n	number of electrons
$\dot{n}$	molar flow rate
P	power density
R	internal resistance
R	universal gas constant

S	entropy
t	time
T	temperature
T	period
T_{Lag}	lag time
T_{Vmax}	maximum voltage time
V	cell potential
$\dot{V}$	volumetric flow rate
$W_{electrical}$	electrical work

Greek Letters

α	charge transfer coefficient
Δ	change
$\prod$	product
η	polarization
η_t	thermodynamic ideal efficiency
η_v	voltage efficiency
ν	reactant coefficient

SUMMARY

The methanol crossover phenomenon, wherein membrane permeability allows the undesirable species transport of methanol from anode to cathode, is a major problem in direct methanol fuel cells (DMFCs). This phenomenon causes the requirement of dilute fuel mixtures, which is undesirable from an energy density viewpoint. In addition, the crossover is capable of promoting, at least in part, lower power density, increasing cost, and uncertain reliability.

Steady flow polarization curves were first analyzed at various methanol concentrations. An optimal concentration range was found wherein the combination of methanol crossover and concentration losses was effectively minimized. During the study of transient phenomena, the fuel flow was first temporarily discontinued. It was found that a significant cell potential enhancement occurred due to anodic fuel concentration reduction and thus diminished reactant crossover. The percentage voltage increase was considerably greater at higher concentrations.

Based on the temporary fuel discontinuation, a hydraulic pulsing operation was developed and tested. During some of these continuous pulsing schemes, fuel discontinuation did not result in an instantaneous cell potential enhancement mainly due to the internal inertia of the membrane. Nonetheless, a significant cell potential and performance enhancement were observed. In addition, the pulse of both fuel and current density resulted in a significant power density increase.

1. Introduction

Fuel cells are a promising source of energy due to their high efficiencies, quiet operation, and negligible emissions. They convert chemical energy into electricity via an electrochemical reaction. There are numerous types of fuel cells, including direct methanol fuel cells (DMFCs). DMFCs use a polymer electrolyte as the ion conductor membrane between the anode and cathode, and they draw hydrogen ions directly from the methanol fuel mixture using methanol rather than hydrogen as a fuel. Due to their capability of operating at low temperatures and without a fuel reformer, DMFCs are an excellent candidate for battery replacement in many portable electronics such as cellular phones and laptops. However, there are some unresolved challenges that have prevented the commercialization of DMFCs. A large quantity of precious metal catalyst is required to achieve significantly high power densities, thus greatly increasing the overall cost of the cell. Another major issue with DMFCs is the methanol crossover phenomenon wherein methanol is transported from the anode diffusion layer to the cathode catalytic surface. Figure 1.1 shows a general illustration of a DMFC including the undesired methanol crossover phenomenon. The permeated methanol reacts at the cathode creating a mixed potential that significantly lowers the cell performance.

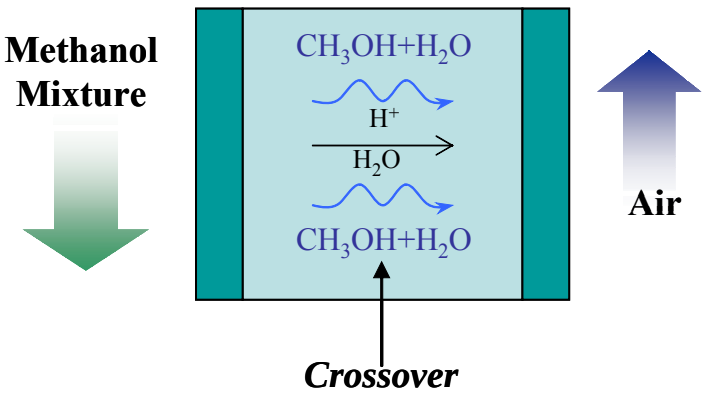

Figure 1.1: Illustration of DMFC including the methanol crossover phenomenon

The methanol permeation is predominantly driven through diffusion and is greatly enhanced when operating at high methanol mixture concentrations (Jiang, 2004). As a result, methanol crossover also hinders cell performance by limiting the operation at higher concentrations wherein lower electrochemical losses, which will be further discussed in Chapter 2, would otherwise enhance cell potential.

Many researchers have attempted to mitigate methanol crossover in DMFCs by changing the thickness and/or material of the electrolyte membrane (Heinzel, 1999). However, sufficient improvement through both techniques has not been achieved mainly due to the complexity of the required membrane properties (e.g., good ionic conductivity and reactant separator). An alternative method to potentially diminish methanol crossover and consequently increase cell performance is through the application of a fuel flow transient operation (Sundmacher, 2001). This type of operation has been *briefly* studied, both analytically and experimentally. Additionally, the characterization of transient phenomena is important because real-world applications (e.g., portable electronics) are

unlikely to operate under continuously static conditions. The current work was primarily devoted to perform an extensive experimental analysis on the fuel flow transient operation at various fuel mixture concentrations, current densities and stoichiometries. It also included the effect of cell degradation on the transient response. Furthermore, this fuel flow transient operation, which is also referred to as hydraulic pulsing throughout this work, was implemented in order to periodically reduce the anodic methanol concentration during the fuel discontinuation phase, thus promoting crossover reduction and higher cell potential/efficiency. The same analysis was performed during an electro-hydraulic pulsing experiment wherein both the fuel flow and current density were pulsed. Various hydraulic and electro-hydraulic schemes were investigated and analyzed in order to select an optimal transient scheme that resulted in the most significant performance enhancement.

The possible advantages of both hydraulic and electro-hydraulic pulsing are shown in Figure 1.2. As stated previously, hydraulic pulsing facilitates a significant reduction in methanol crossover that consequently results in a cell performance enhancement. The operation at high fuel concentrations has a considerable effect on the overall size of the system because the corresponding size of the fuel tank can be significantly reduced. The electro-hydraulic pulsing can possibly result in higher power density output, which might be desired on certain applications. While it is difficult to precisely quantify the cost impact of both hydraulic and electro-hydraulic pulsing, it is feasible to hypothesize that both operations could result in lower capital costs by reducing the catalyst requirement. Nonetheless, it is important to mention that there would be other added cost due to the required flow control system and power electronics.

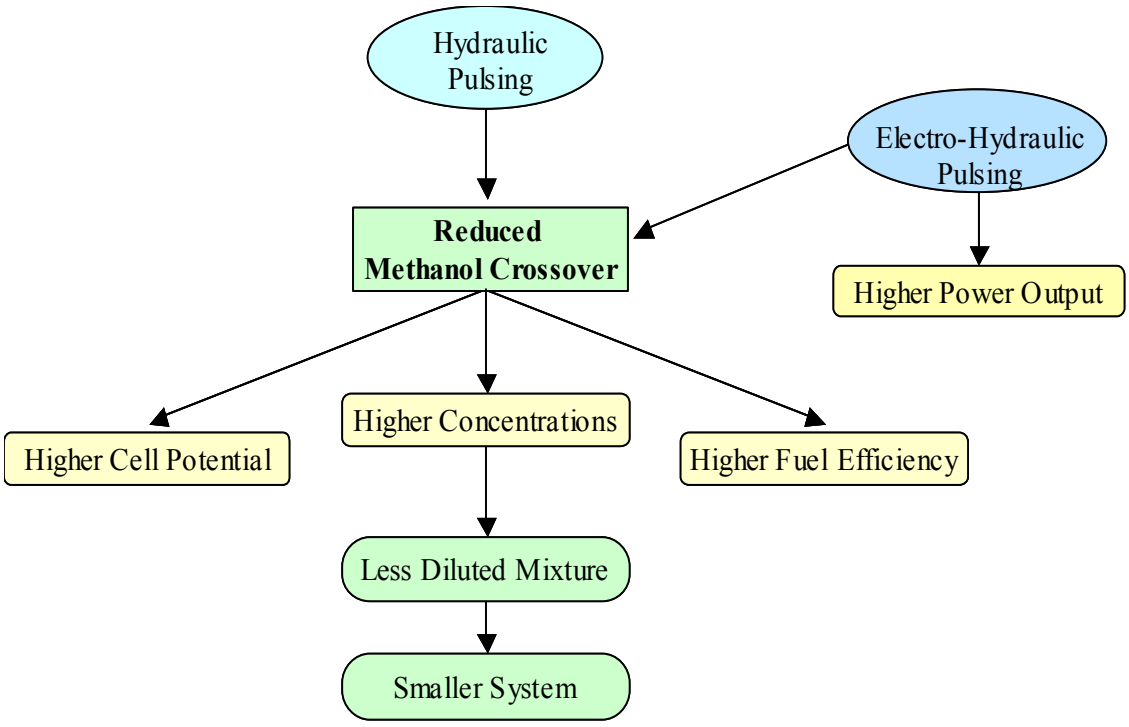

Figure 1.2: Advantages of hydraulic and electro-hydraulic pulsing

In the following chapters, a more detailed discussion of methanol crossover and transient operation is presented. In the second chapter, a detailed description of DMFCs is introduced including some of their advantages and disadvantages such as methanol crossover. Chapter three outlines some of the relevant research previously performed, especially regarding DMFC fuel permeation and transient phenomena. Chapter four reports the experimental apparatus and procedures used. Steady flow polarization curves were performed at various concentrations and are presented in the fifth chapter. The subsequent chapters (six and seven) include analysis of temporary fuel discontinuation and continuous fuel flow pulsing as well as the tested electro-hydraulic pulsing schemes.

2. Background and Research Motivation

2.1. Fuel Cell Background

A fuel cell is an electrochemical device that directly converts chemical energy into electrical energy. Usually a fuel cell uses a hydrogen rich compound or pure hydrogen to electrochemically react with either oxygen or air, which serves as an oxidant, to produce electricity, heat, and water. Unlike energy-storing conventional batteries, a fuel cell continuously produces electricity and heat as long as sufficient reactants are supplied to the cell. The basic electrochemical phenomenon occurring in a fuel cell was first discovered in 1839 by Sir William Grove, a Welsh judge and amateur scientist. He discovered that mixing hydrogen and oxygen in the presence of an electrolyte produced electricity and water. However, the idea was not significantly further developed until the 1930's when Francis T. Bacon applied Grove's fuel cell conception utilizing alkaline electrolytes and nickel electrodes. In the 1950's, the National Aeronautics and Space Administration (NASA) designed and built fuel cells to generate power and water for some of their space flight programs, such as the Apollo and Gemini.

There are several types of fuel cells, and they can be classified depending upon their characteristics (e.g., fuel, oxidant, temperature operation, fuel reformation, electrolyte, and feed mode (i.e., active, semi-passive, and passive mode)). Fuel cells are more often categorized based upon their electrolytes, and the five most common types are listed below.

- Alkaline Fuel Cells (AFCs)
- Phosphoric Acid Fuel Cells (PAFCs)
- Molten Carbonate Fuel Cells (MCFCs)
- Solid Oxide Fuel Cells (SOFCs)
- Polymer Electrolyte Fuel Cells (PEFCs[1])

The present work focuses upon PEFCs. In the early 1960's, General Electric (GE) invented the polymer electrolyte fuel cell. These PEFCs use a thin polymer electrolyte to act as an ion conductor and reactant separator. Figure 2.1 shows a general illustration of a PEFC with the polymer electrolyte at the heart of the cell.

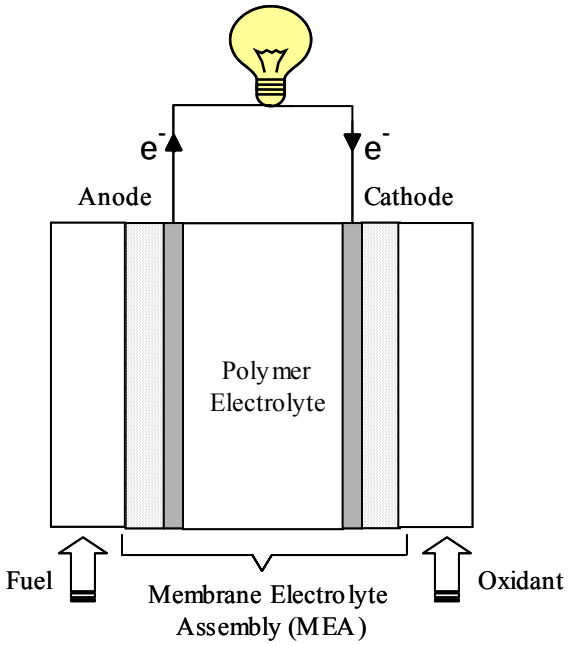

Figure 2.1: General illustration of a PEFC

[1] PEFCs are sometimes referred to as proton exchange membrane fuel cells (PEMFCs)

The solid polymer electrolyte in a PEFC has fewer corrosion issues in comparison to liquid electrolytes. Other advantageous characteristics of PEFCs are their higher power density and low operating temperature (i.e., 60-80 ºC), which enables a faster fuel cell start-up. Nonetheless, PEFC technology has some disadvantages, such as relatively high cost and challenging water management; the latter is extremely difficult to control and can have severe effects upon the cell's performance and efficiency. The water management of PEFCs will be further discussed in the forthcoming sections.

In most PEFC applications, nearly pure hydrogen is used as the fuel and air-based oxygen[2] as the oxidant. These fuel cells are more commonly known as PEM cells. There is a type of PEFCs known as direct methanol fuel cell (DMFC) that uses either liquid or vapor methanol as the fuel instead of hydrogen. Liquid DMFCs are the specific topic of discussion in the present work.

2.2. DMFC Structure

In essence, a DMFC consists of the polymer electrolyte membrane and negatively and positively polarized electrodes (i.e., the anode and cathode, respectively). In liquid DMFCs, the fuel solution, which is a mixture of methanol and water, is oxidized at the anode to form hydrogen protons, electrons and carbon dioxide (CO_2) byproduct. The protons travel through the polymer electrolyte membrane from the anode to the cathode, where they combine with returning electrons and oxygen to form water. The electrons that are transported through an external circuit load produce useful electricity. Figure 2.2 is a schematic of the electrochemical process occurring in a DMFC.

[2] PEFCs very often uses air as the oxidant because of its availability.

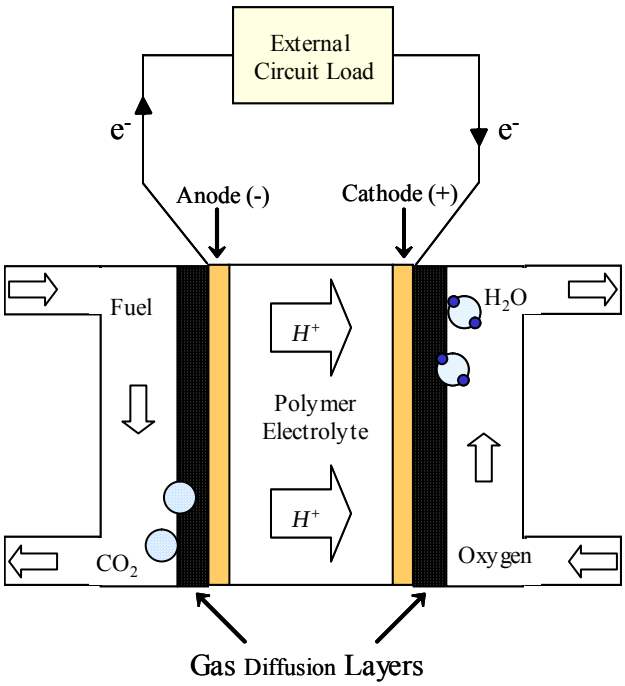

Figure 2.2: Description of a DMFC operation

The different components of a DMFC are shown in Figure 2.3. Located at the center of the cell, is the membrane electrolyte assembly (MEA), which is sandwiched between the gas diffusion layers (GDLs) and the endplate fixtures. Gaskets are used to seal the MEA contact with the endplates. The anode and cathode endplates are used to deliver the fuel and oxidant to the cell through a flow channel configuration. The current collectors, made out of a conductive metal, are attached at each endplate interface.

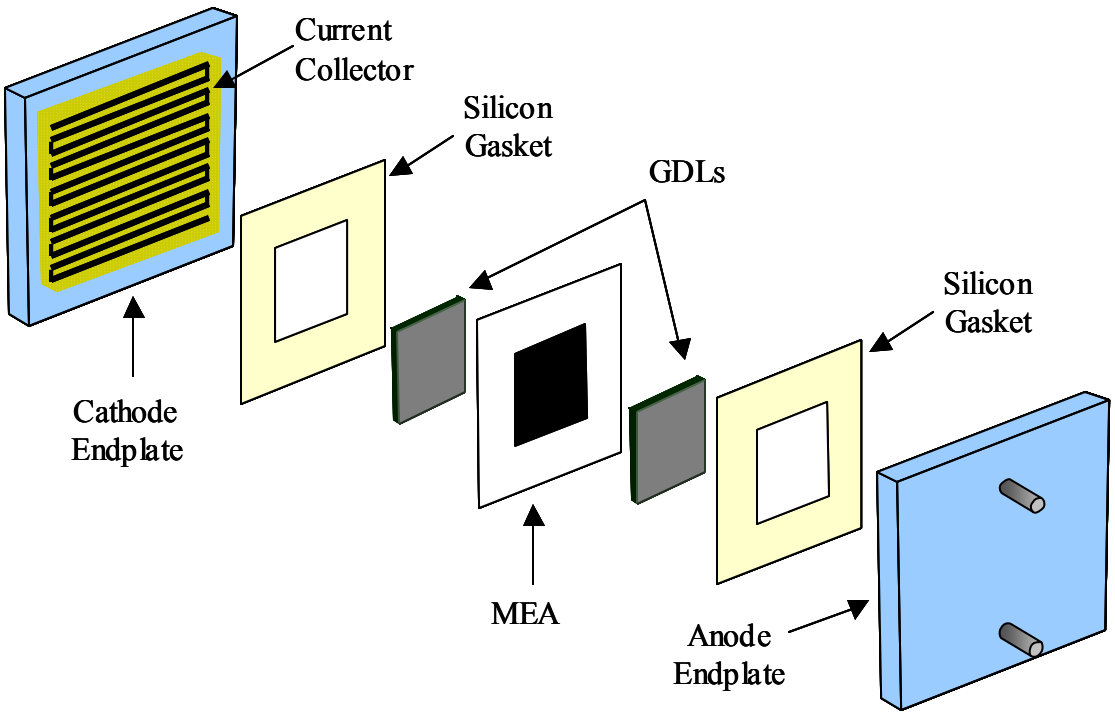

Figure 2.3: DMFC structure

2.2.1 Membrane Electrolyte Assembly (MEA)

The electrochemical portion of the MEA is composed of the solid polymer electrolyte and the anode and cathode electrode catalyst layers. Note that it is customary to include the GDLs within the MEA structure, thus forming a five-layer MEA. Lately, some manufacturers, such as 3M Corporation, have started to market seven and nine-layer MEAs The 7-layer has a gasket edge seal included in the 5-layer, while the 9-layer includes both the anode and cathode endplate fixtures. During this study, a 5-layer MEA was utilized and its illustration is shown in Figure 2.4.

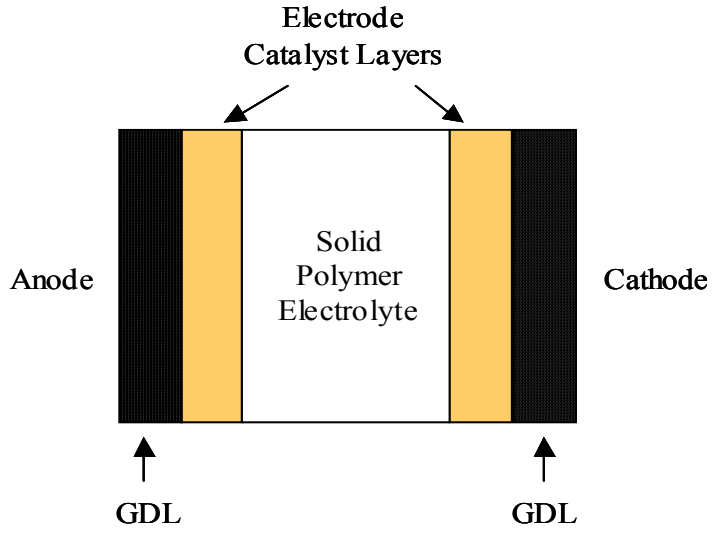

Figure 2.4: Five-layer MEA illustration

The most widely used solid polymer electrolyte material is Nafion®, a registered trademark of E.I DuPont de Nemours & Company. This membrane material structure consists of a polytetrafluoroethylene (PTFE)-based polymer backbone. PTFE is better known as the trade name Teflon®, which is also a product of DuPont. The Nafion® electrolyte has two main purposes, and they are to transport the protons (hydrogen ions) to the cathode and to serve as a physical barrier between the reactants. While Nafion® has good mechanical, thermal, and chemical stability, its proton conductivity, which is directly related to the water management of DMFCs, and reactant permeability characteristics have been a major problem in DMFC operation. The latter is extensively addressed throughout this work.

Attached to the surface of the Nafion® electrolyte are the anode and cathode electrodes. The electrochemical reactions occur at the triple-phase boundaries between the electrode, electrolyte and reactants. In order to increase the chemical reaction rate at

the anode and cathode, a platinum catalyst is dispersed over the electrode surfaces. Typically, ruthenium is used in conjunction with platinum on the anode, because it enhances the tolerance of the catalyst to certain species such as carbon monoxide. In order for the MEA to be effective, it must form an intimate three-phase boundary between the catalyst, membrane, and reactants allowing for the electrochemical reactions to occur. Therefore, a careful and accurate dispersion of the catalyst onto the electrolyte may readily increase the cell's efficiency while reducing the noble metal content, which consequently reduces the overall fuel cell cost. For this reason, a porous carbon supported thin layer, consisting of the electrode catalyst, is usually directly applied onto the Nafion® electrolyte surfaces. The carbon support enables an even dispersion of the catalyst over the active area while reducing the amount of platinum or platinum-ruthenium alloy. However, it has been reported that unsupported catalysts exhibit intrinsically better activity than the carbon-supported catalysts (Arico, 1999). Figure 2.5 shows an illustration of the three-phase region in a carbon-supported MEA.

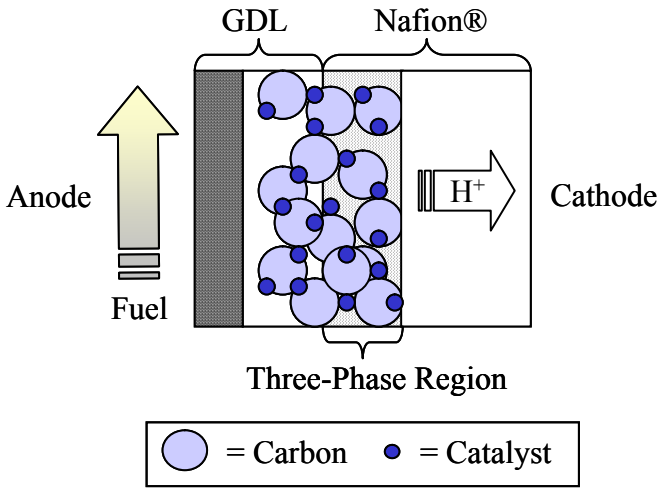

Figure 2.5: Illustration of the three-phase region in a carbon-supported MEA

As shown in Figure 2.5, the GDL[3] is located next to the three-phase region of the MEA. The GDL serves as a path for the reactants and water and as an electronic and thermal contact between the electrodes and the endplate fixtures. GDLs are usually made out of porous conductive carbon-based paper or cloth.

2.2.2 Endplate Fixtures

At the outer surfaces of a single DMFC are the endplate fixtures or bipolar flow field plates. These endplates are usually made out of an electrically and thermally conductive material, such as graphite, to allow for effective heat dissipation and flow of electrons to/from the external circuit load. Some ceramics endplates have been developed (e.g., sintered green ceramic plates). Since most ceramics are non-electrically-conductive, a highly conductive material, such as gold, is placed between the endplate and GDL to serve as a current collector.

The endplates are also used to route the reactants along the fuel cell. Thus, the endplate geometry is an important characteristic in order to improve cell performance by effectively distributing reactants to the catalytically active area. Active DMFCs, where both fuel and oxidant feed are actively controlled, usually incorporate serpentine flow patterns to distribute the reactants. Often, the air feed is allowed to naturally convect to the endplate, while the fuel supply is actively controlled. This DMFC operation is more commonly known as semi-passive[4].

[3] The GDL is also known as the gas diffusion electrode (GDE), electrode backing, diffuser, and gas diffusion backing

[4] Note that it is possible to operate the cell with active control of the oxidant feed and not the fuel; however, such operation has not been found to be significantly beneficial.

2.3 Performance Characterization

The electrochemical process occurring at the anode is the oxidation half-reaction of the methanol solution, while at the cathode it is the reduction half-reaction of the oxygen molecules. These half-cell reactions and the total overall chemical reaction in the DMFC are presented below.

Oxidation Half-Reaction:	$CH_3OH + H_2O \rightarrow CO_2 + 6H^+ + 6e^-$
Reduction Half-Reaction:	$3/2O_2 + 6H^+ + 6e^- \rightarrow 3H_2O$
Total Cell Reaction:	$CH_3OH + 3/2O_2 \rightarrow CO_2 + 2H_2O$

As can be observed from the total cell reaction, water and carbon dioxide are two byproducts of the overall process.

2.3.1 Ideal Cell Potential

The maximum electrical work ($W_{electrical}$) of a DMFC under constant pressure and temperature is equal to the Gibbs free energy change of the total reaction. This Gibbs free energy is dependent on temperature (T) by the relation

$$\Delta G = \Delta H - T\Delta S \tag{2.1}$$

where ΔH and ΔS are the enthalpy and entropy "of reaction", respectively. The enthalpy of reaction is indicative of the thermal energy theoretically available, given a (combustive) chemical reaction.

Under standard conditions[5], the Gibbs free energy change of the total electrochemical reaction is related to the ideal cell potential by

$$\Delta G^{o} = -nFE^{o}{}_{ideal} \qquad (2.2)^{6}$$

where n is the number of electrons involved in the reaction (6 for a DMFC), F is the Faraday's constant (96,487 coulombs per mole of electron), and E^{0}_{ideal} is the reversible standard potential under thermodynamic equilibrium. The ideal voltage is normally referred to as Nernst potential, and it is the difference between the cathodic and anodic thermodynamic equilibrium potentials, which are obtained by the dynamic equilibrium electrochemical reactions occurring at each electrode when no current is drawn from the cell (i.e., when the cell is at open circuit voltage). It has been reported that the anodic and cathodic standard Nernst potentials of a methanol-air DMFC are 0.02 and 1.23 V, respectively (Shukla, 2002). Thus, the ideal standard potential of a DMFC under standard conditions is around 1.21 V. The ideal voltage (E_{ideal}) at any other temperature and pressure can be obtained from the standard ideal potential (E^{0}_{ideal}) with the use of the Nernst equation

$$E_{ideal} = E^{0}{}_{ideal} - \frac{RT}{nF} \ln \frac{\prod |\text{ reactant activity }|}{\prod |\text{ product activity }|} \qquad (2.3)$$

[5] Standard condition usually refers to a 1-atm pressure and a temperature of 25 ºC.
[6] Note that the 0 superscript indicates values at standard conditions.

where R is the universal gas constant and T is the temperature of the reaction. The reactant and product activities measure the concentration relative to the standard conditions. For ideal gases, the activity is a measure of their partial pressures; therefore, the reactant and/or product activities in Equation 2.3 would be relative to 1 atm (standard pressure). For liquids, the activity is a measure of their molarities. Thus, the methanol solution activity (molarity) would be relative to 1 molar, the methanol standard concentration. The other liquid present in a DMFC is water and its activity is equal to one.

2.3.2 Efficiency

The ideal thermodynamic efficiency (η_t) of a fuel cell, as shown in Equation 2.4, is the ratio of the change in Gibbs free energy (ΔG) to the enthalpy (ΔH) of the overall cell reaction.

$$\eta_t = \frac{\Delta G}{\Delta H} \tag{2.4}$$

At standard conditions, the Gibbs free energy and enthalpy of reaction of a liquid methanol-air DMFC are –706.7 kJ/mole and –745.96 kJ/mole, respectively. Using these values and Equation 2.4, the ideal DMFC thermal efficiency at standard conditions is found to be 0.95. The voltage efficiency (η_v) of a DMFC can be calculated using Equation 2.5.

$$\eta_v = \frac{V_{actual}}{E_{ideal}} \tag{2.5}$$

Since the ideal cell potential of a DMFC is 1.21 V, the *standard conditions* voltage efficiency of the cell can be simplified as

$$\eta_v = \frac{V_{actual}}{1.21} = 0.83 \times V_{actual} \tag{2.6}$$

The above voltage efficiency assumes that all the fuel and oxidant supplied to the cell is electrochemically reacted. However, excess supply of both fuel and oxidant is always required in DMFC operation. Thus, a sufficiently high "number-of-stoichs" (NOS); i.e., a stoichiometry ratio greater than one, of each reactant is supplied to the cell. Taking into account the NOS of the reactant supply rate, the total efficiency (η) of the cell can then be calculated using equation 2.7.

$$\eta = \frac{\eta_t \times \eta_v}{NOS_{\text{reactant}}} \tag{2.7}$$[7]

where $NOS_{reactant}$, which is the inverse of reactant utilization, is defined as the ratio of the reactant actual to theoretical molar flow rate ($\dot{n}$):

[7] If recirculation is incorporated, the *net* percentage consumption of fuel should be considered in the efficiency calculation.

$$NOS_{reactant} = \frac{\dot{n}_{\text{reactant,actual}}}{\dot{n}_{\text{reactant,theoretical}}} \tag{2.8}$$

The theoretically needed reactant molar flow rate can be calculated using Faraday's Law:

$$\dot{n}_{\text{reactant,theoretical}} = \frac{i \times v_{reactant}}{nF} \tag{2.9}$$

where v is the reactant reaction coefficient. Substituting Equation 2.9 into Equation 2.8, the actual reactant molar flow rate can then be expressed as

$$\dot{n}_{\text{reactant,actual}} = \frac{i \times v_{\text{reactant}}}{nF} \times NOS_{\text{reactant}} \tag{2.10}$$

Furthermore, the reactant actual volumetric flow rate ($\dot{V}$) can be calculated as a function of reactant concentration (m_{soln}) and molar flow rate:

$$\dot{V}_{\text{reactant,actual}} = \frac{\dot{n}_{\text{reactant,actual}}}{m_{\text{soln}}} \tag{2.11}$$

2.3.3 Polarization Curve

In practical applications, the actual DMFC open circuit voltage (OCV) is lower than the ideal value stated in the previous section (i.e., 1.21 V for a methanol/air cell under

standard conditions). This is due to sluggish electrokinetics associated with dynamic equilibrium cell half-reactions and the mixed-potentials formed at the cathode, with the latter caused by the undesired methanol crossover from the anode to the cathode. The methanol crossover phenomenon will be later discussed in further detail. In addition, fuel and/or oxidant impurities could poison the electrodes and consequently degrade the OCV of the cell. During galvanostatic DMFC operation (i.e., when power is generated), various electrochemical losses occur. The three categories of these losses are activation, ohmic and concentration polarizations.

The activation polarization arises from the kinetic energy barrier associated with reacting oxidant and fuel molecules, and it is the dominant overpotential at low current densities. This polarization is directly related to the reaction rates occurring at the anode and cathode and increases with the stoichiometrically related current density. In particular, the DMFC has higher activation polarization than the hydrogen PEM cell because its anodic half-reaction requires six electrons per fuel molecule as opposed to the two electrons corresponding to PEM cells. The activation polarization can accordingly be expressed by the Tafel equation

$$\eta_{act} = -\frac{RT}{\alpha F} \ln \frac{i}{i_o} \tag{2.12}$$

where α is the charge transfer coefficient, i is the current, and i_o is the electrode reaction exchange current.

The ohmic polarization, which is also known as IR-loss, results from the internal resistances within the fuel cell. These resistances exist in every fuel cell component.

These include the ionic resistance of the membrane, the ionic and electronic resistance of the electrodes, the electronic resistance of the GDLs, endplates and terminal connections. However, the dominant contributor to the ohmic overpotential is the ionic resistance of the electrolyte membrane (i.e., the resistance to proton transport). Since the internal resistance of the cell obeys the Ohm's law, the ohmic polarization is expressed as

$$\eta_{ohmic} = iR \tag{2.13}$$

where i is the current and R is the internal resistance.

The concentration polarization occurs predominantly at higher current densities when there is not a sufficient presence of reactants to meet the high current demand. When this occurs, the limiting current density of a specific cell is reached. The hydrodynamic transfer and porosity of the GDLs, along with the diffusivity of the three-phase region in the MEA, are critical characteristics that can affect the limiting current[8] behavior of a cell. The concentration polarization as a function of the limiting current can be expressed as

$$\eta_{concentration} = -\frac{RT}{nF}\ln[1-\frac{i}{i_l}] \tag{2.14}$$

where i_l is the limiting current.

[8] When the limiting current is achieved, the cell potential lowers precipitously due to high concentration polarization.

Therefore, the actual cell potential of a DMFC at a given current density (j) can be obtained by taking into account the aforementioned polarizations. Equation 2.15 is the expression of the actual cell potential.

$$E = E_{ideal} - \eta_{act,a} - \eta_{act,c} - \eta_{ohmic} - \eta_{conc,a} - \eta_{conc,c} \tag{2.15}$$

where the a and c subscripts refer to the polarizations of the anode and cathode, respectively. It is customary to represent the cell potential as a function of current density[9] and, graphically, is usually referred to as the polarization curve or V-j curve. Given the three polarizations that contribute to the V-j curve, there are specific current density ranges where each polarization predominantly dictates the shape of the curve. Figure 2.6 shows the dominant regions of each polarization in a typical DMFC V-j curve.

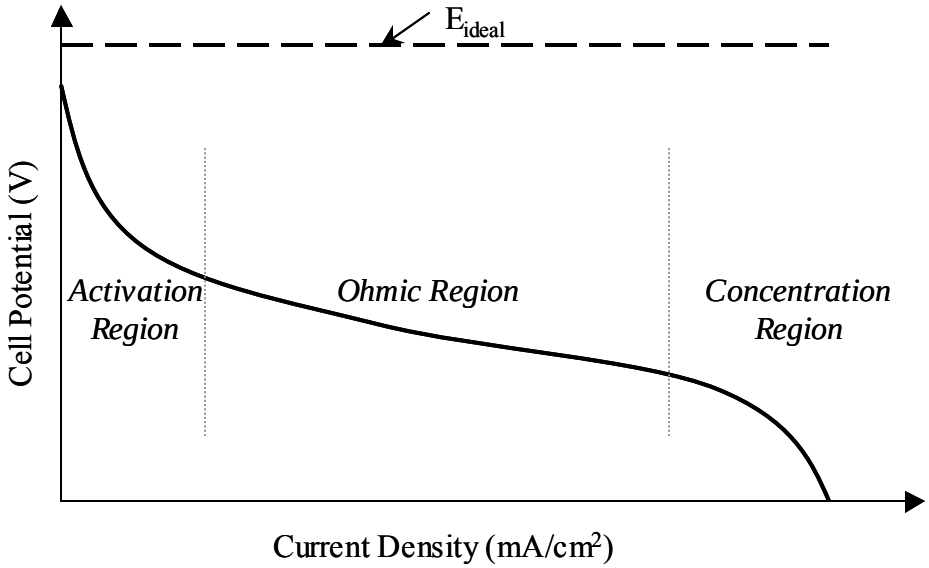

Figure 2.6: Typical V-j curve illustration with its distinctive polarization regions

[9] Current density is the current divided by the active area of the cell and its unit is mA/cm^2.

As can be observed from Figure 2.6, the activation and concentration regions occur at the lower and higher current densities, respectively. Also they show a steeper slope than the ohmic region, which is nearly linear and occurs at the middle region of the current density range. In order to characterize the electrochemical performance of a DMFC, the power density (P), which is the current density times the cell potential, is usually plotted as a function of current density in conjunction with the V-j curve. Figure 2.7 shows the typical V-j and P-j curves of a DMFC.

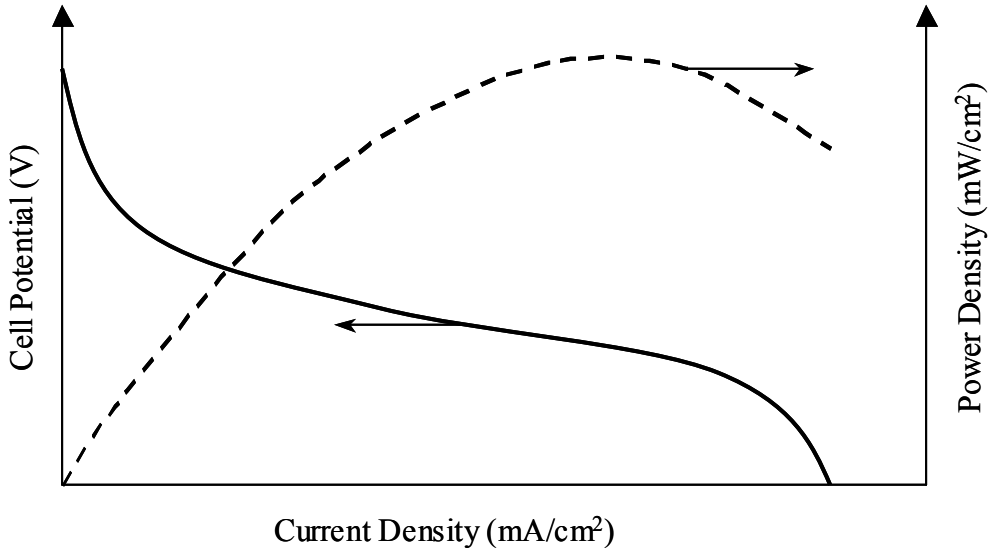

Figure 2.7: Typical V-j and P-j curves of a DMFC

In Figure 2.7, the power density is observed to have a maximum that occurs just before the dominant concentration polarization region. While it may be desired to attain a maximum voltage from a DMFC, a specific application may require a significant amount of power density. Hence, the DMFC operation can be tailored to meet certain power densities and/or cell efficiencies.

2.4 Methanol Crossover

Methanol crossover occurs when methanol solution permeates from the anode to the cathode through the electrolyte membrane. Most of the permeated methanol is reacted at the cathode creating a "mixed potential", which reduces the cathode potential and consumes some of the oxidant. Therefore, this methanol crossover phenomenon significantly reduces the cell's performance. Figure 2.8 shows an illustration of the methanol crossover phenomenon in a DMFC.

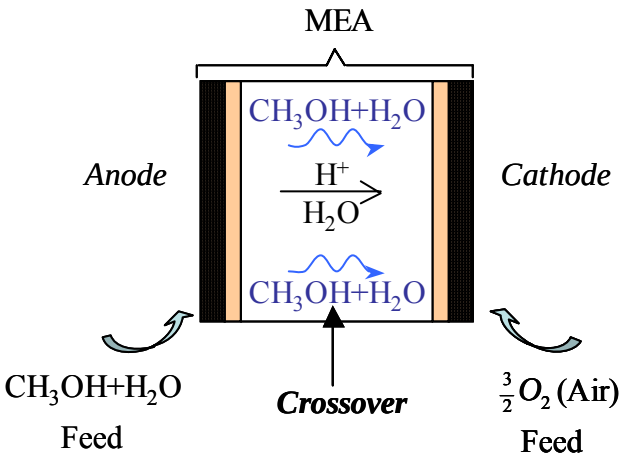

Figure 2.8: Illustration of methanol crossover in a DMFC

DMFC operation has encountered many difficulties due to methanol crossover, which occurs via diffusion, electro-osmosis, and pressure difference across the electrolyte; with diffusion being the dominant contributor to methanol crossover in comparison to electro-osmosis and pressure differentials (Wang, 2003). This diffusion increases at lower current densities due to smaller electro-oxidation rates that allows a

greater reactant presence at the fuel side of the MEA; hence, a larger diffusional driving force. Thus, it is expected that the maximum crossover occurs at OCV when there is no current density drawn. Another factor that affects the amount of methanol crossover due to diffusion is the fuel mixture concentration. Significantly high fuel mixture concentrations increase the crossover phenomenon again due to a larger diffusional driving force.

Electro-osmosis is the movement of a liquid through a porous material induced by an electrical field. In a DMFC, protons are conducted through the electrolyte when a current density is demanded from the cell. During this operation, protons "drag" water and methanol molecules from the fuel mixture to the cathode side. The magnitude of this electro-osmotic drag increases with current density and with temperature. The presence of a pressure gradient within the MEA can also cause methanol to crossover due to "leakage" forces. These two phenomena are again less influential than diffusional crossover.

The methanol permeation in DMFCs decreases the voltage and fuel efficiency of the cell. When the methanol reaches the cathode catalytic layer, it is potentially reacted with the oxidant creating a mixed potential that decreases the cell potential. In addition, this reaction masks the cathodic catalytic sites that are needed for the oxygen reduction half-reaction. As stated previously, the diffusion contribution to methanol crossover limits the practical (i.e., allowable) fuel concentration, thus limiting the energy density metrics actually achievable by DMFC systems.

2.5 Water Management/CO_2 Formation

Another major disadvantage of DMFC operation is its complex water management. Water content within the MEA, GDLs and flow channels can have severe negative effects on the cell's performance due to either the lack, or excess, of water. Excess water production in a DMFC can flood the cathode layer and obstruct active catalytic sites and thus reduce the cell's performance and efficiency. On the other hand, limited water content reduces the conductivity of the MEA. This increases the fuel cell internal resistance, which means an increase in ohmic losses.

Particular to DMFCs, the carbon dioxide (CO_2) byproduct from the methanol oxidation can temporarily attach to the anode and obstruct catalytic sites, thus degrading the cell's performance. Literature has mentioned that this degradation is a reversible phenomenon occurring to greater extent at higher current densities (Fowler, 2002).

2.6 Research Motivation

Most of DMFC research has focused on the steady state performance of the cell and not as much on its dynamic behavior. However, most real-world applications will likely operate the fuel cell system under transient conditions. There is thus the need to characterize associated transient phenomena, which may include the active control of fuel supply (also referred to as hydraulic pulsing), current density and/or pressure. The primary motivation of this research was to investigate the effective steady flow and hydraulic pulsing behavior of high fuel concentration DMFCs. These characterizations also include different current densities, NOS and catalyst loadings.

As mentioned previously, methanol crossover plays a major role in the design limitations of DMFC systems, requiring the cells to typically operate with highly diluted fuel mixtures. This constrains the compact design of the system, which is most desirable for the application of DMFCs to portable electronics. In comparison to steady flow operation, hydraulic pulsing can lead to significantly better DMFC performance and efficiency via cyclical reductions in methanol crossover (Sundmacher, 2001). This enables the system to operate at higher fuel concentrations. These concepts are further discussed within the body of this work.

Active fuel feed control may improve the overall feasibility of many DMFC applications, hence the need of a more comprehensive understanding of this transient phenomenon at various operating conditions. The present work attempts to find important trends and characteristics of this transient phenomenon.

3. Literature Review

In this chapter, some of the relevant literature that discusses and/or analyzes the methanol crossover phenomenon and the transient operation of a DMFC is presented. While there has been a relatively significant amount of investigation pertaining to methanol permeation in DMFCs, there has been limited research devoted to characterizing the transient response of this type of fuel cell.

3.1 Methanol Crossover

Jiang, *et al.* (2004) measured the amount of methanol crossover in a DMFC by monitoring the amount of carbon dioxide produced from the cathodic methanol reaction. The carbon dioxide byproduct was reacted with barium hydroxide in order to form barium carbonate, a solid compound. Based on the amount of this compound, an equivalent current of the permeated methanol was calculated and analyzed. It was found that the amount of methanol crossover was greater at lower current densities and higher methanol mixture concentrations. The experiments were performed for methanol concentrations between zero and four molar, and it was found that the cell efficiency was significantly degraded when operating at concentrations higher than one molar. At concentrations lower that one molar, high concentration polarization was observed at higher current densities thus limiting the power density output. Therefore, it would be ideal to operate at higher mixture concentrations without significant methanol permeation in order to potentially enhance the cell's power density and efficiency. This was the

major motivation for the present work, wherein the cell potential and power output were significantly increased by operating the DMFC under a specific fuel flow pulsing scheme. A steady flow operation at various concentrations was performed in order to corroborate the findings obtained by Jiang, *et al.*

Wang, *et al.* (2003) developed a two-phase model to analyze the methanol permeation phenomenon in DMFCs. It also showed the methanol concentration distribution within the gas diffusion layers, electrodes, and electrolyte membrane that was caused due to the undesired methanol permeation. This distribution varied almost linearly from the anode diffusion layer to the cathode catalytic surface. The tested methanol concentrations were one and two molar. The model assumed that the permeated methanol was completely reacted at the cathode; however, Mench *et al.* (2005) stated the presence of some methanol in the cathodic effluent, especially when operating at high methanol mixture concentrations (i.e., greater than one molar). This is indicative that not all permeated methanol necessarily reacts at the cathode.

In addition, Wang, *et al.* (2003) reported the effect and extent of methanol transport due to diffusion, convection and electro-osmosis drag. Each of these affected the amount of methanol permeation differently under various operating conditions. Table 3.1 summarizes the results obtained for two different current density demands. It includes the percentage contribution of each transport source to the overall quantity of methanol crossover.

Table 3.1: Percentage contribution of the methanol permeation sources (Wang, 2003)

	Percentage Contribution (%)	
Permeation Source/ Current Density	0.45 A/cm^2	0.14 A/cm^2
Diffusion	70	85
Electro-osmosis	30	15
Advection	~ 0	~ 0

As can be observed in Table 3.1, methanol crossover predominantly occurred through diffusion from the anode to cathode. The electro-osmosis drag occurs when water particles and hydrogen ions literally *drag* along some of the methanol to the cathode side. Therefore, it was expected that the extent of this source was greater at higher current densities wherein more water and ions are produced. Nonetheless, as shown in Table 3.1, methanol diffusion was the primary source even at higher current densities. Note that the advective (pressure-driven) mass transfer was negligible due to the lack of significant pressure gradients between the electrodes. These results obtained by Wang, *et al.* were extremely important for some of the steady flow and pulsing analyses that are presented in this work.

3.2 Transient Operation

Sundmacher, *et al.* (2001) presented experimental and analytical results of a DMFC operated under a particular methanol concentration pulsing scheme. First, it analyzed the cell response when fuel concentration was reduced from near two molar to zero, and it was observed that the cell potential temporarily increased before significant concentration polarization occurred. This was done for three different current densities (30, 50 and 60

mA/cm^2) and both the reactant flow rates were maintained constant throughout the experiments. The work stated that a fifteen percent increase in cell potential was observed during fuel discontinuation mainly due to a reduction in methanol crossover. However, it did not quantify the exact voltage rise for the various tested current densities. The second transient operation consisted of a continuous fuel concentration pulsing strategy, and a ten percent average voltage enhancement was reported during this pulsing operation. Similar cell response was obtained for both the experimental and analytical experiments. Only one pulsing scheme was tested, and the specific duty cycle and period were not reported. Also, the work did not present a detailed quantification and analysis of the transient response. Therefore, the present work focuses on experimentally quantifying and analyzing the transient cell response under various operating conditions including different feed concentrations, current densities, and fuel flow rate.

The present thesis primarily continues the work of Leahy, *et al.* (2004). They reported the steady flow and transient operations of both hydrogen PEM cells and DMFCs. The steady flow polarization curves were performed at two different fuel flow rates (0.125 and 0.25 cc/min), and an insignificant difference between these results was observed. In the present work, the polarization curves were performed at a constant fuel flow rate of 0.25 cc/min and at various fuel mixture concentrations as well as different catalyst loadings. This was done because the major focus of the thesis was to investigate the possible cell potential enhancement during fuel transient operation at higher mixture concentrations.

Leahy, *et al.* analyzed the fuel discontinuation cell response at three different current densities (10, 25 and 50 mA/cm^2). Also, they performed the experiments on two

different catalyst loadings, two and four mg/cm^2. It was found that the voltage increase was slightly greater at lower current densities. The fuel flow rate (i.e., the flow rate prior to the fuel discontinuation) was maintained constant throughout the experiments and only one and two molar concentrations were tested. Again the present work mainly focused upon testing higher methanol concentrations.

In addition, Leahy, *et al.* performed a continuous fuel flow pulsing scheme at one and two molar. The period and duty cycle of the pulsing scheme was 550 seconds and 50 percent, respectively. Nearly a ten percent cell potential enhancement was attained and no other duty cycles or periods were tested. Therefore, this work attempted to further investigate the fuel transient operation at various pulsing schemes with different duty cycles and periods as well as fuel mixture concentrations. Furthermore, a transient operation consisting of continuous pulsing of both fuel and current density was tested and analyzed.

4. Experimental Setup

4.1 Experimental Equipment

The system utilized during this study, as shown in Figure 4.1, consisted of a set of flow meters and solenoid valves, a DMFC, an electronic load, and other peripheral components.

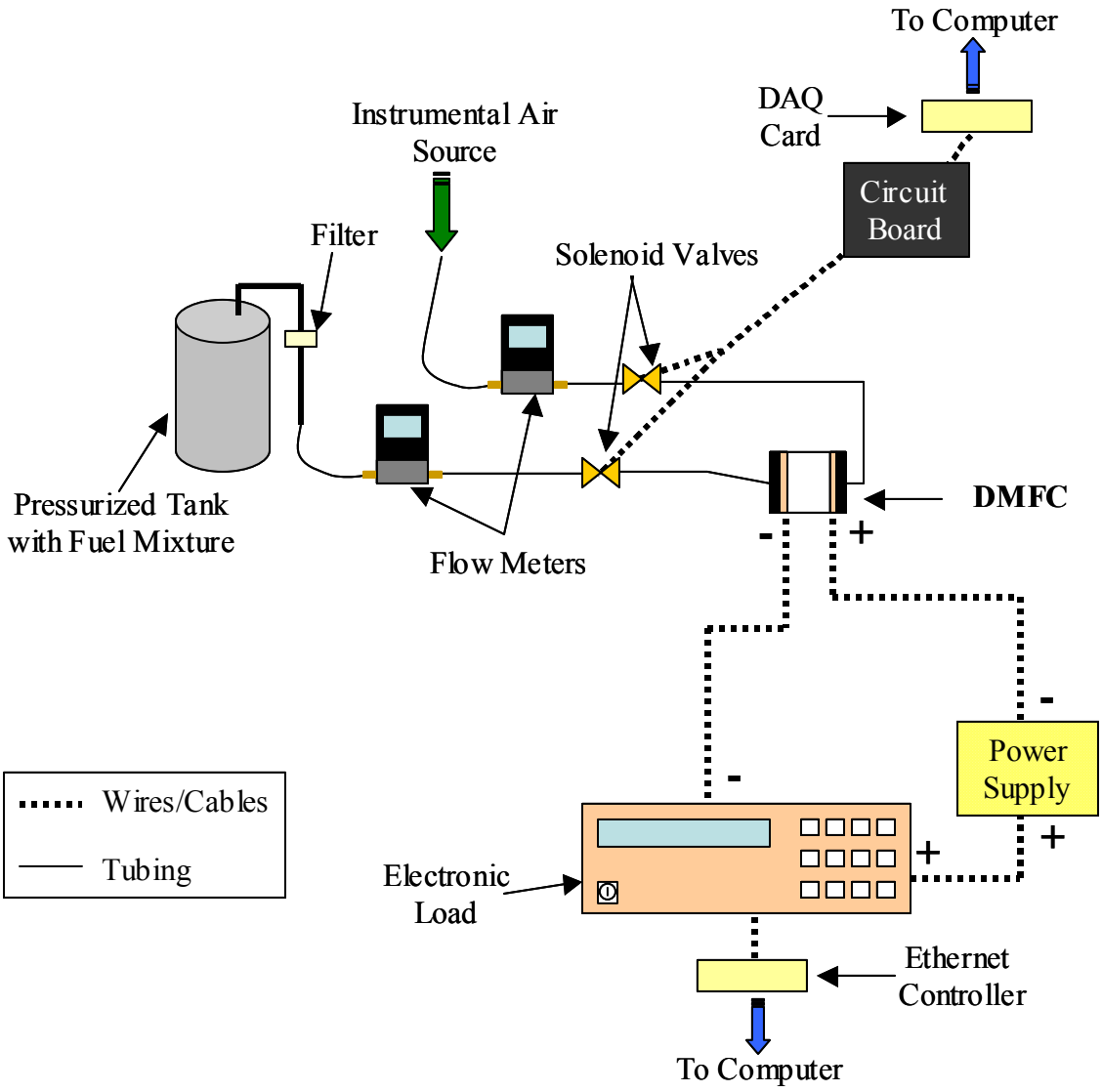

Figure 4.1: Schematic of DMFC experimental setup

The fuel (i.e., the methanol-water mixture) was placed in an aluminum tank that was pressurized at 15 psig with pure nitrogen from an in-house supply system. In order to assure the purity of the fuel mixture, a filter from Osmonics Inc., model number DCN01000T6, was connected between the fuel tank and flow meter. This filter also facilitated the removal of undesired particles capable of obstructing the solenoid valve. The oxidant in this research was air and was also supplied from an in-house system.

The fuel flow meter utilized during this work was from Alicat Scientific series 16 model L. This meter was calibrated for a maximum flow rate of 1 ccm, which was sufficient for the tested flow rate range. The air flow meter was from Omega Engineering, model FMA-1618, and was calibrated for a maximum flow rate of 200 standard cc/min (scc/min). Throughout the present work a constant air flow rate of 60 scc/min was utilized, which was suitable for the given flow meter calibration. The accuracy of the fuel and air flow meters were +/- 0.01 cc/min and +/- 2 scc/min, respectively; also, the response time of each flow rate was 10 ms, which resulted in a maximum feasible flow oscillation of 25 Hz. (Leahy, 2004)

The fuel and air flows were controlled with proportional solenoid valves from the Pneutronics Division of Parker Hannifin Corporation and were model numbers E-20568 and E-20336, respectively. The valves were actuated with a 0-5 voltage signal to open or close the reactants path. This digital signal was sent from a National Instruments data acquisition card model number SCB-68 and was controlled with a specific program that will be discussed later in this chapter. The actuation voltage required a specific gain and offset that was tailored based on the given flow rates. Therefore, a circuit board consisting of adjustable resistors and op-amplifiers was utilized to regulate this gain and

offset in order to more accurately control the target flow rates. Unfortunately, it was difficult to maintain a constant accuracy level for the various tested flow rates. Therefore, the gain and offset were strategically adjusted for a given flow rate in order to maintain a percentage error no greater than ten percent.

Although the temperature of the cell was not controlled, in some instances it was monitored with a Fluke Inc. thermometer, model number 52-II. This thermometer was calibrated and its accuracy within the temperature range associated with this work (i.e., 25-50 °F) was found to be +/- 0.25 °F. The temperature measurement was taken with a thermocouple from the outer surface of the DMFC endplate fixtures.

Throughout the present work, the DMFC was always operated galvanostatically wherein the current demand was always controlled[10]. This was accomplished with a DC electronic load from Agilent Technologies model number N3300A. In addition to controlling the current density, the electronic load was used to record the cell potential as well as the demanded current density. Since the cell potential output was always less than one-volt, a power supply from Acopian model number VA5H1700 was connected in series with the DMFC and electronic load. This boosted the voltage across the load terminals to above three-volts, which is the threshold associated with this particular DC load. It is not recommended to operate the load below this threshold because the slew rate and input current are derated. Power from both the boost supply and DMFC was absorbed by the electronic load. The voltage readback was measured directly from the DMFC using the remote sensing feature of the load. This load was capable of measuring the current and cell potential within a percentage error of +/- 0.1 and +/- 0.05 percent,

[10] If the voltage is controlled instead of the current density, the operation is referred to as potentiostatic.

respectively. The electronic load was controlled through an Ethernet-based GPIB controller model number IEEE-488.

A single DMFC with a 4 cm^2 square active area was utilized during this work and was fitted with an MEA of that same size. The DMFC components including the MEA, endplate fixtures, and silicon gaskets are shown is Figure 4.2.

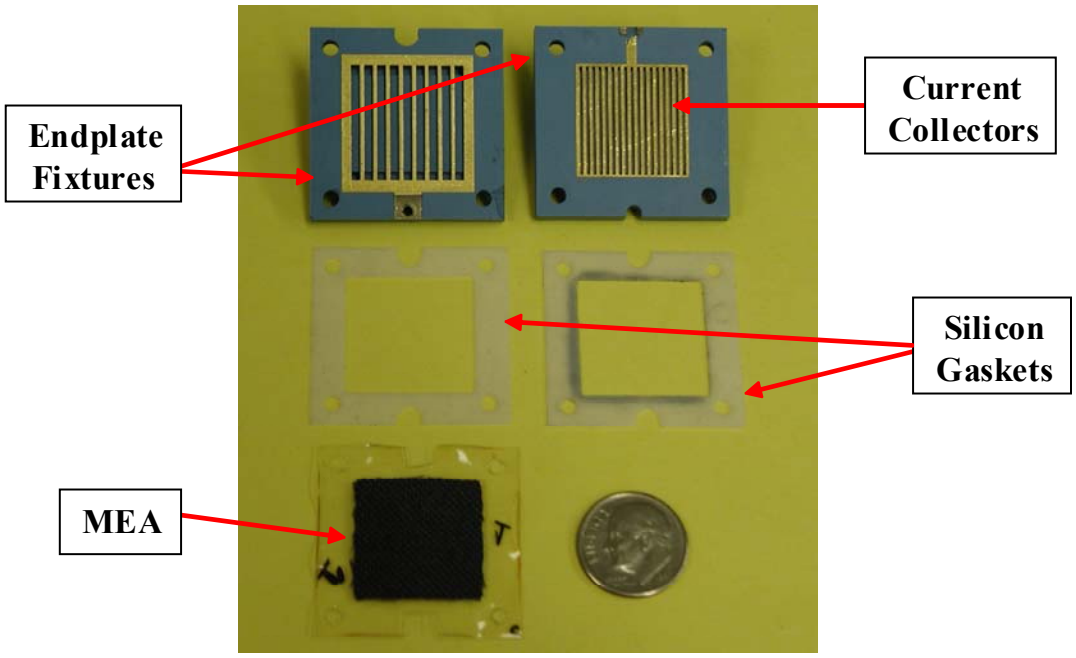

Figure 4.2: DMFC components

The 5-layer MEAs were purchased from E-Tek, a division of Gruppo De Nora, and were made based upon central electrolyte material Nafion® 117. The cathode and anode consisted of unsupported black Platinum and Platinum-Ruthenium alloy, respectively. The catalyst loadings on these electrodes were either three or four milligrams per

centimeter square. However, a given MEA always had the same catalyst loading on both the anode and cathode. The gas diffusion layers were made out of carbon cloth and placed onto each side of the electrodes. The anode and cathode silicon gaskets had a thickness of 10 and 15 micrometers, respectively.

The endplate fixtures were donated by Motorola and were made out of Dupont 951 ceramic green tape. Each fixture had a serpentine flow pattern that was used to uniformly distribute the reactants to the MEA active area. The inlet and outlet ports of the endplates had a 5/64 inch diameter. The cell was operated vertically with the fuel supply inlet at the upper port and the outlet at the lower port. This operation allowed gravitational forces to facilitate the fuel flow through the endplate channels. The air was supplied into the lower port in order to more effectively remove the water byproduct from the cathode flow channels.

A main part of this research was to investigate the cell response to specific fuel flow pulsing schemes; therefore, a detailed description of the anode endplate is necessary to determine the minimum flow rate associated with a given pulsing duty cycle and period. The cathode endplate description is not needed because the air flow rate was maintained constant throughout the work. Nonetheless, it is worth mentioning that the only difference between the endplates was the number of channels. The anode had 18 channels while the cathode only 10 channels, but both had the same serpentine surface area. As a result, the cathodic channels were bigger mainly because the air flow rate was significantly higher than the fuel rate thus enabling a faster dispersion throughout the larger flow channels. The anode endplate schematic is shown in Figure 4.3. It includes the dimensions of the serpentine surface area as well as the dimensions of the flow

channels and fuel inlet connector. Note that the inlet and outlet had identical configurations.

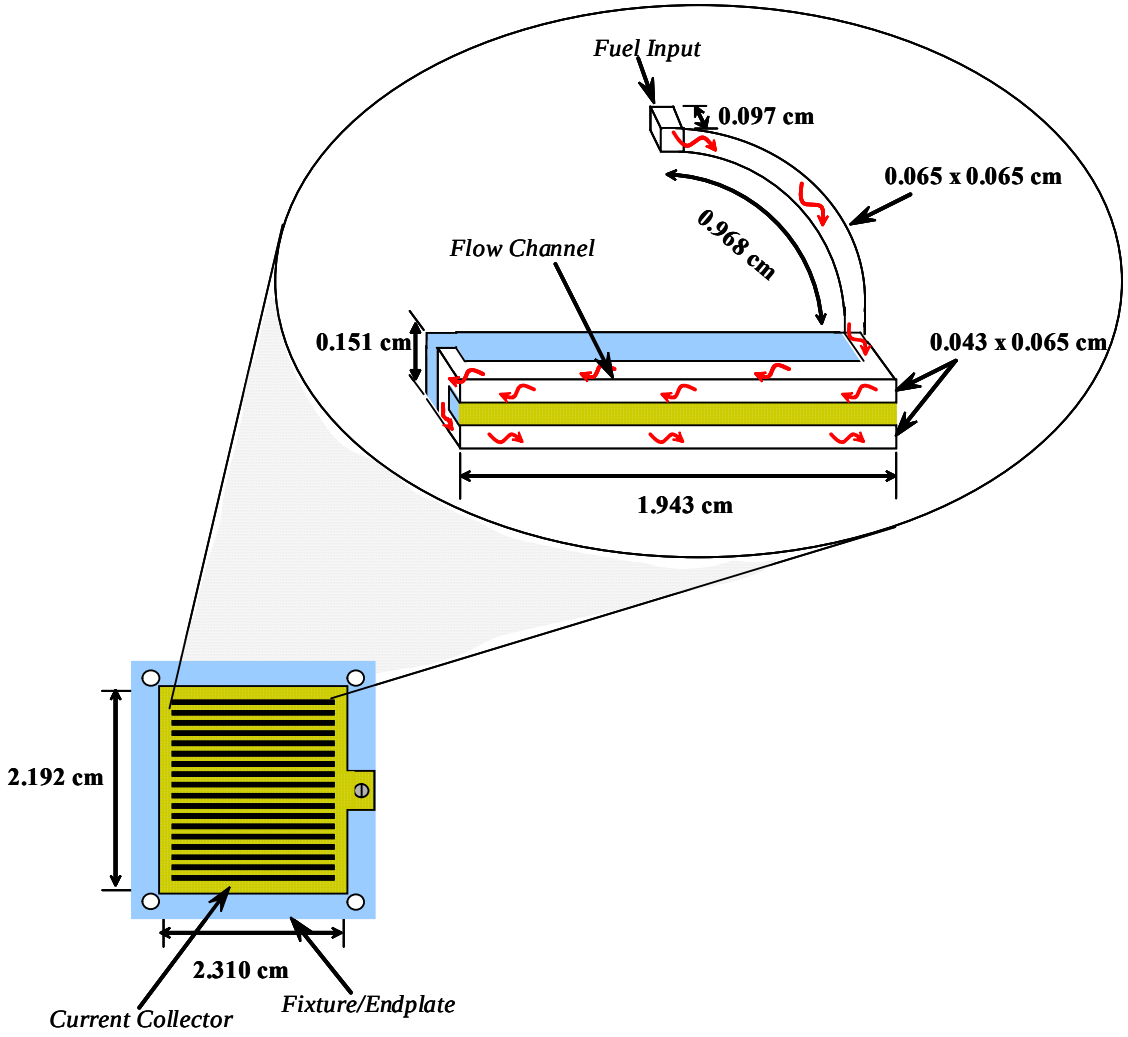

Figure 4.3: Anode endplate fixture schematic

The total volume of the channels and peripheral connectors was *0.116 cm*^{3}. Based on this volume and a given fuel supply time, an appropriate flow rate can be chosen in order to assure that the channels are completely filled with methanol mixture solution. In

Table 4.1, a range of minimum flow rates for a given fuel supply time are presented. These values are important for developing an effective fuel flow pulsing scheme.

Table 4.1: Minimum fuel flow rate for a given supply time

Supply Time (min)	Minimum Flow Rate (ccm)
0.5	*0.23*
1	*0.12*
1.5	*0.08*
2	*0.06*

Another typical purpose of the endplates is to serve as current collectors. Since the endplates material (i.e., green ceramic) was not electrically conductive, thin sheets of gold were built into the inner surface of the endplates enabling a continuous current flow between the cell and the external load.

4.2 Software

The DMFC system was controlled through Labview, a graphical programming language distributed by National Instruments. The software communicated with the experimental system through the data acquisition card, Ethernet GPIB controller and the flow meters. It was capable of controlling and recording the current density and cell potential as well as the fuel and air flow rates.

A specific current density value was input into the program and sent directly to the DC electronic load via the Ethernet GPIB controller. This controller also continuously sent to the computer the readback values of the corresponding cell potential and

prescribed current demand, which were recorded and displayed in Labview. An important feature of the program was the ability to suddenly stop the experiment if the cell potential reached a prescribed minimum value, which was also input into Labview.

As stated previously, digital signals to the proportional solenoid valves were sent through the data acquisition card. A calibration was performed to obtain the DC voltage value associated with a given flow rate. This DC voltage value was then used by Labview as a reference to initialize the operation. Since the valves were constantly fluctuating, the required DC voltage for a given flow rate was also changing. Therefore, Labview continuously compared the flow measurements and adjusted the DC voltage signal, if necessary, in order to closely achieve the target flow rate. The Labview code recorded the flow rates directly from the flow meters, which had the capability of sending RS-232 digital output signals to the computer serial ports.

The Labview program was capable of running manually from the front panel or automatically through a scripted file. During manual operation, the input values (i.e., current density and flow rates) were directly specified in the front panel of the program. Alternatively, the program was able to input the values from a script wherein the operating values were set for a desired running time. The script consisted of different steps with each specifying the values including the step time. This automated mode was primarily utilized.

The voltage, current density, reactant flow rates and running time were automatically saved into a comma separated value (csv) file. Data was saved every 0.3 seconds. In order to simplify the data analysis of certain operations, two different saving modes were developed. Under V-j curve mode, the voltage and current of each step was

averaged and saved into the csv file. As a result, the final csv file consisted of only one voltage and current density entry from each step. The other saving mode only collected data within a specific step range, which was specified in the Labview program. This mode helped collect data more effectively during the transient operations wherein the initial steps, as discussed later in this chapter, were not needed for the analysis.

4.3 Experimental Procedure

During both steady and transient flow operations, a careful experimental procedure was developed in order to obtain more accurate and repeatable results. Prior to testing, the MEA underwent a "break-in" process wherein the new membrane was soaked in deionized water for at least twenty-four hours. This process facilitated an appropriate hydration level, which is required for proper membrane conductivity. The cell was then operated at a mixture concentration of one molar with no current demand for four to five hours until a reasonable open circuit cell potential was attained. Note that during this phase a higher fuel mixture concentration was not utilized in order to minimize the methanol crossover effect.

Throughout the experiments, the minimum cell potential was set to 0.1 volts. It is not recommended to operate below this value because the membrane could be severely damaged. As previously discussed, nearly all of the experiments were performed through a scripted file. The first step in the file, which was not considered a part of the experimental data set, was always used to allow the given reactants flow rates to stabilize during open circuit voltage operation (i.e., no current demand). This stabilization was usually attained within two to three minutes. Another procedural condition was to always

drain the methanol out of the cell before extended break periods to assure that no methanol crossover occurred and consequently eliminate the detrimental effect on the membrane.

During steady flow polarization curves, the current density demand was first slowly incremented from 0 to 50 mA/cm^2. In the scripted file, each step was used to change the current density by increments of 2.5 mA/cm^2. The time of each step was set to fifteen seconds in order to allow sufficient time to achieve a stable cell potential for the prescribed current density. The same procedure was applied when the current density demand was decremented from 50 to 0 mA/cm^2. Three replicates of each experiment were performed, and the average of the three was used in the final data analysis. A five minute break between the trials was taken in order to establish the same initial cell conditions for each trial.

The rest of the experiments involved transient fuel flow operations. Each test was performed at a specific current density (i.e., either 25 or 40 mA/cm^2). Before running the transients, the current density was slowly increased to the target value by increments of five mA/cm^2 every fifteen seconds. During the fuel discontinuation tests, the cell was operated at the prescribed current density and reactants flow rates for three minutes before the fuel flow was set to zero. Only the last step, where fuel was discontinued, was recorded and analyzed. The continuous fuel pulsing schemes consisted of four pulsing cycles. The first cycle was used to establish a uniform cell condition and was not considered in the data analysis. Only the last three cycles of the scheme were used in the analysis. As with the steady flow polarization curves, three replicates of each experiment were performed during the various fuel discontinuation and continuous pulsing

operations. Again, the average of the three trials was used to analyze the results. For both the steady and transient flow experiments, the replicates had a percentage error less than ten percent.

5. Experimental Results of Steady Flow

A major aspect for DMFC technology improvement is the ability to successfully operate at higher fuel mixture concentrations. However, methanol crossover from anode to cathode, which severely degrades the cell's performance, increases with methanol concentration. This phenomenon is detrimental to the overall fuel cell cost, fuel efficiency, cell lifetime, and power density. As mentioned in Chapter 3, Ge *et al*. (2004) performed steady flow polarization curves on DMFCs at different methanol feed concentrations and found that the optimal concentration was between 0.5 and 2 M. Based on these results, similar testing was performed to determine the steady flow behavior of galvanostatically operated DMFCs with various fuel feed concentrations and catalyst loadings. The air and fuel flows were kept constant at 60 scc/min and 0.250 cc/min, respectively. The cell was operated nominally at room temperature.

5.1. Hysteresis Effect

It is customary to produce a steady flow polarization curve (i.e., V-j curve) with a continuous current density sweep cycle. First, the current density is incrementally increased to the maximum desired value and then decrementally decreased to 0 mA/cm^2 (i.e., no load, or open circuit). The cell response during the decreasing sweep is rarely identical to the increasing sweep. In most cases tested, the increasing sweep was higher than the decreasing sweep[11]. This phenomenon has been attributed to reversible losses caused by the cell's water management and other parasitic formations (e.g., carbon

[11] This phenomenon is also referred to as "hysteresis" or a "lagging effect".

dioxide agglomeration) at the electrodes (Ge, 2004). Figure 5.1 shows the complete polarization cycle up to 50 mA/cm^2 for a 6 molar concentration fuel mixture wherein the hysteresis effect was observed.

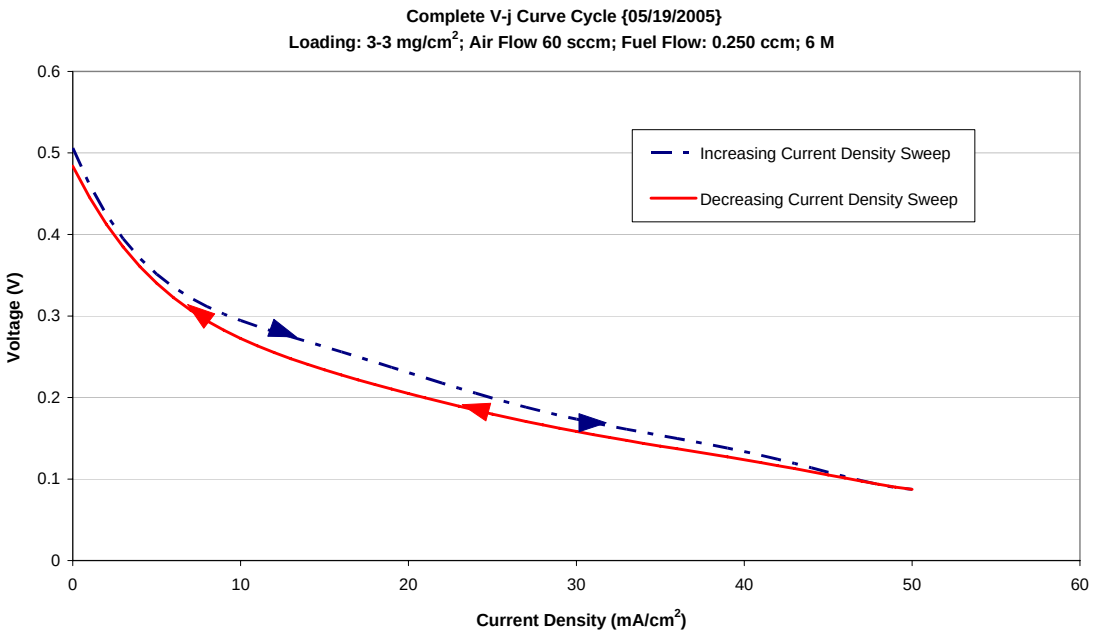

Figure 5.1: Complete V-j cycle plot at 6 molar

During this work, complete steady flow polarization cycles were performed with different fuel mixture concentrations, and only the increasing current density sweep was used.

5.2. Performance Analysis

Figure 5.2 (a) and (b) show the cell polarization (V-j) and power (P-j) curves at various fuel concentrations as current density is increased from 0 to 50 mA/cm^2 for a 3:3 mg/cm^2 loaded MEA (i.e., a loading of 3 mg/cm^2 on each electrode).

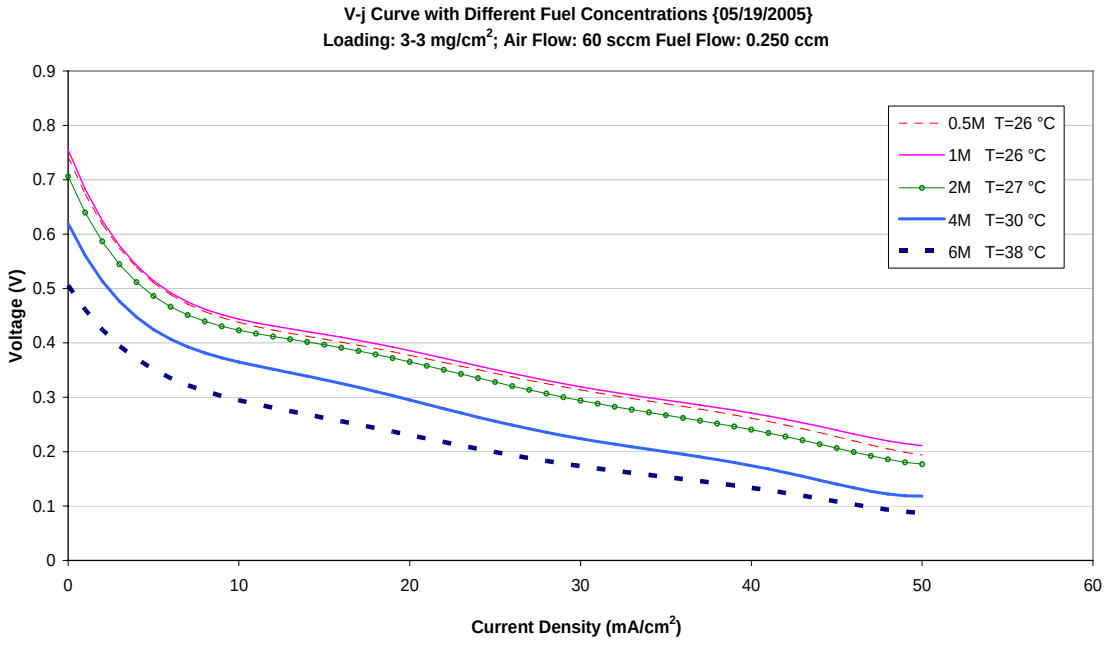

Figure 5.2 (a): V-j curve of 3:3 mg/cm^2 loaded MEA under various fuel feed concentrations

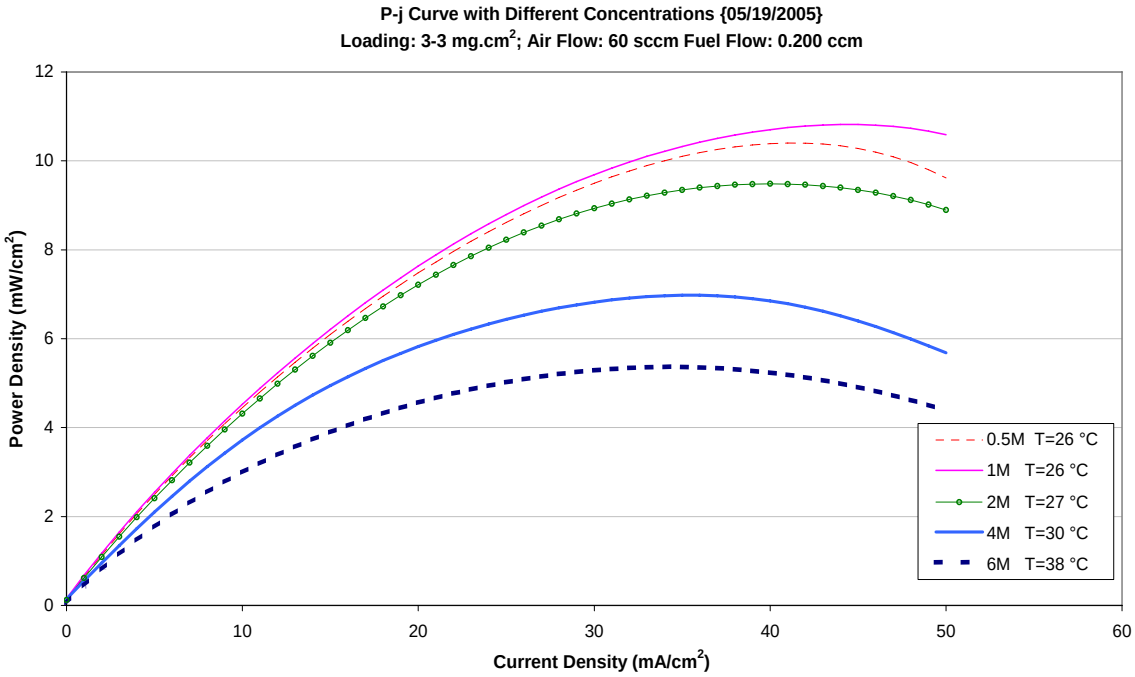

Figure 5.2 (b): P-j curve of 3:3 mg/cm^2 loaded MEA under various fuel feed concentrations

As can be observed from Figure 5.2, the best cell performance was attained at a fuel feed concentration of 1 M. At the lower concentration (i.e., 0.5 M), the performance was degraded predominantly due to high concentration polarization. In accordance with the literature, the cell performance significantly degraded at concentrations higher than 2 M (Ge, 2004). This behavior is the result of a relatively high methanol concentration presence at the anode layer that allows more methanol diffusion to the cathode. As described in chapter 2, the permeated methanol negatively impacts the cathode (e.g., catalytic reaction with oxygen) and lowers the cathodic potential. Based on these results, it can be hypothesized that there is an optimal fuel concentration where there is relatively low methanol crossover but not too large an effect of concentration polarization. Based

on the test results, it is feasible to state that the optimal concentration was between 0.5 and 2 M. An important parameter shown in Figure 5.2 is the representative average cell temperature of each polarization curve. In general, it was found that the average cell temperature increased with concentration. This increase in average temperature is attributed to lower Faradaic efficiencies primarily resulting from greater methanol crossover and catalytic combustion at the cathode.

The same testing was performed on a MEA with higher catalyst loading. Figure 5.3 (a) and (b) show the cell polarization (V-j) and power (P-j) curves at various fuel concentrations as current density was increased from 0 to 50 mA/cm^2 for a 4:4 mg/cm^2 loaded MEA.

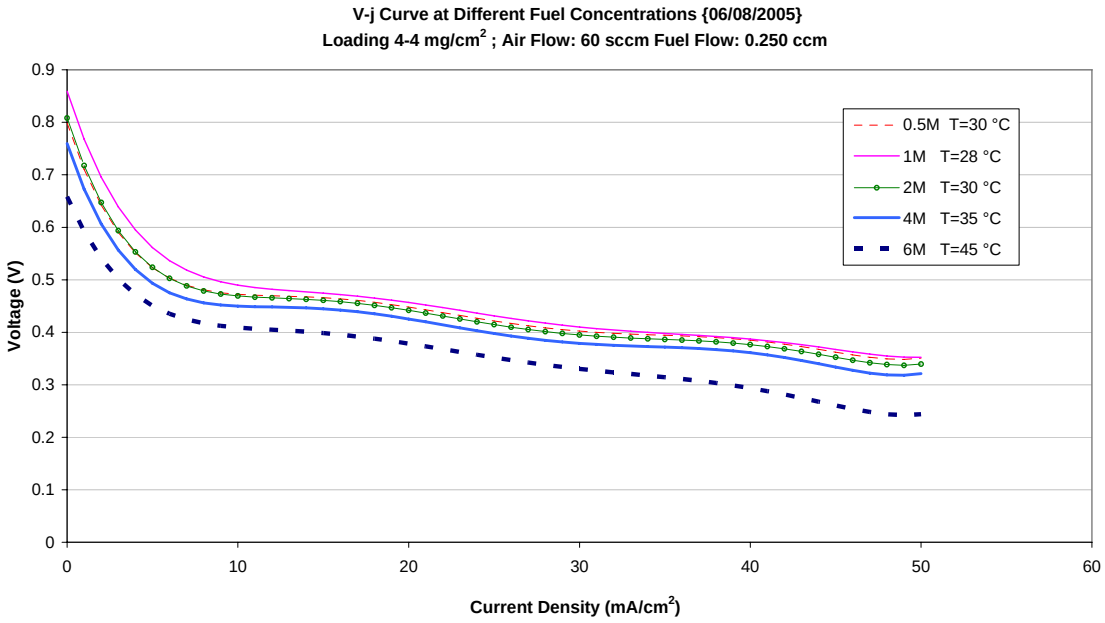

Figure 5.3 (a): V-j curve of 4:4 mg/cm^2 loaded MEA under various fuel feed concentrations

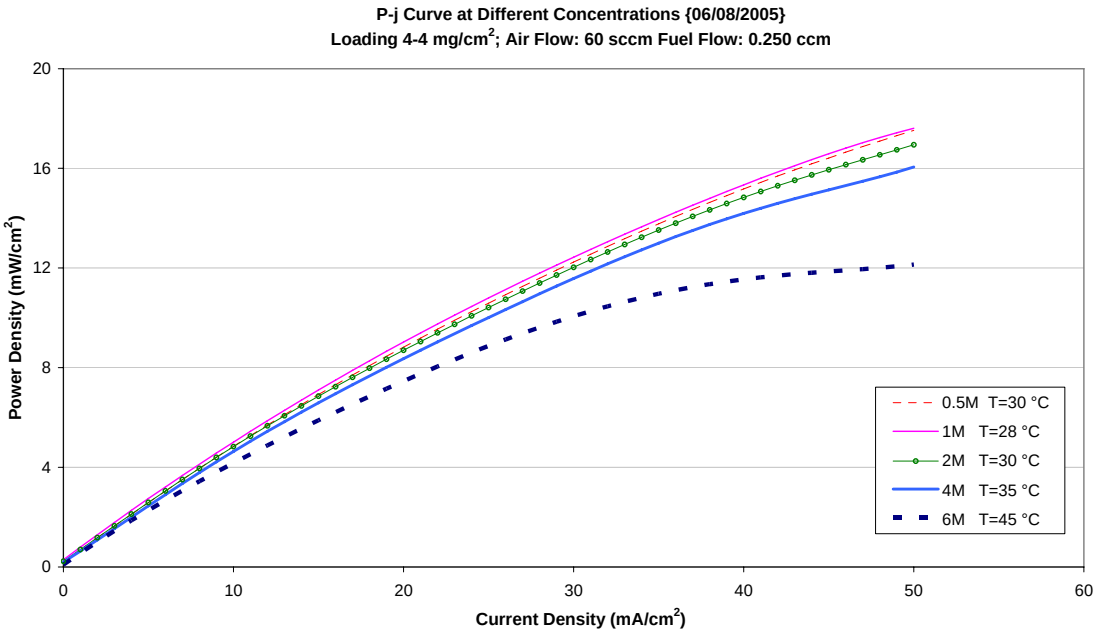

Figure 5.3 (b): P-j curve of 4:4 mg/cm^2 loaded MEA under various fuel feed concentrations

In general, the higher catalyst loading tests showed the same trends observed in the lower loading results. The possible optimal concentration region was the same as that of the lower catalyst loading (i.e., between 0.5 and 2 M). The temperature also generally increased with concentration. Again, this occurs due to greater methanol crossover at the higher concentrations. The overall performance and temperature at the various concentrations was different for each catalyst loading, indicative of differing cell activity.

As can be observed from Figures 5.2 and 5.3, the overall performance of the higher catalyst loading was significantly better than the lower loading. The activation polarization was greatly reduced with the use of higher catalyst loading. However, it is

important to note that higher catalyst loading considerably increases the overall fuel cell cost due to the high cost of noble metals.

Another major difference between the two loading results is the degree of degradation caused by the 4 M concentration in comparison to 0.5 and 1 M cases; the additional degradation was more pronounced given the lower loading cells. According to some literature, there is less methanol crossover at the higher loading because the catalyst layer thickness increases with loading (Havranek, 2001). Nonetheless, the present data is insufficient to conclusively determine whether there is a reduction in methanol crossover at the higher loading. A more sophisticated experimental procedure, such as a gas chromatography-based test, is required.

In theory, a DMFC without methanol crossover would have a significantly lower temperature at the higher catalyst loading because the heat generation is inversely proportional to the cell potential. However, Figure 5.4 shows that the average cell temperatures for the higher loading were actually greater than the lower loading. The higher temperature behavior can then only be attributed to an increase in methanol cathodic reaction. In fact the presence of unreacted methanol in the cathode effluent has been reported (Mench, 2005), so greater methanol cathodic reaction due to the higher catalyst loading is plausible. Again, a more sophisticated experimental procedure would be needed to fully corroborate this reasoning.

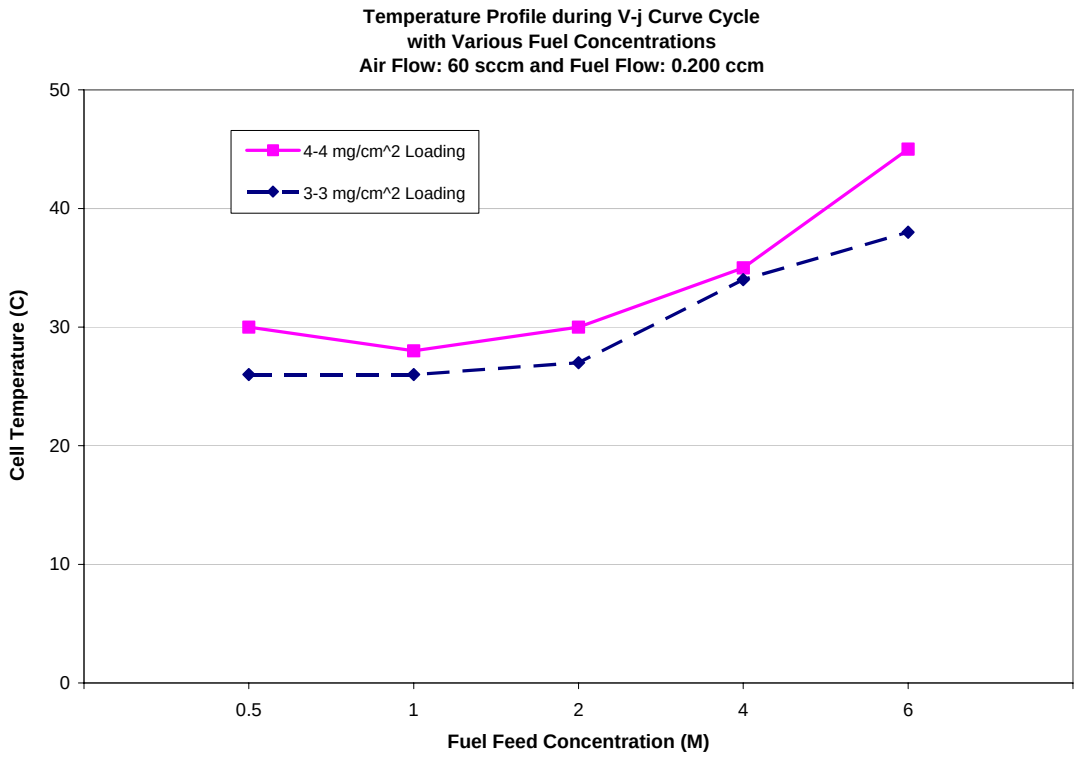

Figure 5.4: Average temperature difference[12] between a 3:3 and 4:4 mg/cm^2 loaded MEA under various fuel feed concentrations

5.3. Summary

It was found that concentrations higher than 2 M significantly degraded the cell performance predominantly due to greater methanol crossover. At lower concentrations, the performance was hindered by high concentration polarization. However, as shown in Figure 5.5, there is an optimal concentration region with a relatively low amount of combined "mixed potential" and concentration polarization. Although the thermal effect on the cell's performance was not investigated in depth, it was found that the temperature of the cell increased when operating at higher methanol concentrations. This is indicative

[12] Note that this is the average cell temperature recorded throughout the polarization curve.

of the greater methanol crossover that can possibly generate more heat byproduct from catalytic methanol combustion at the cathode.

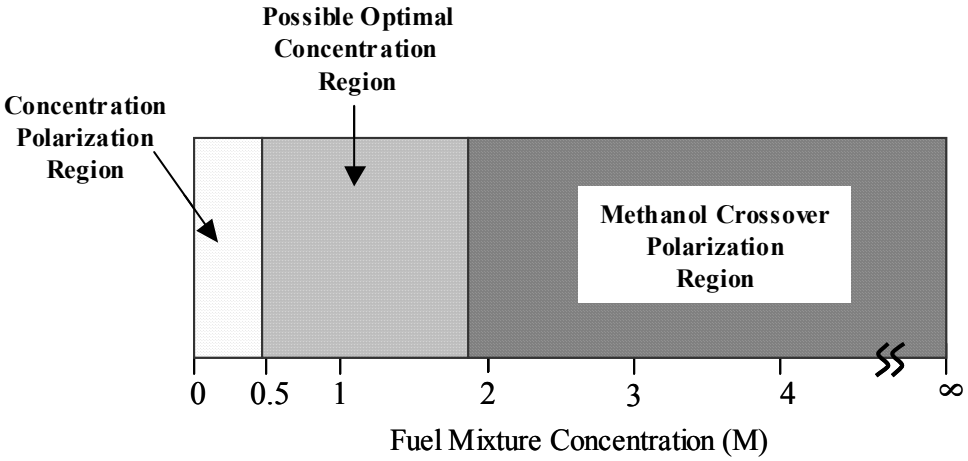

Figure 5.5: Illustration of the possible optimal concentration region

6. Experimental Results of Temporary Fuel Discontinuation

Due to the nature of many DMFC applications, such as portable electronics, it is important to characterize the fuel cell's transient behavior. Despite the fact that in recent years there have been more initiatives to investigate the dynamic behavior of DMFCs, there is still more research needed to sufficiently characterize the transient phenomena of these fuel cells. Pressure, fuel and oxidant flow rate, current density, and fuel feed concentration are some parameters to consider when analyzing the dynamic behavior of DMFCs. The present chapter analyzes a DMFC's transient response to a sudden fuel flow discontinuation while the oxidant flow rate was kept constant at 60 sccm. This was done at different NOS levels, current densities and fuel mixture concentrations.

Leahy *et al.* (2004) and Sundmacher *et al.* (2001) have shown that a discontinuation of fuel mixture supply results in a temporary increase in cell potential, and it has been hypothesized to occur due to a reduction of fuel concentration at the electroactive region, which consequently reduces the amount of methanol crossover. Based on these findings, a comprehensive experimental analysis was performed wherein a DMFC fuel feed solution was discontinued. During this set of experiments, fuel was supplied for three minutes at a constant stoichiometry (NOS) before its discontinuation. Furthermore, a specified current density was demanded throughout the given experiment.

6.1 Influence of Fuel Feed Concentration

During the steady polarization analysis in Chapter 5, it was found that higher fuel feed concentrations significantly degraded cell performance. Researchers have attributed this phenomenon to an increase in methanol crossover as fuel mixture concentration is increased (Havranek, 2001). Figure 6.1 shows the voltage responses when various fuel mixture concentrations were discontinued while a 25 mA/cm^2 current density was applied. The cell response for each concentration is plotted as a function of "normalized time[13]".

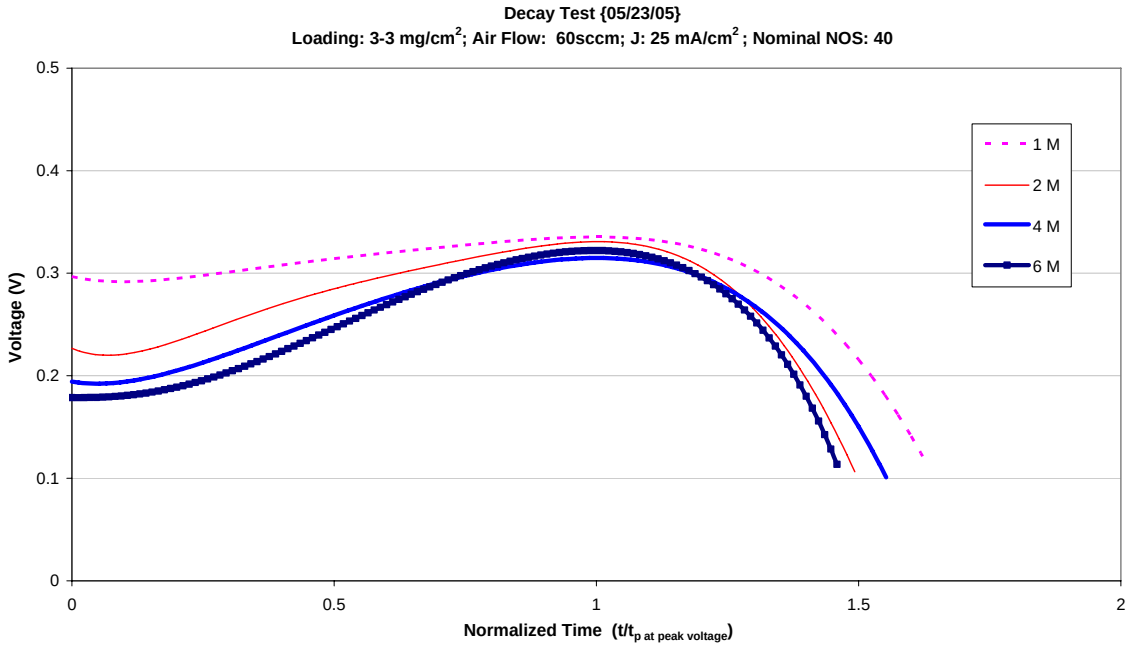

Figure 6.1: Semi-normalized voltage plot when fuel supply was discontinued on a 3:3 mg/cm^2 loaded MEA with a 25 mA/cm^2 applied current density

[13] Throughout this work, normalized time is defined as the ratio between the test-run time and the time to reach maximum voltage that occurs during the fuel discontinuation phase.

As can be seen from Figure 6.1, the initial voltages decreased as fuel concentration increased. This is in agreement with the steady flow polarization findings of the previous chapter, where the voltage significantly degraded with increasing concentration due primarily to the greater methanol crossover. Table 6.1 lists the observed maximum voltage for each concentration and the respective time taken to rise from initial to that maximum value.

Table 6.1: Maximum voltage and time data from fuel discontinuation for a 3-3 mg/cm^2 loaded MEA with a 25 mA/cm^2 applied current density

Concentration (M)	**V_{max} (V)**	**t_{Vmax} (min)**
1	0.34	3.4
2	0.33	6.0
4	0.32	6.6
6	0.32	7.3

It is important to note that, due to the large fuel NOS, the initial methanol concentration at fuel discontinuation was approximately the same as that of the fuel feed. As a result, it would take longer to reach the optimal (lower) concentration given higher methanol feed concentrations. In each concentration case, the maximum voltage was approximately one-third of a volt. This common maximum voltage for the various *initial* fuel mixture concentrations is indicative of a lower, optimal concentration universally reached, given sufficient time for methanol depletion within the resident fuel mixture. After the optimal concentration was reached, the cell potential started to rapidly diminish

due to growing concentration polarization effects. Figure 6.2 is an illustration of the optimal concentration reached during the fuel discontinuation test along with the voltage change from the initial (i.e., steady state) to the maximum voltage.

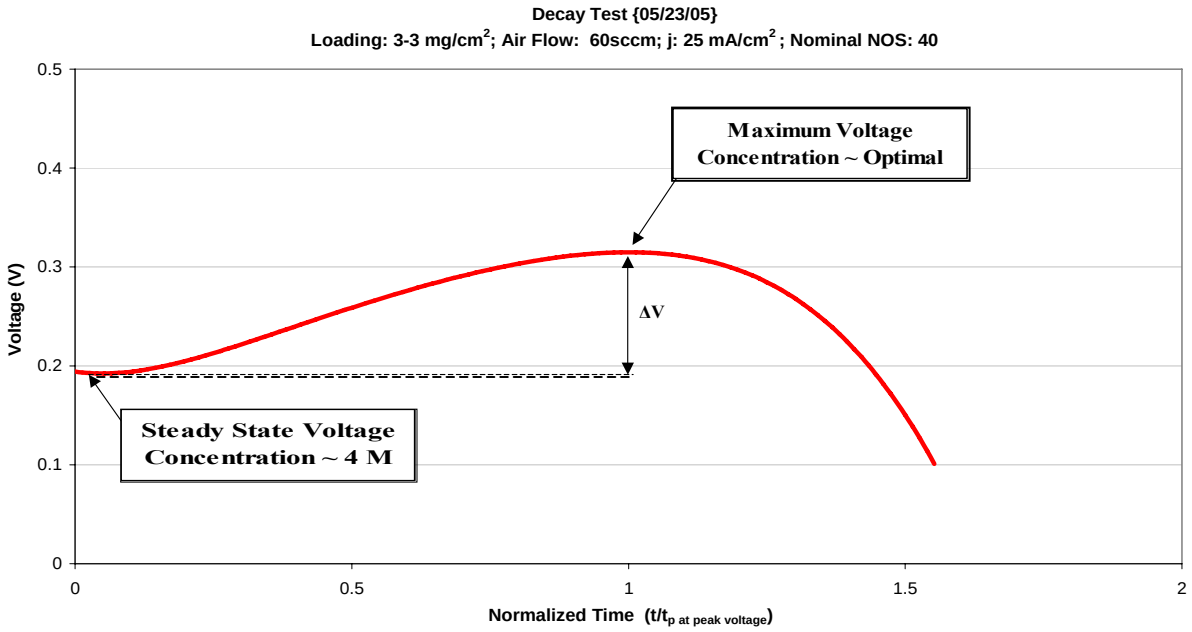

Figure 6.2: Illustration of voltage rise occurring when fuel is discontinued

The only feasible explanation for the voltage rise is methanol crossover depletion caused by a decrease in fuel concentration at the electrodes. Thus, it is plausible to hypothesize that the same maximum voltage can be obtained at steady flow operation if the fuel feed concentration is the same as that reached during the peak of the fuel discontinuation response. This steady flow response might vary due to secondary effects that occur during fuel discontinuation, such as carbon dioxide agglomeration at the electrode and convective mass transfer. The analytical/experimental measurement of the optimal concentration was beyond the scope of this work. Nonetheless, an illustration of the steady flow polarization for a *hypothetical* optimal concentration is compared to a

high concentration response in Figure 6.3. Note that, theoretically, the voltage change should be similar in magnitude to the voltage change attained when fuel is discontinued.

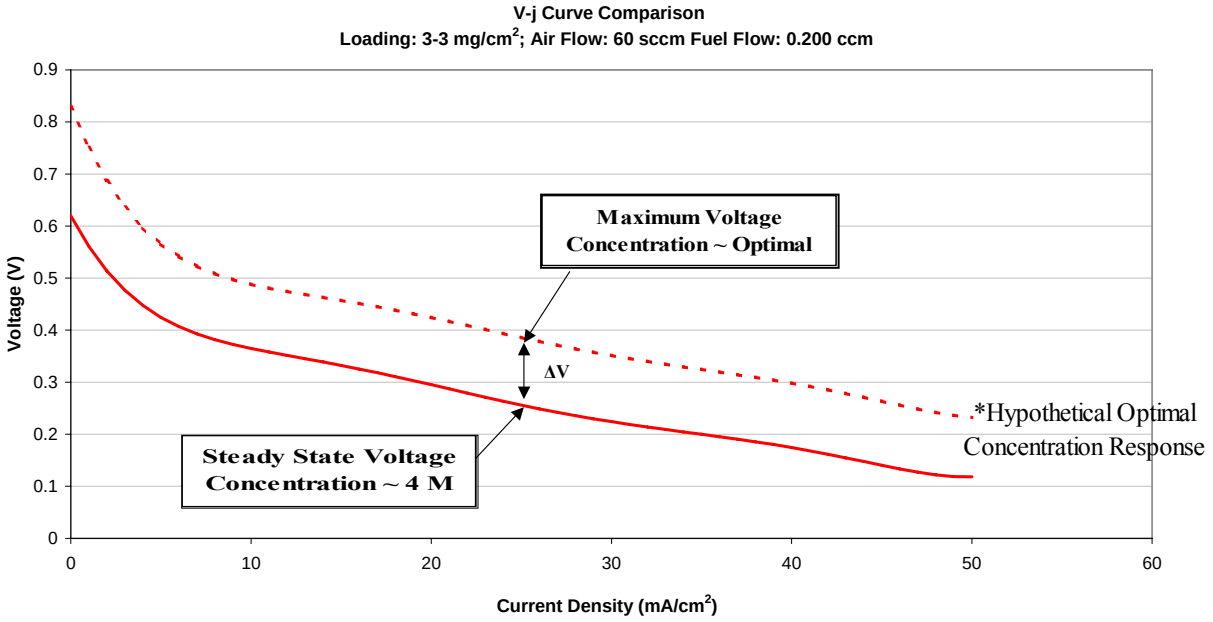

Figure 6.3: Illustration of the voltage response difference between a hypothetical optimal and actual higher concentration

To extend the analysis of this phenomenon, the cell potential response for each concentration was normalized with respect to the initial voltage (i.e., the voltage at the beginning of the fuel discontinuation test). Figure 6.4 shows the normalized cell response for each fuel feed concentration with its corresponding percentage overshoot.

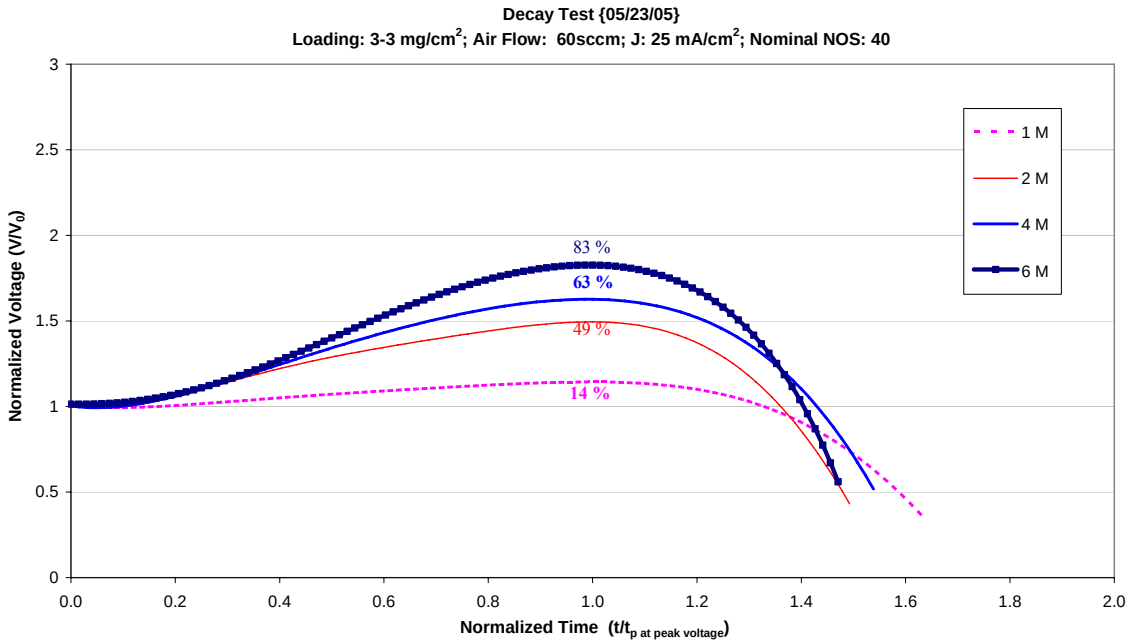

Figure 6.4: Normalized voltage plot when fuel supply was discontinued on a 3:3 mg/cm^2 loaded MEA with a 25 mA/cm^2 applied current density

As can be seen in Figure 6.4, the percentage overshoot increased with fuel feed concentration. Since more methanol crossover due to diffusion is expected at higher feed concentrations, it is again reasonable that the percentage overshoot would increase with feed concentration. In Chapter 5, it was hypothesized that the optimal concentration was between 0.5 and 2 M. However, Figure 6.4 shows that there was a 14% overshoot at 1 M. This is indicating that at 1 M there was still a significant concentration decrease needed to reach maximum voltage or the optimal concentration. Therefore, it would feasible to further suggest that the optimal concentration is between 0.5 and 1 M.

The exact same test was performed at a higher current density. Figure 6.5 shows the voltage response when various fuel mixture concentrations were discontinued with a 40 mA/cm^2 current density demand.

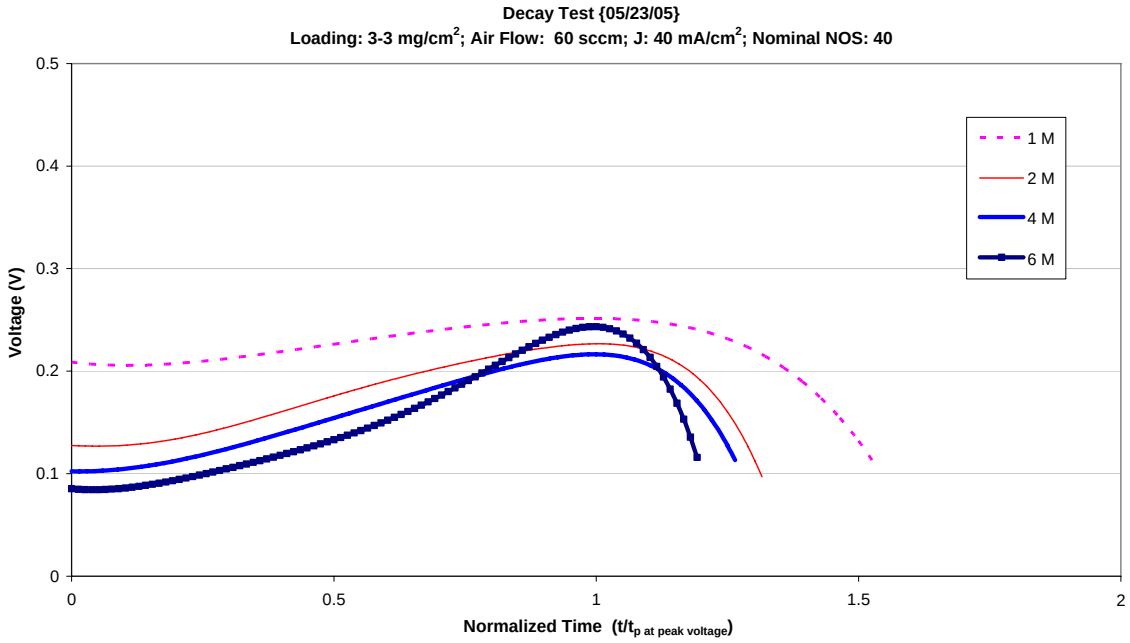

Figure 6.5: Semi-normalized voltage plot when fuel supply was discontinued on a 3:3 mg/cm^2 loaded MEA with a 40 mA/cm^2 applied current density

Similarly to the lower current density results, the initial voltage of each response was lower at the higher concentration. Again, this is the result of greater methanol crossover. The time to reach the maximum voltage, as shown in Table 6.2, was longer for the higher concentrations, while the maximum voltage for each case was about one-fifth of a volt. The overall response trend, however, was different from that observed at the lower current density. In particular, the 6-molar case had a relatively faster response and higher maximum voltage than the 2 and 4-molar cases. While it is believed that the

dominant phenomenon occurring during the fuel discontinuation is methanol crossover depletion, there are secondary effects (e.g., differing bubble agglomerations) causing the responses to somewhat deviate at different current densities. Specifically, current density electrochemically produces more carbon dioxide, and thus presumably greater agglomeration, on the fuel stream side. Fuel discontinuation trends of voltage versus time may thus be more influenced by two-phase flow effects.

Table 6.2: Maximum voltage and time data from fuel discontinuation of a 3-3 mg/cm^2 loaded MEA with a 40 mA/cm^2 applied current density

Concentration (M)	**V_{max} (V)**	**t_{Vmax} (min)**
1	0.25	2.4
2	0.23	4.6
4	0.22	4.9
6	0.25	6.6

The effect of the catalyst loading on the fuel discontinuation cell response was analyzed by testing two different loadings. The results, shown up to this point, have been for a 3:3 mg/cm^2 loaded MEA. Similar testing was performed on a MEA with a 4:4 mg/cm^2 catalyst loading. The fuel discontinuation cell response at various methanol concentrations and the normalized voltage plot for a 4:4 mg/cm^2 catalyst loading are shown in Figure 6.6 (a) and (b), respectively. The current density demand was 25 mA/cm^2.

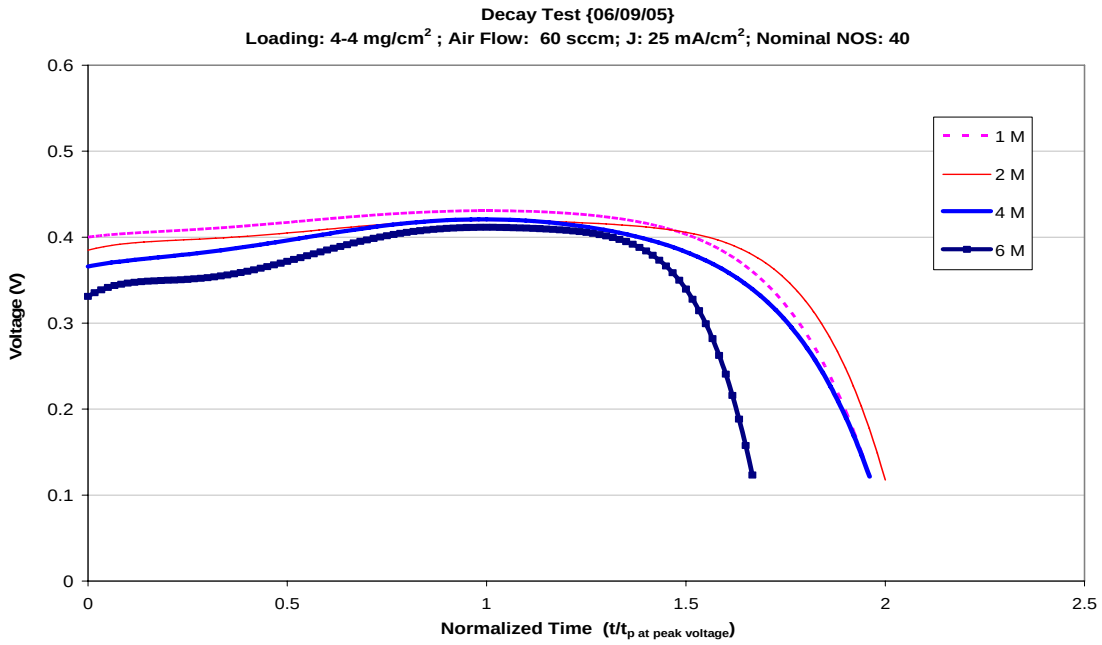

Figure 6.6(a): Semi-normalized voltage plot when fuel supply was discontinued on a 4:4 mg/cm^2 loaded MEA with a 25 mA/cm^2 applied current density

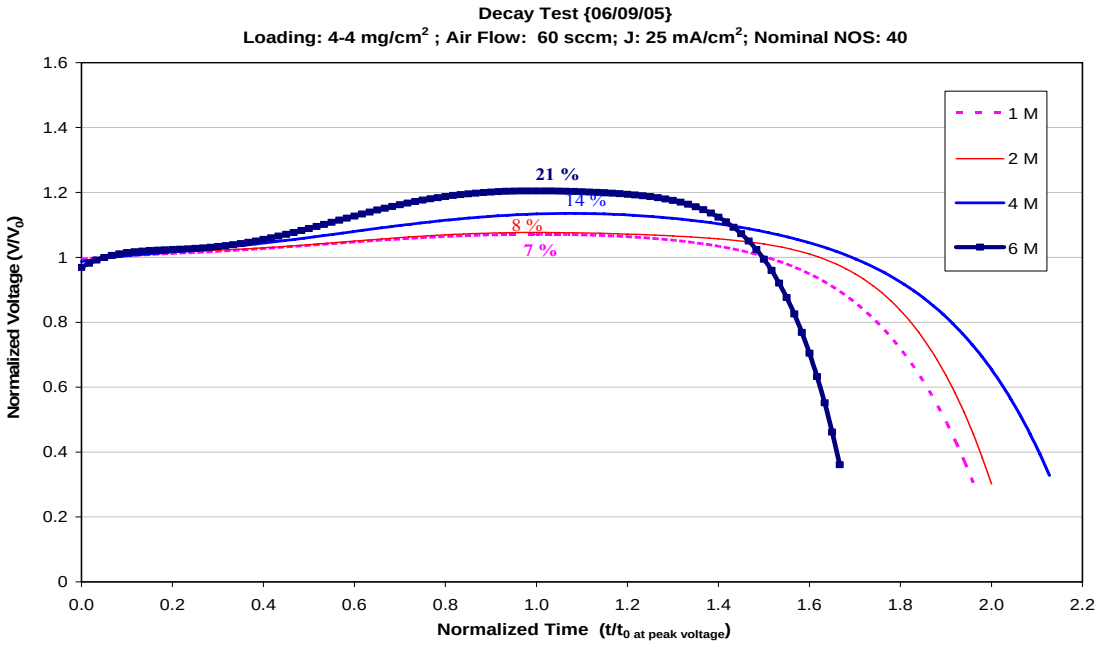

Figure 6.6(b): Normalized voltage plot when fuel supply was discontinued on a 4:4 mg/cm^2 loaded MEA with a 25 mA/cm^2 applied current density

The polarization curves presented in Chapter 5 showed that the higher loadings had a significantly better performance than the lower catalyst loadings. Since the activation polarization was significantly lower at this higher catalyst loading, the fuel discontinuation cell response, as shown in Figure 6.6, was expected to have lower percentage overshoot at each concentration in comparison to the lower loading results. This is not necessarily the result of less methanol crossover occurrence, but possibly due to better electrochemical kinetics. As shown in Figure 6.7, the initial voltage of the higher catalyst loading was significantly higher than the lower loading. Again, this is predominantly due to lower activation energy required for the half-reactions to occur. Nonetheless, the hypothesis presented in some literature that there is less methanol permeation at the higher loading may also be true, and thus may have an impact on the observed results.

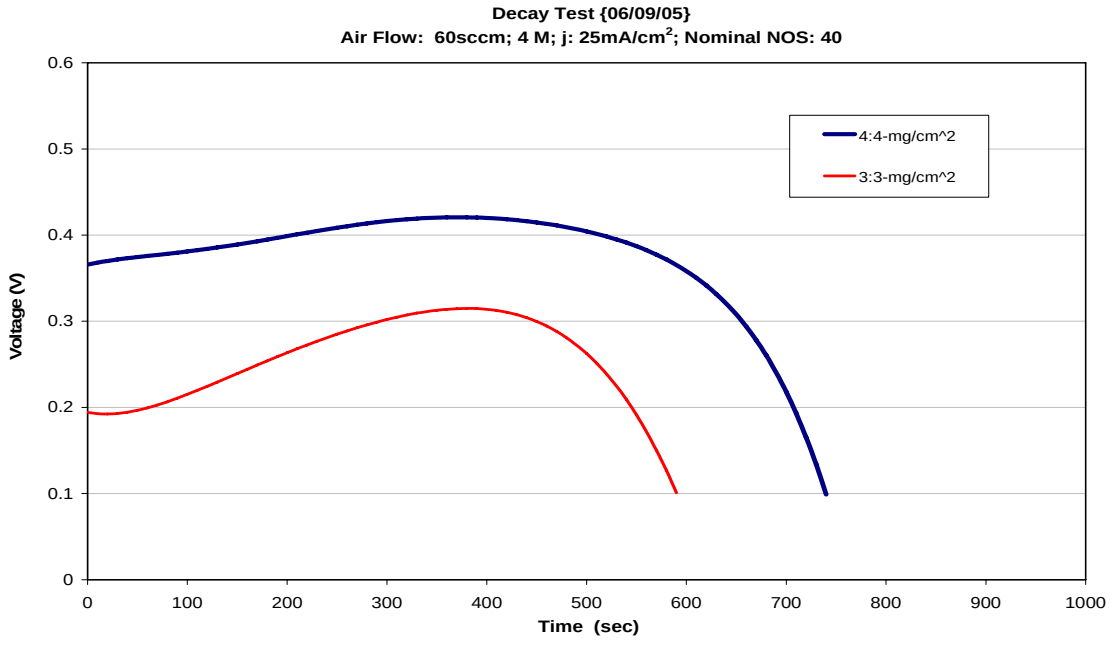

Figure 6.7: Cell response when fuel supply was discontinued on a 4:4 and 3:3 mg/cm^2 loaded MEA with a 25 mA/cm^2 applied current density

6.2 Influence of Current Density

Figure 6.8 shows the voltage response for a fuel feed concentration and NOS of 2M and 40, respectively. The current densities tested were 10, 25, and 40 mA/cm^2.

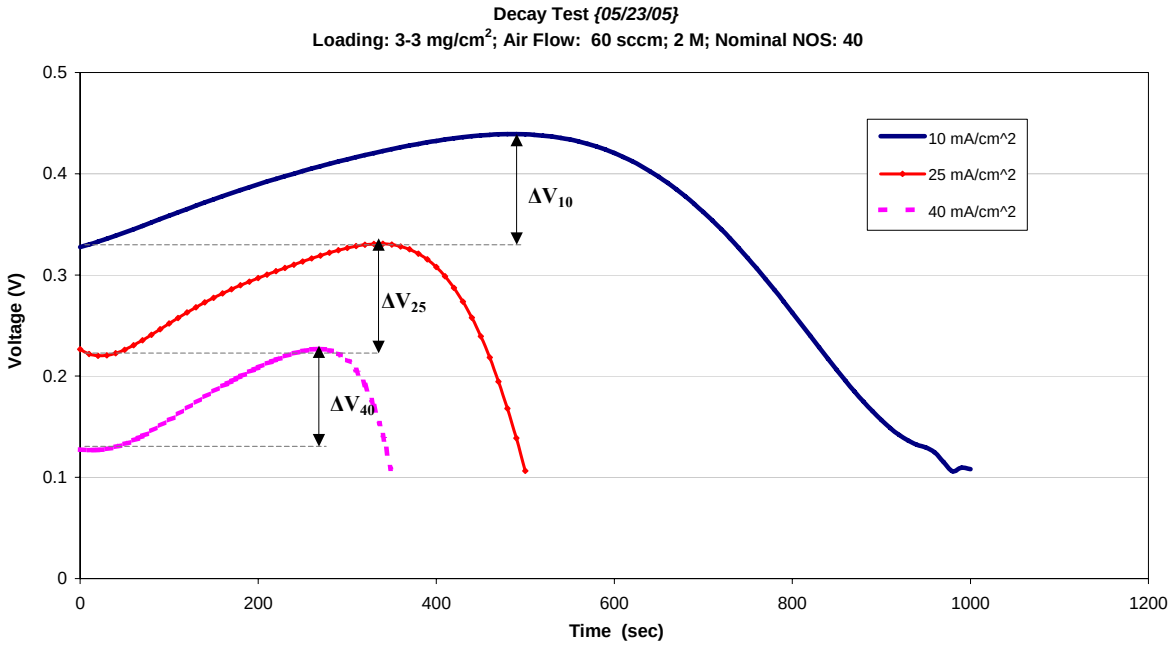

Figure 6.8: Cell response when fuel supply was discontinued on a 3:3 mg/cm^2 loaded MEA with a 10, 25, and 40 mA/cm^2 applied current density

As it was expected, the initial and maximum voltages were lowest for the largest current density demand. Furthermore, the time to reach maximum voltage was less for the higher current densities due to the higher reaction rates enabling faster concentration depletion at the electrode. In theory, methanol permeation in DMFCs is never completely eliminated, even at the optimal concentration. However, at lower current densities there is conceptually more methanol crossover because the lower reaction rates allow for a greater methanol concentration at the anode three-phase region. Based on this reasoning,

it is believed that for a given fuel feed concentration, a maximum methanol crossover occurs at open circuit voltage (i.e., when no load is applied).

An important parameter shown in Figure 6.8 is the voltage change from the initial to the maximum voltage for each current density. This voltage change, to some extent, can be a correlated measurement of the amount of methanol crossover reduction. The voltage change for 25 and 40 mA/cm^2 at different concentrations is shown in Figure 6.9.

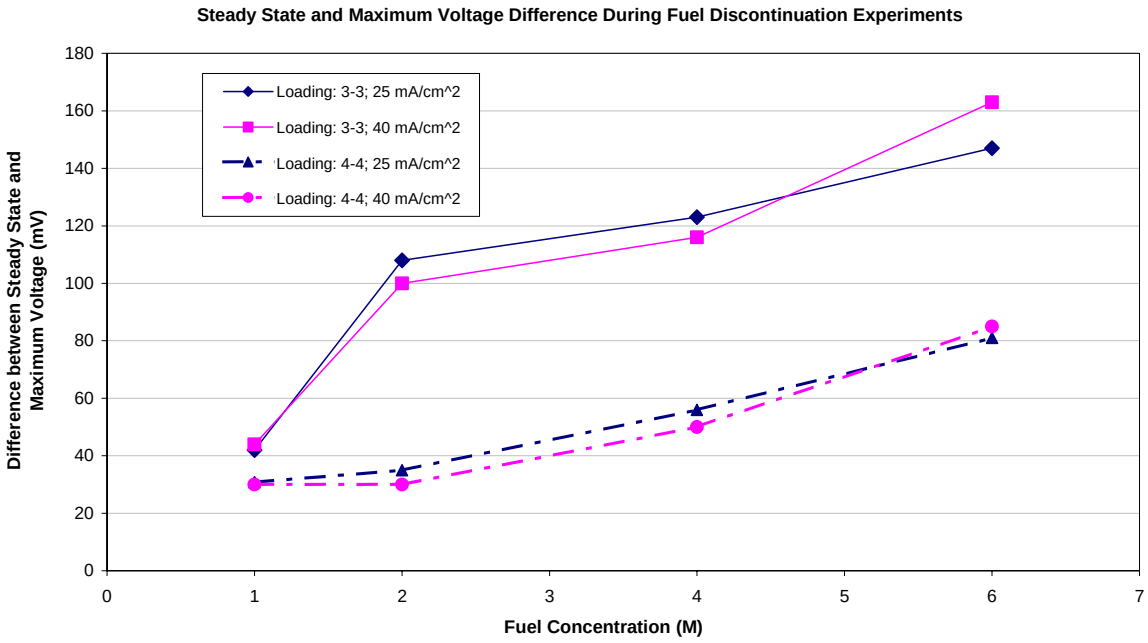

Figure 6.9: Voltage difference comparison of a 3:3 and 4:4 mg/cm^2 loaded MEA at 25 and 40 mA/cm^2 applied current density

The disparities between the voltage change of 25 and 40 mA/cm^2 were less than 6% at the various concentrations. However, it is interesting, as shown in Figure 6.8, that very similar trends were observed at the two different catalyst loadings. The voltage change

for the two loads was very similar at 1-molar. Meanwhile, the 25 mA/cm^2 voltage change was slightly larger than the 40 mA/cm^2 at 2 and 4 molar but smaller at 6-molar.

When the voltage changes were very close, it would indicate that the amount of methanol crossover depletion, in magnitude, were very similar for each concentration. On the contrary, a noticeable difference in voltage change could possibly lead to the conclusion that there was less methanol crossover depletion during one of the current density tests and/or that secondary effects had a greater impact on the response. Since the test was performed at a constant NOS, the flow rate for each current density case was significantly different due to differing fuel stream concentrations. This flow rate deviation could cause noteworthy differences of carbon dioxide agglomeration at the anode and convective mass transfer when fuel was discontinued.

Based on the obtained results, it is reasonable to conclude that, in general, the same amount of methanol concentration/crossover reduction occurred for given initial concentrations. Again, the relatively small deviations in voltage change for variable current densities are believed to be a result of secondary effects occurring during the fuel discontinuation phase. Therefore, the voltage rise is primarily a function of fuel feed concentration and cell design (e.g., MEA thickness and active area).

The methanol crossover ratios of the two current densities are nearly uniform at tested concentrations, with the lower current density always having the greater methanol crossover. However, it is important to note that, for the given cell and operating conditions, 25 and 40 mA/cm^2 were current densities within the ohmic polarization region. Current densities corresponding to the activation and concentration polarization

regions might result in different behaviors than the presented loads, primarily due to the impact of the associated polarizations.

Figure 6.10 shows the normalized voltage plot for 10, 25, and 40 mA/cm^2 at a feed concentration and NOS of 2 M and 40, respectively.

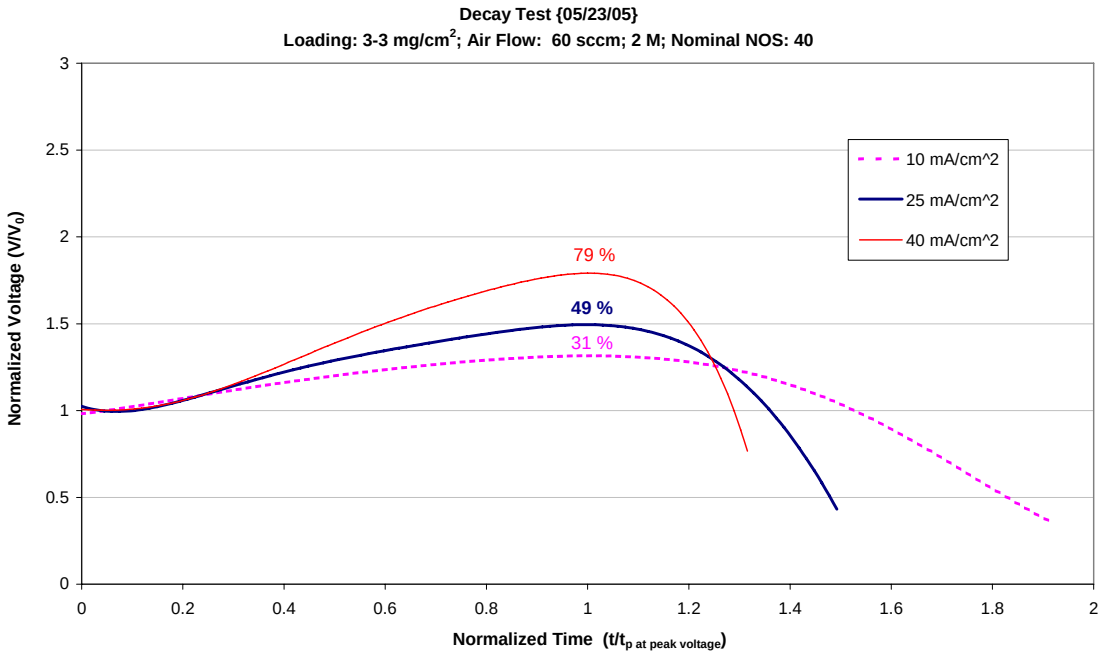

Figure 6.10: Normalized voltage plot when fuel supply was discontinued on a 3:3 mg/cm^2 loaded MEA at various current densities

As can be observed from Figure 6.10, the percentage overshoot increased with current density. Since the absolute voltage change was almost the same *(ref. Fig. 6.8)* for each current density, the highest current density, which results in the lowest *initial* voltage, would be significantly more affected than the other current densities. In some literature, it has been reported that a slightly lower percentage overshoot was observed at higher current densities (Mench, 2005). The literature attributed the results to the greater

steady state methanol crossover at the lower current density in comparison to the higher load, thus allowing the lower current density to deplete more methanol crossover. The reason for the discrepancy between the present results and those of the literature is not fully clear. However, there are several factors that can directly affect the response during the fuel discontinuation test, such as operating temperature and type/size of MEA. These two aspects were different between this work and that of the literature.

Figure 6.11 shows the percentage overshoots at a current density of 25 and 40 mA/cm^2 for various fuel feed concentrations. As stated previously, the percentage overshoot at a particular current density increased with feed concentration; since there is greater methanol permeation at higher feed concentrations.

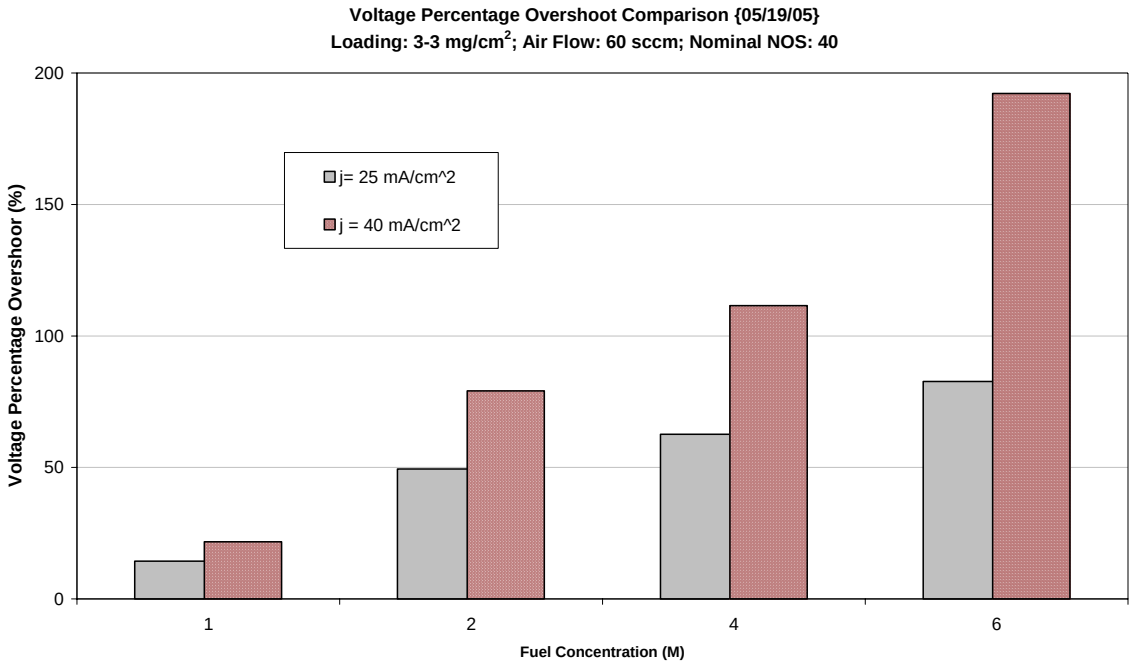

Figure 6.11: Comparison of the voltage overshoot at j= 25 and 40 mA/cm^2 for a 3:3 mg/cm^2 catalyst loading DMFC

The same analysis was performed for the higher catalyst loading (i.e., 4:4 mg/cm^2), and the results are shown in Figure 6.12. In comparison to the lower catalyst loading, the percentages overshoot were significantly lower. This could have been caused by either lower methanol crossover rates or simply the result of lower activation polarizations. At 6-molar, there was a significant difference between the two current densities' overshoots, as expected. However, the same was not observed for the other feed concentrations (i.e., 1, 2, and 4 molar) where the percentage overshoots were almost identical at the lower and higher current densities. This could be the result of lower methanol crossover and/or the lower activation polarization promoting a smaller deviation between the initial voltages at the given loads.

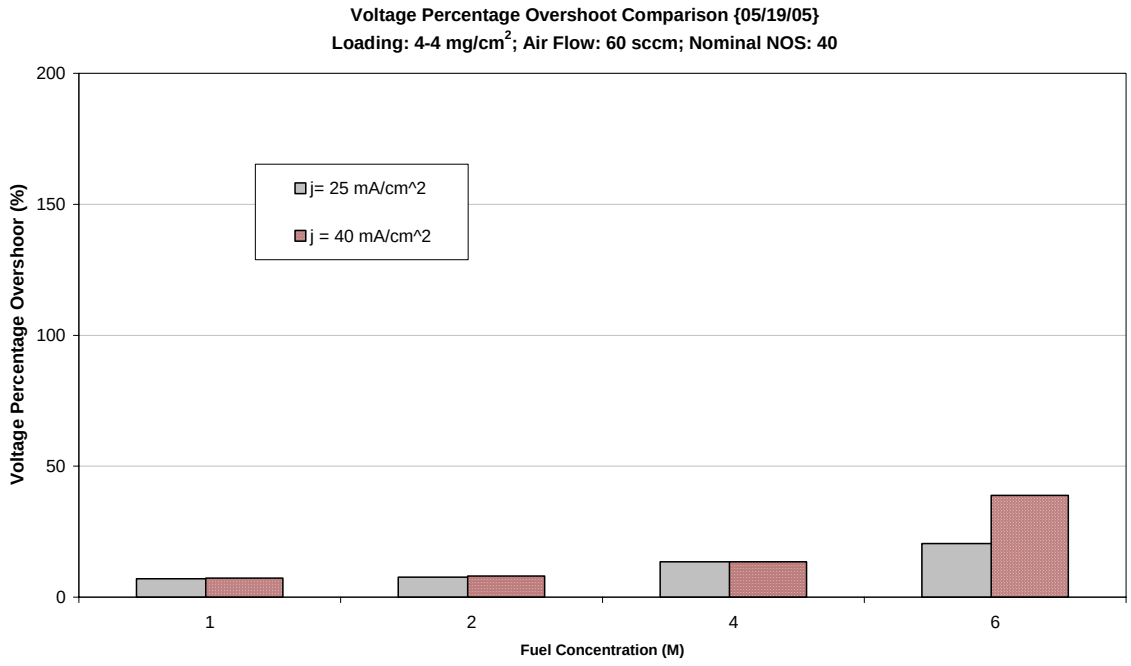

Figure 6.12: Comparison of the voltage overshoot at j= 25 and 40 mA/cm^2 for a 4:4 mg/cm^2 catalyst loading DMFC

6.3 Influence of fuel NOS

The stoichiometry (i.e., NOS) at a given feed concentration and current density can have a significant effect on methanol crossover via changes in convective mass transfer. Furthermore, the fuel flow rate directly influences the carbon dioxide (CO_2 bubbles) removal rate at the anode, which would ultimately have an effect on the fuel discontinuation response. The fuel discontinuation cell responses at various NOS values are presented in Figure 6.13. The current density and feed concentration were kept constant at 25 mA/cm^2 and 2 M, respectively. Due to the limited flow control in the system, only NOS values of 10, 20, 40 and 60 were tested. 2 M was the only feasible feed concentration for these desired NOS values.

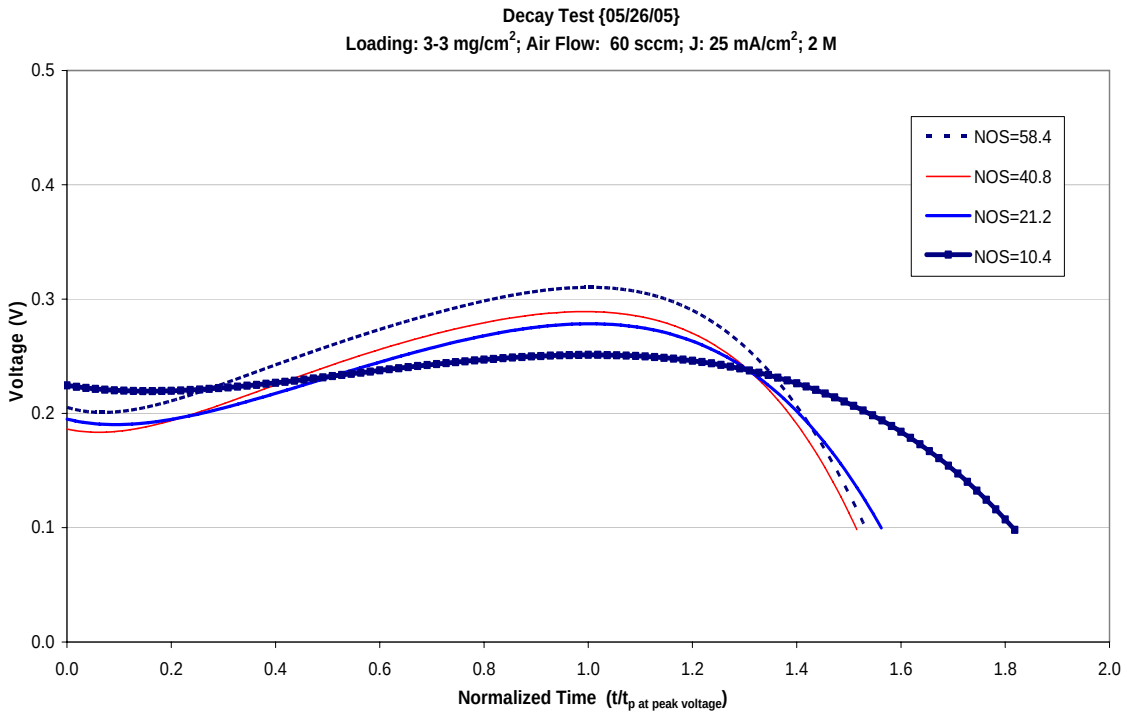

Figure 6.13: Semi-normalized voltage plot when fuel supply was discontinued on a 3:3 mg/cm^2 loaded MEA at various NOS values

As can be observed from Figure 6.13, the voltage response varied when fuel feed was discontinued at various NOS values. The lowest NOS value or fuel flow rate showed the highest initial voltage. This is possibly indicative of the less amount of methanol crossover occurring at this lower flow rate, which is plausible considering a potentially smaller convective mass transfer coefficient within the lower Reynolds number fuel stream. Note, however, that smaller NOS (hence flow rate) values probably also indicate less effective carbon dioxide bubble advection. The initial voltage for the NOS values of 20, 40 and 60 did not show a specific trend. Again, an unknown mix of methanol crossover and CO_2 bubble removal could have affected the response at these NOS values. For example, the initial voltage at NOS of 60 is hypothesized to have been the lowest if there was no bubble formation; however, CO_2 bubbles, which can obstruct active catalytic sites, are being removed at a faster rate prior to fuel discontinuation when the NOS is higher. This may be the reason the initial voltage at NOS of 60 is higher in comparison to initial voltages at NOS values of 20 and 40. Also note the trend that higher NOS values led to higher maximum voltages.

An important aspect shown in Figure 6.13 is the lack of a common maximum voltage. This could be predominantly due to the flux in CO_2 bubble removal prior to fuel discontinuation. In order to better analyze this behavior, a normalized plot is shown in Figure 6.14. The lowest NOS showed the lowest percentage overshoot, presumably due to the lower amount of methanol crossover. The interesting non-monotonic behavior occurs at the higher NOS values, where both methanol crossover and bubble removal could be affecting the voltage response.

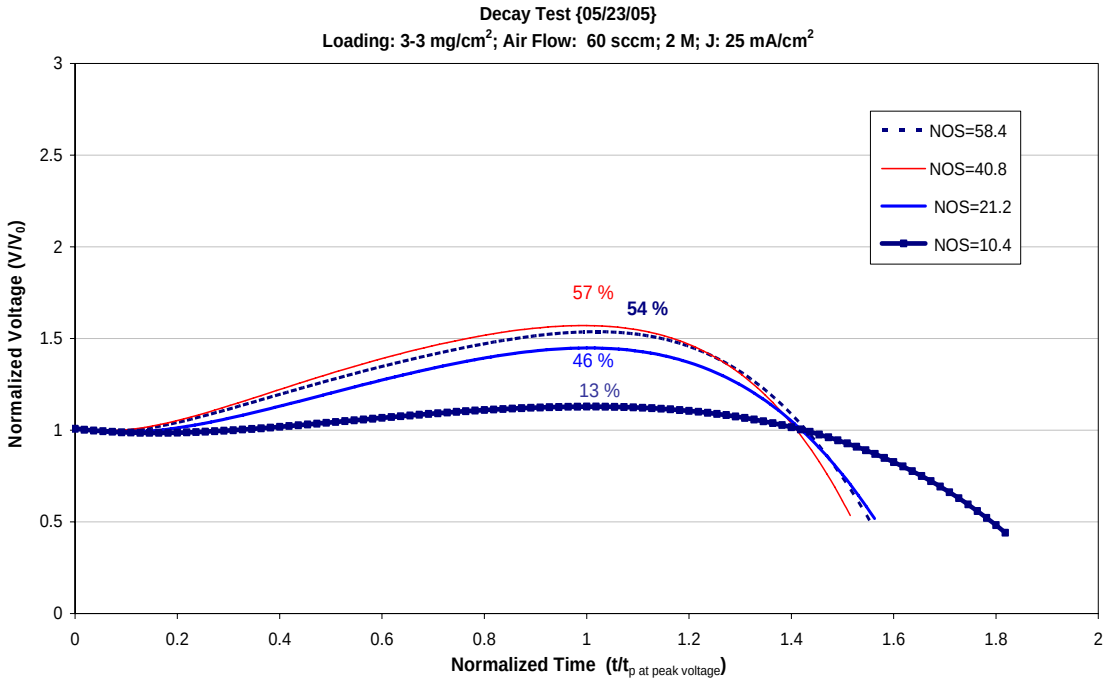

Figure 6.14: Normalized voltage plot when fuel supply was discontinued on a 3:3 mg/cm^2 loaded MEA at various NOS values

6.4 Influence of Cell Degradation

Fowler *et al.* (2002) reported that the degradation of DMFCs can be attributed to three main factors, and they are listed below.

- Loss of apparent catalytic activity
- Conductivity Loss
- Loss of mass transfer of reactants

While each of these factors can separately contribute to fluctuation in the cell response when fuel is discontinued, the catalytic activity losses are more likely to have a greater effect on the response and particularly on the amount of methanol crossover. One of the

causes of this activity loss is the reduction of catalyst surface area throughout the cell operational life, wherein catalytic reactant sites are rendered inactive (Fowler, 2002). Figure 6.15 shows the polarization curve for a 4:4 mg/cm^2 MEA at different stages of its lifetime.

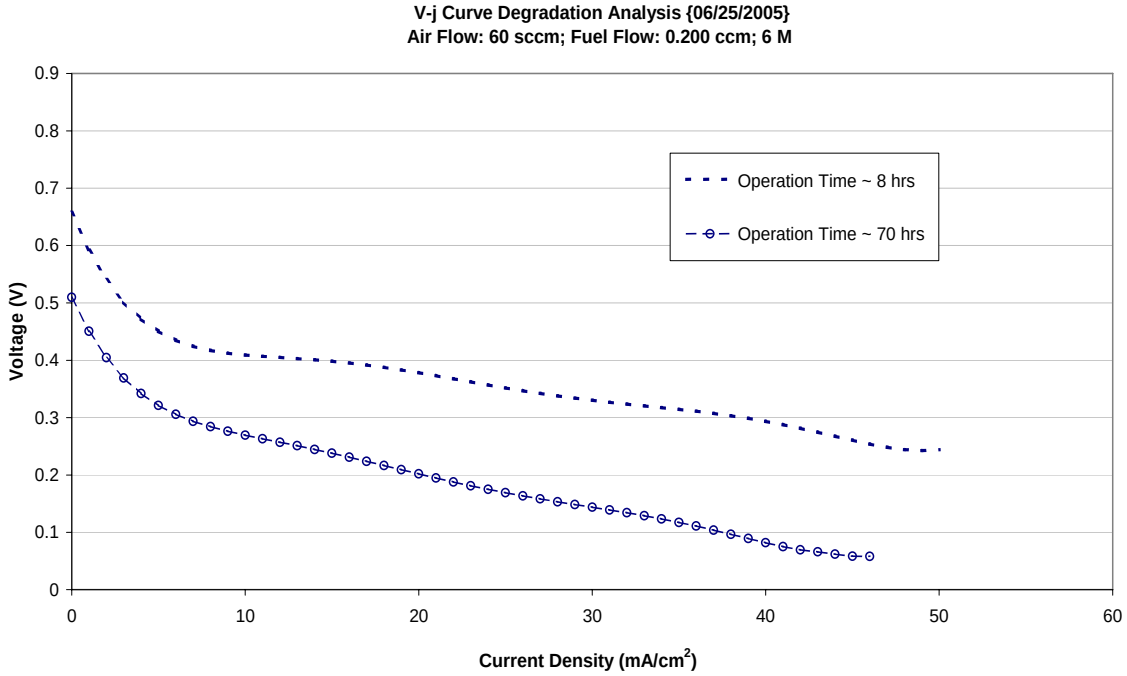

Figure 6.15: Degradation analysis-V-j curve for 4:4 mg/cm^2 loaded MEA

After about 70 hours of operation, the cell performance was significantly degraded. The methanol crossover impact of the overall degradation was analyzed by performing the fuel discontinuation test during these two lifetime stages. Figure 6.16 shows the fuel discontinuation cell response after 8 and 70 hours of operation. The current density and feed concentration were 40 mA/cm^2 and 6 M, respectively.

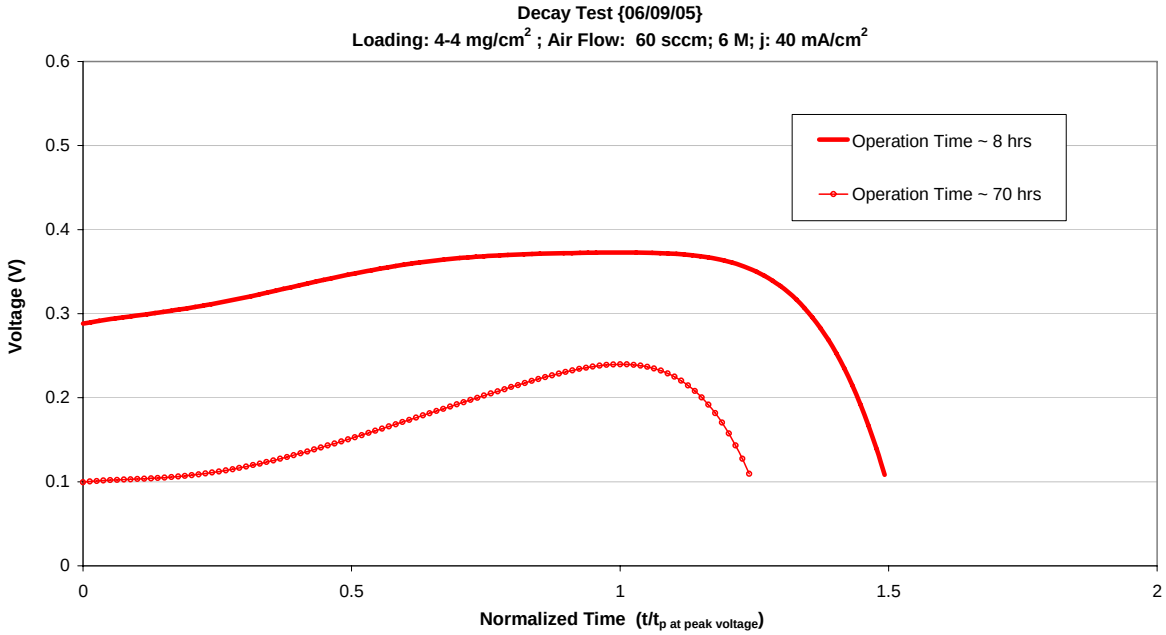

Figure 6.16: Comparison of semi-normalized response when fuel supply was discontinued on a 4:4 mg/cm^2 loaded MEA after different hours of operation

As can be observed from Figure 6.16, the initial and maximum voltage decreased with operation due to the cell's degradation. As a result, the effectiveness of boosting cell potential via purposeful reduction of fuel supply may be significantly greater for the degraded cell. Thus, the fuel discontinuation process is very likely more beneficial when the cell has degraded. However, the degradation level of a particular DMFC is very difficult to predict. Figure 6.17 is the normalized plot of the above responses wherein the greater voltage enhancement for the degraded cell is observed.

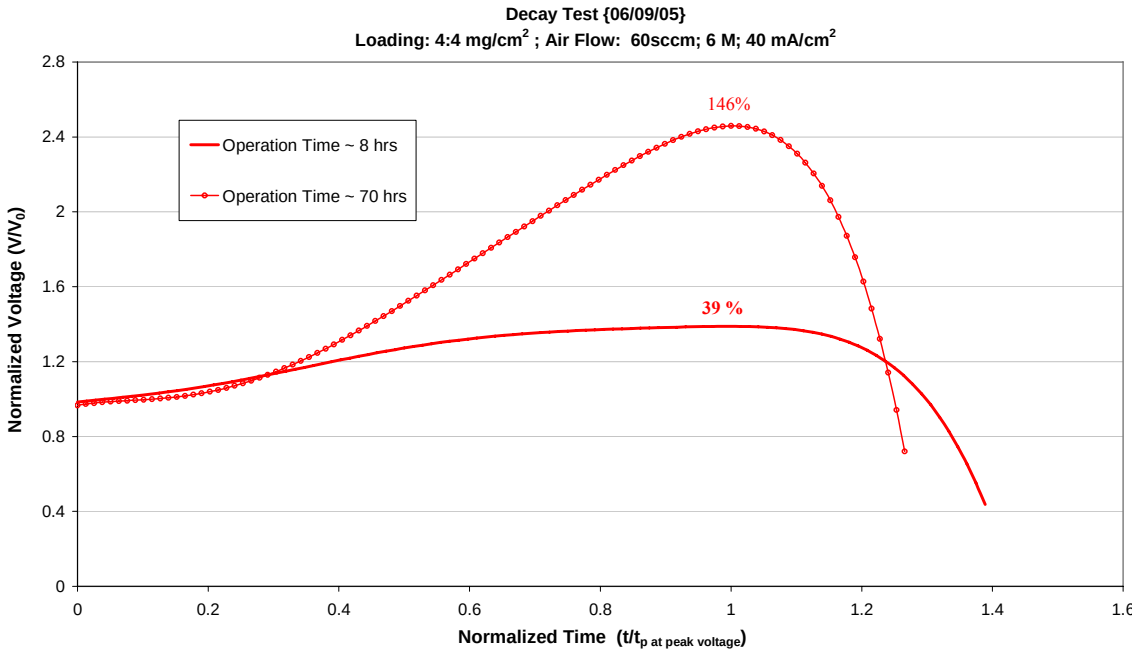

Figure 6.17: Comparison of normalized response when fuel supply was discontinued on a 4:4 mg/cm^2 loaded MEA after different hours of operation

The percentage overshoot increased with cell operation time. The greater percentage overshoot is indicative of larger-scale methanol crossover depletion, given degraded cells. Since the operating conditions were identical for each scenario, a corollary hypothesis is that at the longer cell operation time there was more methanol crossover occurrence.

6.5 Summary

During steady flow DMFC operation, it was resolved that when fuel flow was temporarily discontinued there was a significant voltage enhancement primarily due to a reduction in methanol crossover. Fuel feed concentration, current density, stoichiometry

and cell degradation were investigated as to their individual impacts upon such enhancement. For the tested methanol concentrations, a common maximum voltage was attained during fuel discontinuation. This is indicative of an optimal lower concentration reached after the discontinuation, which balanced the reduced methanol crossover effect against heightened concentration polarization. As a result, a greater voltage enhancement was achieved at higher feed concentrations due to the associated high initial methanol crossover. While there was more methanol crossover at lower current densities, the same crossover depletion was observed at the various current densities tested. Thus, it is plausible to hypothesize that the crossover depletion phenomenon was primarily a function of fuel feed concentration. However, it was found that the NOS (i.e., flow rate stoichiometry) also had a noticeable impact on the transient response, possibly through a combination of changes in CO_2 agglomeration at the anode and convective mass transfer of methanol. Additionally, it was observed that a degraded cell resulted in a more effective voltage enhancement during fuel discontinuation.

In conclusion, the voltage efficiency of a DMFC can be significantly increased with the implementation of a fuel flow pulsing scheme wherein a voltage increase is attained when fuel is temporarily discontinued.

7. Experimental Results of Continuous Fuel Flow Pulsing

During the fuel discontinuation analysis, it was found that the cell potential increased after the fuel supply was temporarily discontinued. Based on these results, a hydraulic pulsing scheme was developed in order to investigate the overall transient fuel cell performance at various feed concentrations.

The motivation for continuously pulsing the fuel supply was to potentially increase the voltage and fuel efficiency of the cell. As found previously, a voltage efficiency enhancement may be attained when local anodic methanol concentration (leading to crossover) is depleted during the fuel discontinuation phase. The present work focused on analyzing the voltage efficiency difference between a transient and steady flow fuel feed operation, wherein the same average flow rate of fuel was supplied in each case.

An *ideal* hydraulic pulsing scheme, as illustrated in Figure 7.1, would consist of a relatively small percentage duty cycle and a large period per cycle, allowing the response to reach a maximum during fuel discontinuation while maintaining significantly high fuel efficiency. The temporary fuel discontinuation time, which is denoted as “b” in Figure 7.1, would be the time required for the response to reach the maximum voltage (i.e., for a given set of operating conditions) that was observed during the previous fuel discontinuation experiments. The influence of the fuel supply time “a” on the overall transient response will be analyzed later in this chapter.

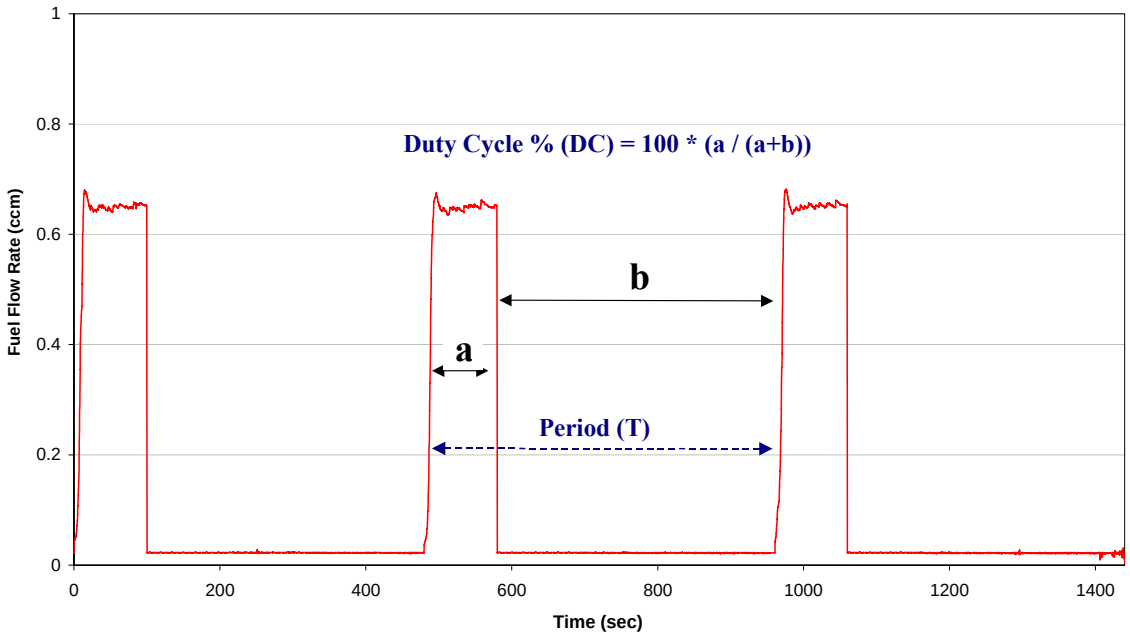

Figure 7.1: Illustration of a hydraulic pulsing scheme with its respective duty cycle percentage and period

7.1 Transient Response Characterization

Figure 7.2 (a) shows the overall voltage response to a hydraulic pulsing scheme with a duty cycle (DC) of 37.5% and period (T) of 480 sec/cycle. The current density and feed concentration were 25 mA/cm^2 and 2 molar, respectively. In order to better examine the result, the voltage response during only one of the cycles is shown in Figure 7.2 (b).

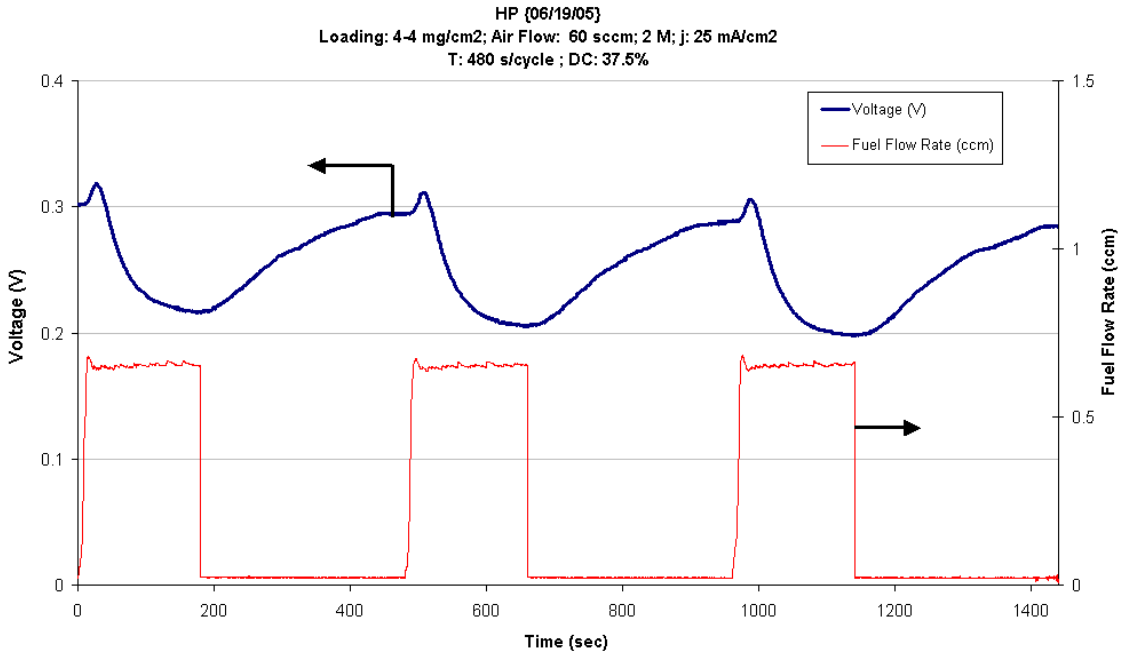

Figure 7.2 (a): Voltage response with pulsed fuel flow (DC: 37.5%; T: 480 s/cycle)

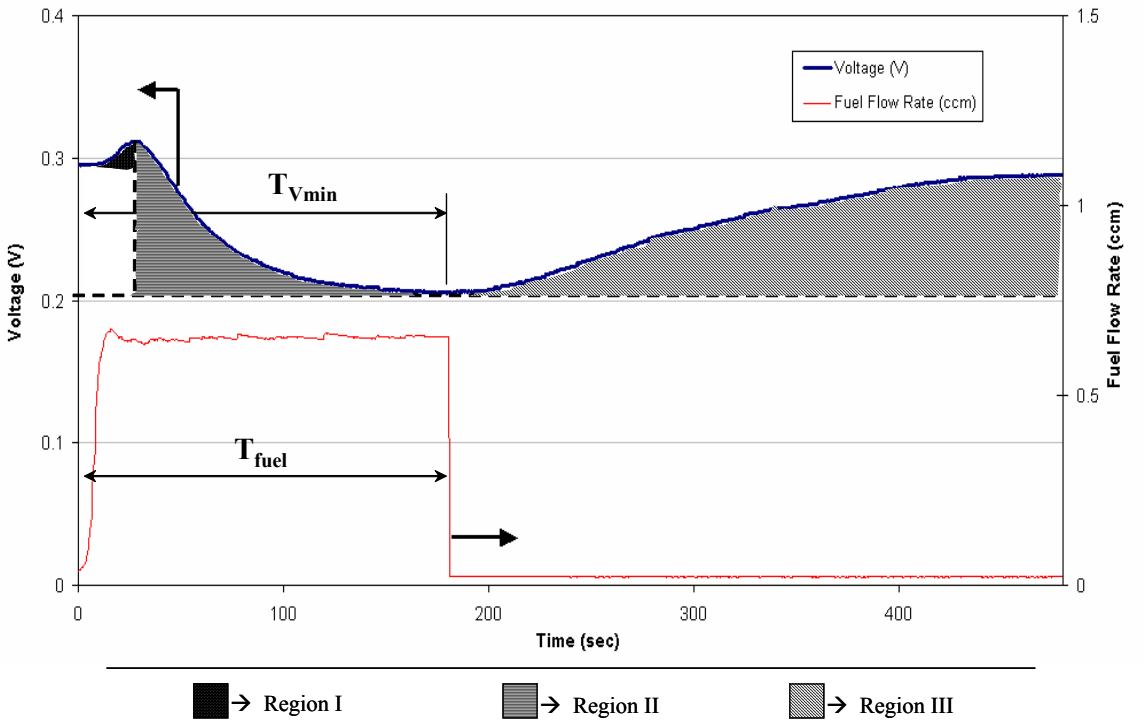

Figure 7.2 (b): Single cycle transient response with denoted distinct regions

As can be observed in Figure 7.2 (b), there are three distinct regions within the voltage response during a single hydraulic pulsing cycle. Each region, along with its respective recommended name, is listed below.

- Region I: Reactant re-institution region
- Region II: Methanol crossover restoration region
- Region III: Methanol crossover depletion region

Region I: Reactant Re-institution Region

Before the fuel feed is reintroduced into the cell, the reactant concentration at the anode has been decreased to a lower value than that of the feed. Thus, the sudden increase in reactant concentration enhances the cell response (e.g., larger Nernst potentials and limiting current densities) in this region until the detrimental methanol crossover phenomenon becomes more dominant. Another factor contributing to the response in this region may be the removal of the carbon dioxide bubbles, which could agglomerate to a larger extent at the anode layer and/or GDL when the fuel flow is discontinued. These formations obstruct the catalytic surface at the anode as well as the path of reactants to the reaction zone. Despite these initial benefits, methanol crossover is never completely alleviated and has a greater negative impact on the performance as the anode methanol concentration continues to increase. As a result, the performance enhancement in this region is very limited and relatively negligible in comparison to the other two regions within the cyclic response.

Region II: Methanol Crossover Restoration Region

When fuel was reintroduced and methanol crossover became a more dominant factor, the cell potential started to rapidly decrease until it approached the steady state voltage associated with a given fuel anodic concentration. As was discussed in Chapter 2, the amount of methanol crossover depends predominantly on the concentration at the anode, which dictates the rate of methanol diffusion from the anode to cathode. For that reason, the voltage in this region decreased until the maximum methanol crossover associated with the feed concentration was reached. As can be observed in Figure 7.3, the steady flow response of a 6-molar concentration coincided with the minimum voltage attained within region II[14].

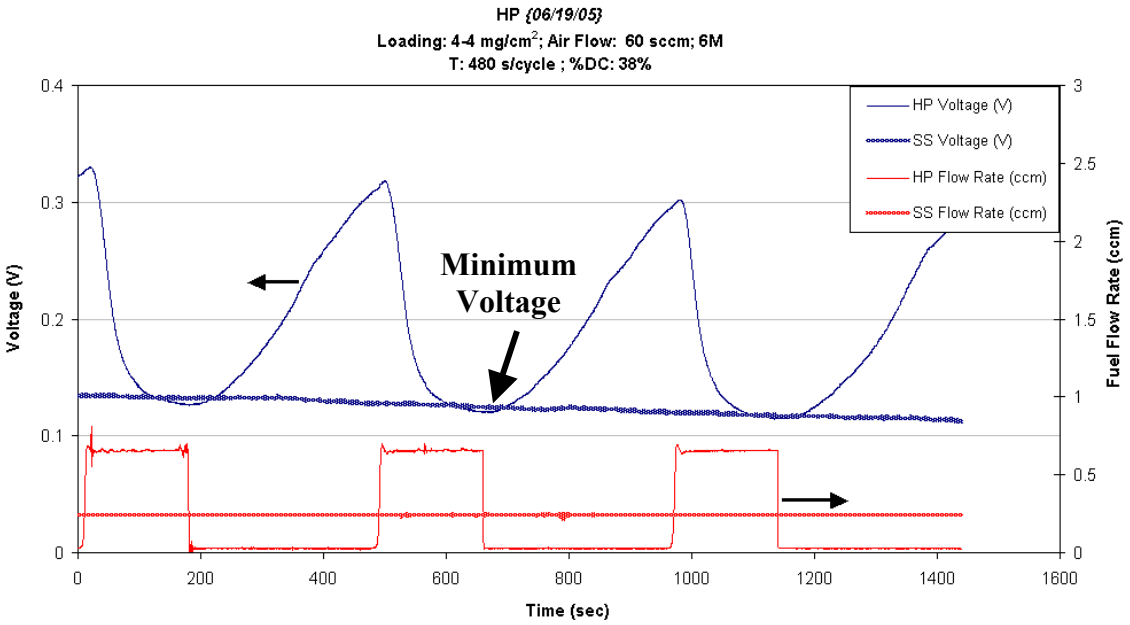

Figure 7.3: Hydraulic pulsing and steady flow response comparison with DC: 37.5 % and T: 480 sec/cycle

[14] Note that the steady flow rate will vary depending on the corresponding transient duty cycle and period.

An interesting trend observed during the hydraulic pulsing and steady supply operations is the continuous decay in overall cell potential throughout the experiment. This behavior has been attributed to the various reversible degradation mechanisms associated with DMFCs (e.g., chemical "intermediates" formation, CO_2 agglomeration at the anode and flooding of the cathode) that are functions of the operation time as well as the immediate history of the cell (Leahy, 2004). As a result of this *drift*, the region II minimum voltage is different for each cycle. Since this is a reversible phenomenon, a careful data acquisition, as discussed in Chapter 4, was required to perform the steady flow analysis presented in Chapter 5.

The dynamics of the response in this region were further analyzed by varying the duty cycle and period of the hydraulic pulsing scheme. The duty cycles tested were 12, 23 and 38 %, and the fuel discontinuation time was kept constant at five minutes per cycle. Note that a lower duty cycle and longer fuel discontinuation time were not investigated due to the fuel flow control limitations of the specific system utilized during this study. Figure 7.4 shows *only* the response within region II during a single cycle for the various pulsing schemes. The current density and fuel feed concentration were 25 mA/cm^2 and 6-molar, respectively. The slope of each response as well as the time to reach the minimum voltage is shown within the graphs.

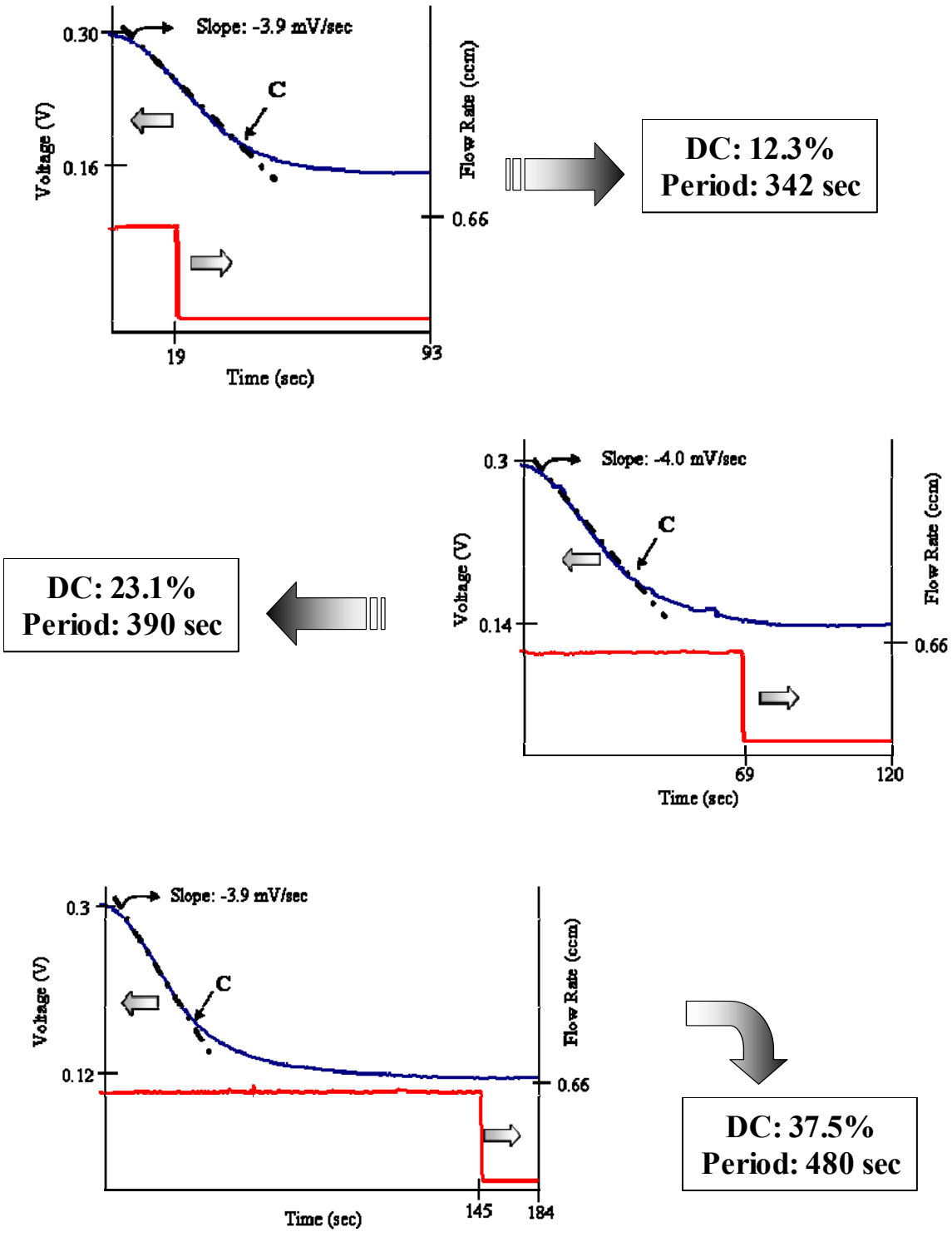

Figure 7.4 (a): Region II response for a pulsing scheme with DC of 12, 24 and 38 %

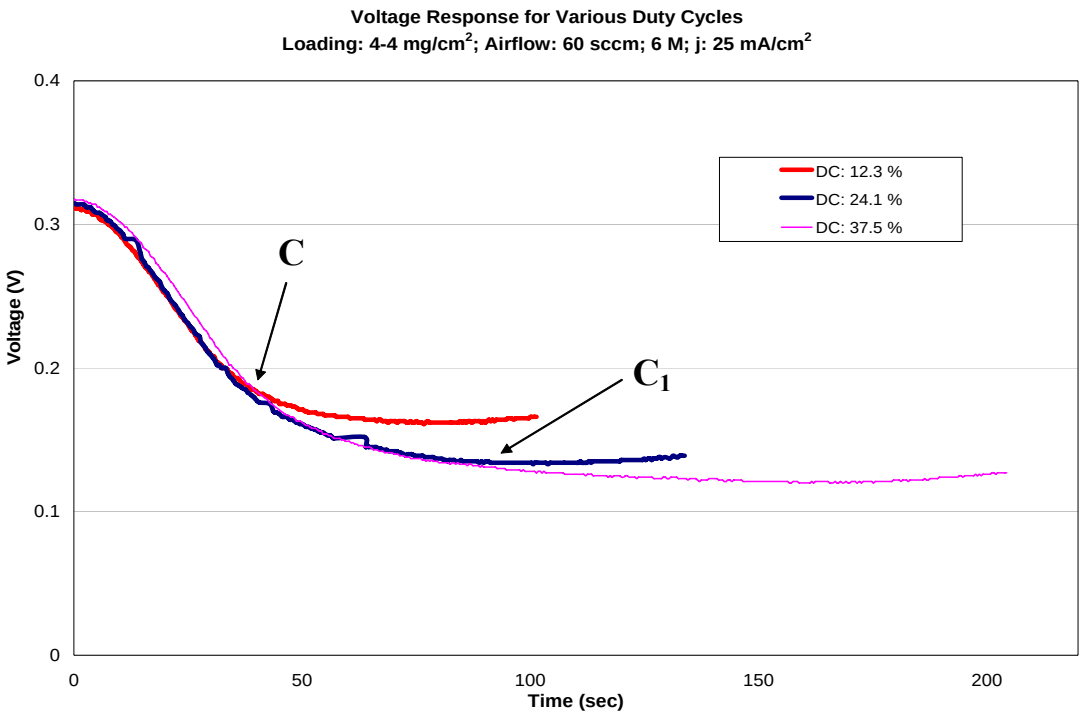

Figure 7.4 (b): Comparison of the region II voltage response for various duty cycles

As can be observed in Figure 7.4, the initial or maximum voltage for each duty cycle was approximately the same. The three responses had common voltage decays up to a certain point, which is denoted as "C" in Figure 7.4; meanwhile, the higher duty cycles continued to behave similarly until a later point "C_1". The common slope among the responses is indicative of the voltage decay dependence on the anodic methanol concentration, which itself depends on the feed concentration and current demand. Again, this rapid decay was a result of the fuel feed concentration reintroduction that caused an increase in methanol permeation. Another interesting behavior observed in Figure 7.4 (a) was the continued decay of cell potential beyond the point of discontinuation. This occurred at lower duty cycles, such as the 12.3 % plot, and is suggestive that for a given feed concentration there is a specific time constant associated with MEA methanol

permeation. Fuel discontinuation before this time constant may not immediately result in voltage rise due to an effective inertial time frame associated with Region II.

It has been reported that for a given fuel feed concentration the amount of methanol within the MEA varies from the fuel flow channel surface to the cathode catalyst layer, wherein the permeated methanol is primarily reacted[15] (Wang, 2003). Figure 7.5 shows a *hypothetical* illustration of the methanol gradient within the MEA.

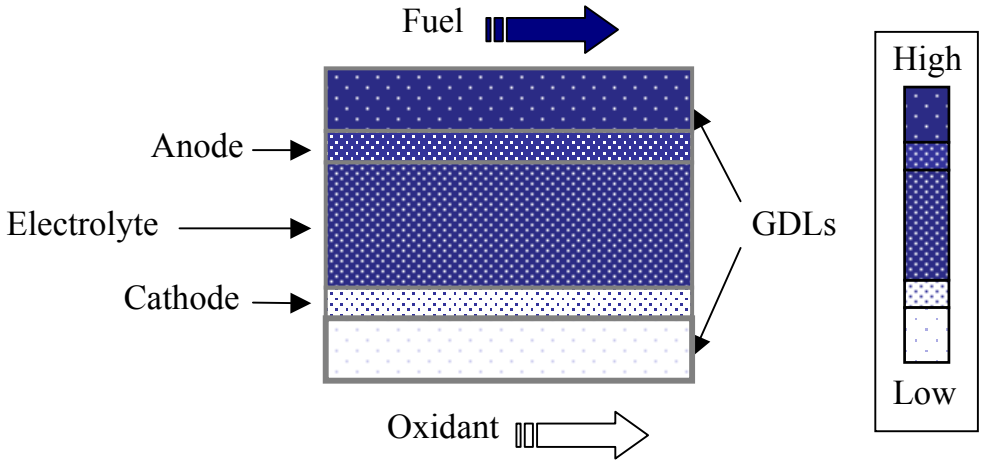

Figure 7.5: Hypothetical illustration of the methanol concentration within the MEA

Although not illustrated in the Figure 7.5 schematic, the concentration of methanol within the electrolyte actually decreases from anode to cathode (Wang, 2004). Since methanol crossover mainly occurs due to diffusion, the methanol concentration within the MEA is directly proportional to the feed concentration. Therefore, a sudden change in fuel feed concentration will consequently cause a change in methanol variation in the MEA. However, the latter change is unlikely to be instantaneous due to the internal inertia of

[15] The methanol concentration gradient from anode to cathode is due to the methanol crossover phenomenon.

methanol permeation into the MEA components, as well as methanol storage (i.e., capacitive) effects within the MEA components.

When fuel was reintroduced, the concentration at the anode flow channel, which is denoted as "A" in Figure 7.6, was suddenly increased to the feed concentration. The concentration within the GDL and electrolyte, however, gradually increased to the "would be" steady state associated with the new fuel feed. Again this is due primarily to inertial effects. Therefore, the mixed potential phenomenon at the cathode gradually increases while concentrations within the MEA increase. Similarly, the cell potential would initially continue to decay and/or remain stagnant despite the fuel discontinuation.

During the fuel discontinuation phase, the amount of methanol was decreased to the optimal concentration causing a significant voltage enhancement. Thus, the methanol permeation level was also decreased and is illustrated in Figure 7.6 (i.e., the $C_{optimal}$ profile). The feed and optimal concentration profiles, which are represented as red lines in Figure 7.6, were assumed to be linear for illustration purposes; however, a linear profile could actually occur if the operation is allowed to reach a quasi-steady state[16]. When fuel was discontinued, a transient methanol reservoir was created at the anode flow channel that was decreasing as a function of applied current density. It is possible that during the fuel discontinuation the concentration at the flow channel was decreased in a linear manner; however, the concentration within the MEA would more likely be a transient change as illustrated in Figure 7.6 (i.e., the blue lines C_1 and C_2). Again, this mainly occurs due to the internal inertia and/or capacitance of the MEA components.

[16] A complete steady state may not be attained due to the aforementioned continuous voltage "drift" associated with DMFCs.

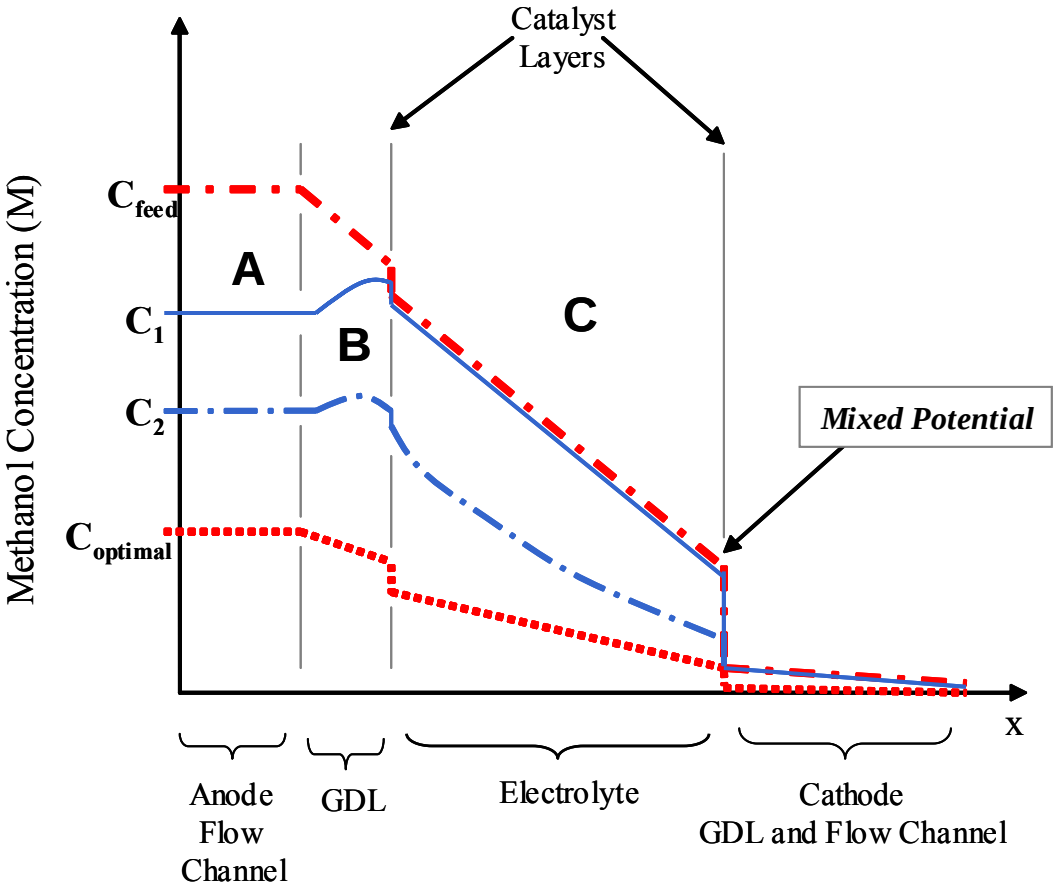

Figure 7.6: Illustration of the amount of methanol within a DMFC for a given fuel feed and the optimal concentration

During the fuel discontinuation analysis, it was hypothesized that cell potential increased when fuel flow was temporarily discontinued due to a change in methanol concentration at the anode that consequently caused methanol crossover depletion. Additionally, the present results showed that for the tested duty cycles a voltage enhancement was not necessarily simultaneous with fuel flow discontinuation. This supports the presumption that the MEA may have an "internal inertia" of MEA permeation. Therefore, a reduction of the mixed potential phenomenon was not

necessarily observed until the completion of MEA permeation (e.g., for a given pulse cycle).

This phenomenon of delayed voltage rise occurred at the lower duty cycles where the voltage continued to decay in spite of fuel discontinuation. Although, in the case of lower duty cycles, the voltage continued decaying immediately after fuel supply discontinuation; the concentration at the anode flow channel was also gradually decreasing due to fuel discontinuation. This led to lower MEA permeation levels. As a result, the minimum voltage, as listed in Table 7.1, was higher at the smaller duty cycles. This is suggestive that when the minimum voltage was reached, methanol MEA presence was still greater for the larger duty cycles.

Table 7.1: Region II pulsing data for various duty cycles

Duty Cycle (%)	**V_{min} (V)**	**t_{Vmin} (sec)**	**t_{Vmin}/t_{fuel}**	**t_{Lag} (sec)**
38	0.11	184	1.15	24
23	0.14	120	1.65	25
12	0.16	93	5.03	22

The time for each duty cycle to reach minimum voltage, as well as its ratio to the fuel supply time, is also listed in Table 7.1. The ratio of the minimum voltage time to the fuel supply time increased with lower duty cycles. As mentioned previously, this trend is thought to be due to the continued internal inertia of the MEA permeation. At the higher duty cycle, however, it was assumed that the membrane was already completely permeated with methanol before fuel discontinuation. Nonetheless, Fig. 7.6 shows that for larger duty cycles fuel discontinuation was still characterized by an increment of

unchanging cell potential, which indicates that there was a lag time, or capacitive effect, preceding the voltage enhancement (i.e., aside from the dynamic permeation inertia). The lag time for each duty cycle was found to be about twenty seconds and is possibly a representative capacitive time constant regarding reduction in MEA methanol presence.

In order to further investigate the dynamics of the response within region II, a hydraulic pulsing scheme consisting of a twenty-three percent duty cycle was tested on a 4-4 mg/cm^2 loaded MEA for different feed concentrations. Table 7.2 lists the data from the hydraulic pulsing tests at the various concentrations.

Table 7.2: Region II pulsing data for various concentrations

Concentration (M)	**V_{min} (V)**	**t_{Vmin} (sec)**
1	0.362	120
2	0.353	113
4	0.338	107
6	0.142	94

As was expected, the minimum (steady state) voltage decreased with feed concentration due to greater methanol crossover. In agreement with the results presented in Chapter 5, the steady state voltage difference among the lower concentrations was relatively small for the given catalyst loading. The decline toward minimum voltage, as shown in Figure 7.7, increased with increasing feed concentration. Since the methanol crossover rate increases with methanol concentration, it is feasible to assume that the saturation rate of the membrane also increased with feed concentration. The rate was slightly different for the lower concentrations but more noticeably different for the higher

concentration. Since the decay rate as well as the steady state voltage depends predominantly on the amount of methanol crossover associated with the feed concentration, they both showed similar trends for the various concentrations.

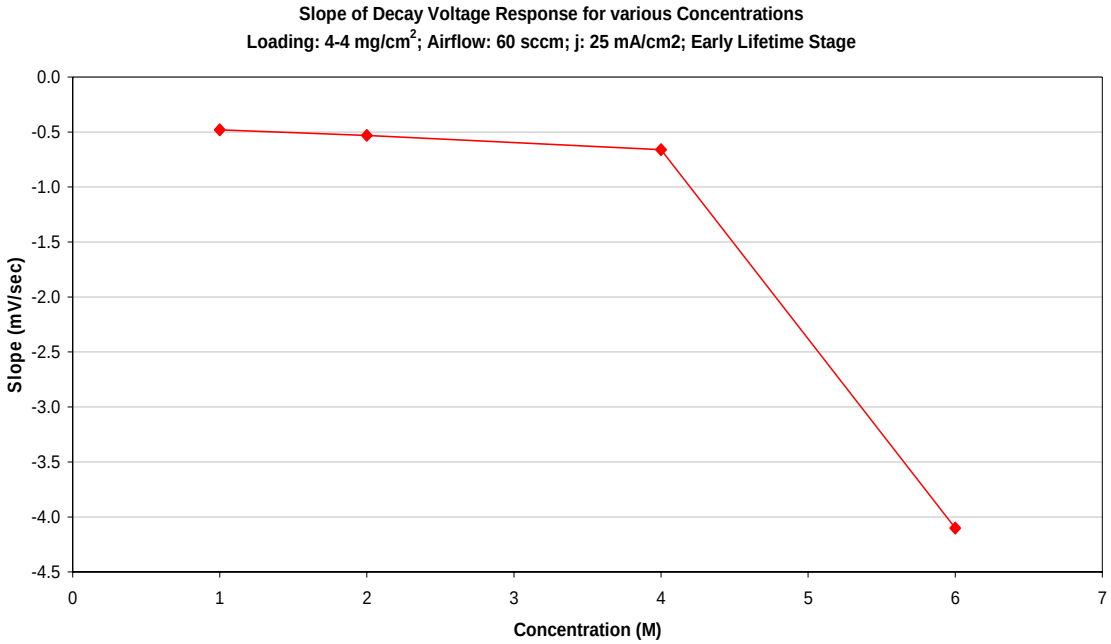

Figure 7.7: Voltage decay slope[17] for various concentrations

Region III: Methanol Crossover Depletion Region

When the membrane is completely permeated and fuel flow is discontinued, beyond the reference "lag time", the voltage response increased due to methanol crossover reduction. The area under the voltage response (curve) within Regions II and III for various duty cycles was measured in order to assess the performance enhancement due to

[17] This is the initial slope within region II response.

methanol crossover depletion relative to the voltage decay in region II. Figure 7.8 shows the areas of region II and III for the three tested duty cycles.

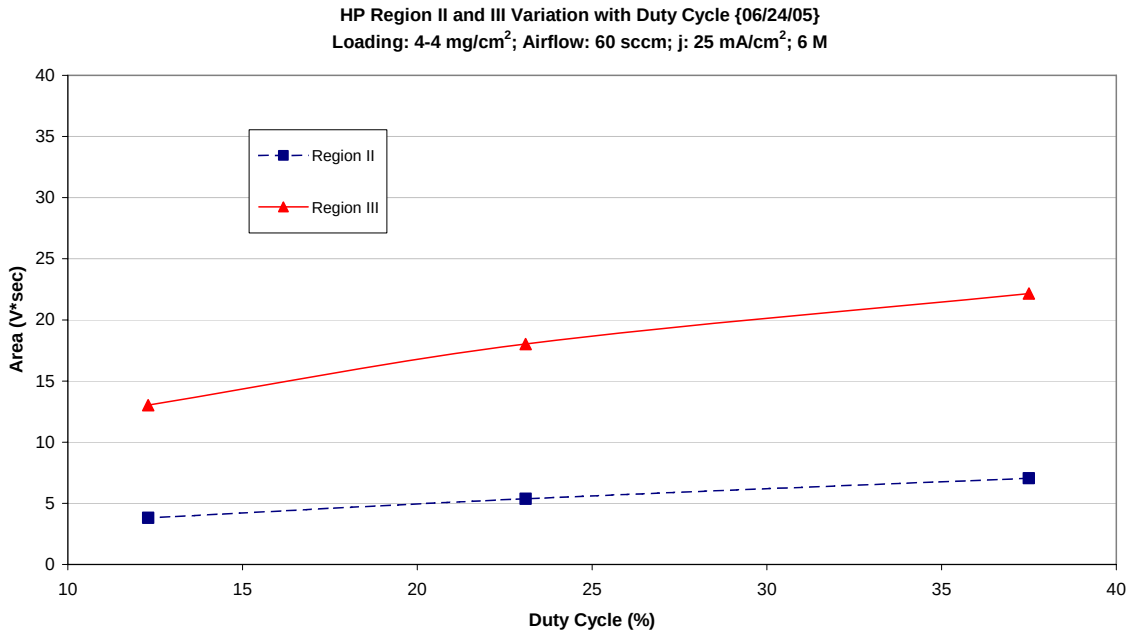

Figure 7.8: Areas of region II and III for various duty cycles

For each duty cycle, the region III area was almost three times larger than the area within region II. This shows that the performance enhancement due to a reduction in methanol crossover played a major role in increasing the average cell potential when hydraulic pulsing was implemented. In agreement with the region II analysis, the area within this region increased slightly with duty cycle. Meanwhile, a greater area variation was observed for the methanol crossover depletion region. This crossover depletion phenomenon is directly related to the amount of methanol permeation associated with the fuel concentration at the anode. Therefore, the higher duty cycle had a greater voltage

enhancement. Again, this occurred because the fuel was discontinued when the membrane was already completely permeated with methanol.

The same analysis was performed for a hydraulic pulsing scheme consisting of a twenty-three percent duty cycle at various concentrations. As shown in Figure 7.9, the areas of region II and III increased with concentration.

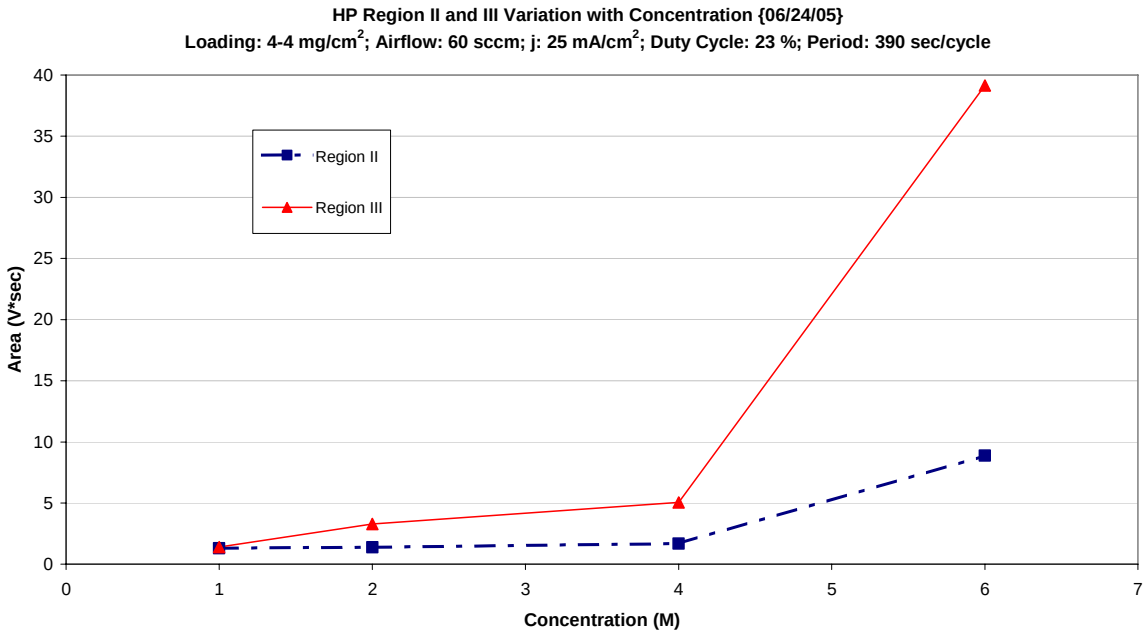

Figure 7.9: Area of region II and III for various concentrations

The difference between the regions was greater at higher concentrations, which indicates that hydraulic pulsing would result in greater performance enhancement due to methanol crossover depletion at higher concentrations.

7.2 Duty Cycle Effect

As was noted in the previous section, the dynamics of the cell response significantly changed with duty cycle. Therefore, the voltage efficiency[18] of a hydraulic pulsing scheme was compared to the corresponding steady flow efficiency for various duty cycles and will be referred to as "voltage efficiency difference" for the rest of the analysis. The voltage efficiency differences between hydraulic pulsing and steady flow operation for various duty cycles are shown in Figure 7.10.

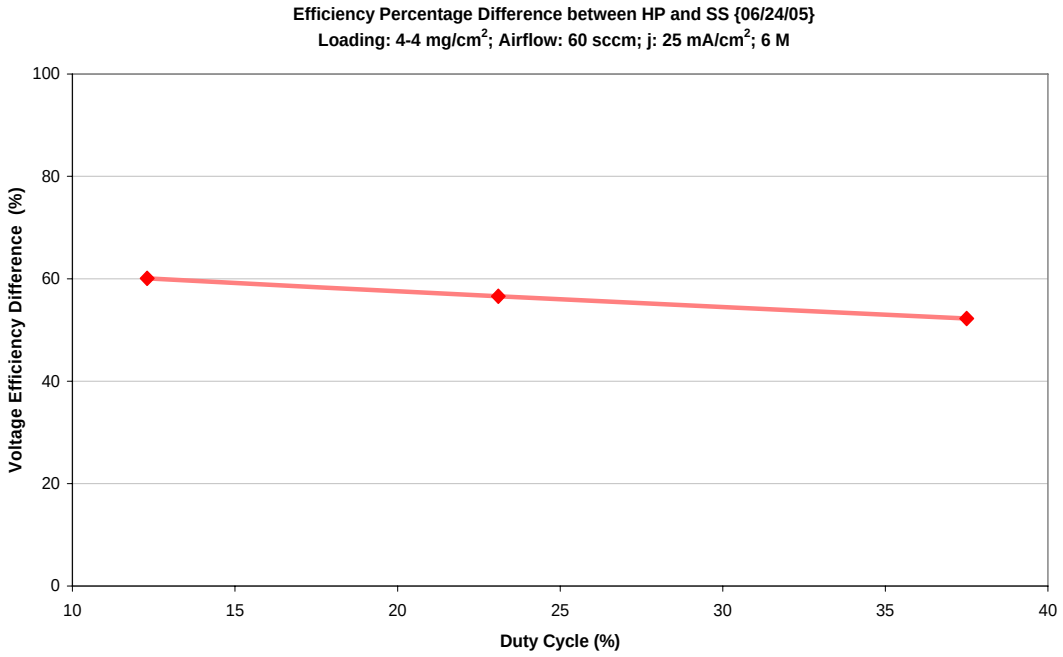

Figure 7.10: Voltage efficiency difference between the hydraulic pulsing and steady flow operation for various duty cycles

[18] The voltage efficiency was defined in Chapter 2 as the cell potential times the value 0.83.

Again, the same amount of fuel per cycle was utilized in the hydraulic pulsing as in the steady flow operation. Since the hydraulic pulsing flow rate was kept constant while the duty cycle was increased, the steady flow rate also increased with increasing duty cycles. Many researchers have reported that, in general, higher fuel flow rates negatively affect the cell response due to greater heat removal and methanol crossover (Scott, 1999). During this study, the response was also found to decrease at higher fuel flow rates. In addition, it was observed that the minimum voltage of the hydraulic pulsing at a given duty cycle coincided with the corresponding steady flow voltage, with both voltages increasing for lower duty cycles (i.e., lower steady flow rates). Interestingly, this indicated that the effect of the duty cycle on the hydraulic pulsing minimum voltage was similar to the effect of the fuel flow rate on the steady flow voltage. While the exact reason for such behavior is unknown, it can be stated that various competing trends (e.g., methanol crossover, CO_2 bubbles, and heat removal) are simultaneous impacted by flow rate.

The voltage efficiency difference was observed to linearly decrease with increasing duty cycle. Therefore, it is feasible to hypothesize that the lower duty cycle would result in a greater cell performance enhancement. Note that due to the aforementioned flow control limitations a lower duty cycle was not analyzed; thus, a possible lower optimal duty cycle might exist for the given operating conditions.

7.3 Voltage Efficiency Comparison for Various Concentrations

The hydraulic pulsing voltage efficiency was further analyzed at various concentrations. Despite the duty cycle (fuel supply time) effect that was found in the previous section, a longer fuel supply was utilized to avoid concentration polarizations associated with the lower feed concentrations. Furthermore, the fuel discontinuation time was modified for the different concentrations in order to allow for a maximum methanol crossover depletion[19] (i.e., allowing the maximum voltage in region III to be reached). Therefore, the duty cycle and period of each pulsing scheme was lower for higher concentrations with the fuel supply time kept constant. Figure 7.11 shows the voltage efficiency difference for the various concentrations.

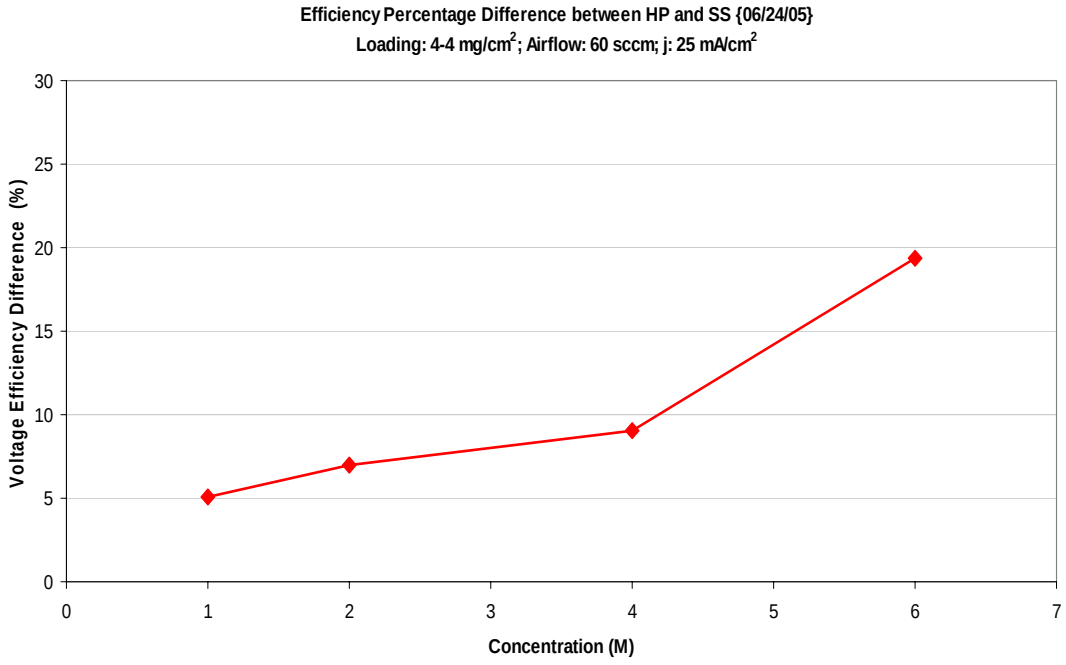

Figure 7.11: Voltage efficiency difference between the hydraulic pulsing and steady flow operation for various concentrations

[19] The fuel discontinuation time was selected based on the previous fuel discontinuation analysis.

For the given catalyst loading (4-4 mg/cm^2), there was a slight efficiency difference increase up to the 4-molar concentration and a more significant difference at the higher concentration. This behavior was expected due to the similar steady flow voltage trend previously observed for these various concentrations. Nevertheless, a more noticeable performance enhancement is observed at higher concentrations mainly due to the larger impact of methanol crossover. Based on these results, it can be concluded that a greater performance enhancement can be achieved when operating at higher concentrations.

7.4 Electro-Hydraulic Pulsing Analysis

During the fuel discontinuation analysis, it was concluded that the amount of methanol crossover depletion for the various current densities was almost the same. It may be possible to significantly increase the power density of a given hydraulic pulsing operation if the current demand is pulsed. The feasibility of this type of transient operation would depend on the specific voltage and/or power density requirements of the application, as well as the power electronics. Based upon the previous pulsing analyses, an efficient electro-hydraulic pulsing scheme was developed wherein both the fuel flow rate and current demand were cyclically pulsed. The electro-hydraulic scheme utilized during this analysis is shown in Figure 7.12.

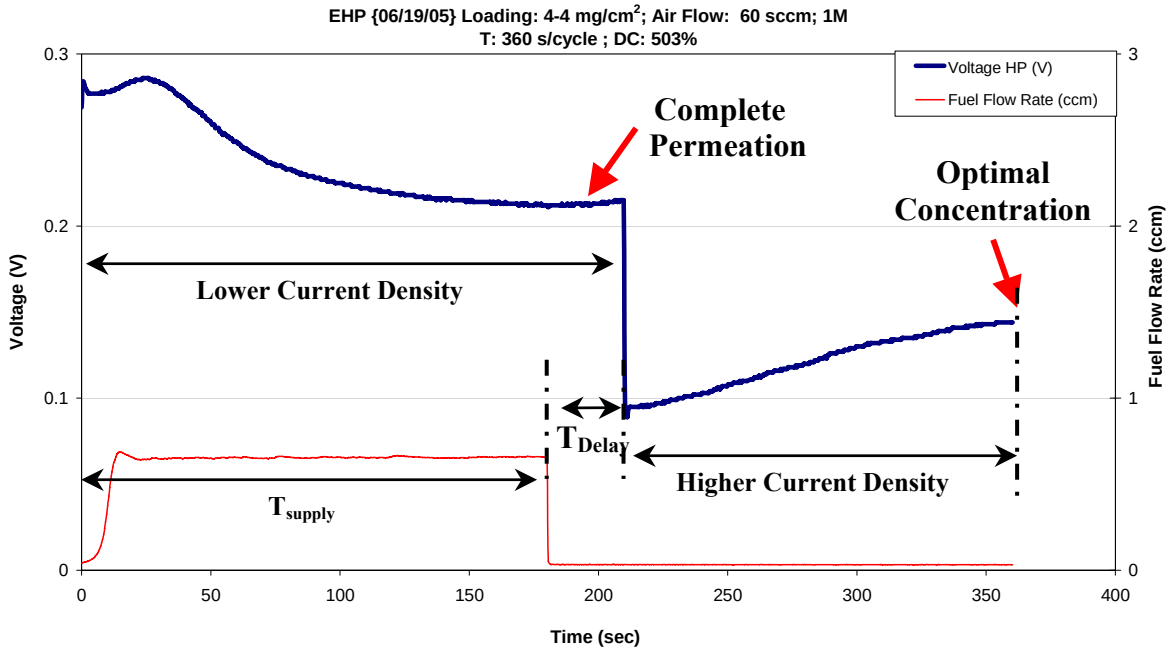

Figure 7.12: Electro-hydraulic pulsing scheme between 25 mA/cm^2 (lower) and 40 mA/cm^2 (higher)

The fuel supply was pulsed at a specific duty cycle and period that were based on the previous hydraulic pulsing and fuel discontinuation analyses. Meanwhile, the current density was pulsed between 25 and 40 mA/cm^2. The lower current density was applied when the fuel supply was reintroduced. Since it was found that for a given concentration there is a specific time constant associated with complete MEA methanol permeation, the current density was increased when this permeation level was reached. As a result, the power density was severely increased during the fuel discontinuation phase (i.e., where methanol crossover was depleted). As noted in Figure 7.12, a delay time[20] (t_{Delay}) was

[20] The delay time was based on the previous hydraulic pulsing results and was lower for higher feed concentrations.

incorporated in the electro-hydraulic pulsing scheme in order to allow for the complete methanol permeation of the MEA before the current density was increased.

7.4.1. Efficiency Comparison for Various Concentrations

Similar to the previous transient analysis, the electro-hydraulic average voltage was compared to the steady flow response wherein both operations used the same amount of fuel per cycle. The steady flow operation, however, also included the same current density pulsing strategy that was incorporated in the corresponding electro-hydraulic operation. Therefore, the voltage efficiency difference between the electro-hydraulic and steady flow responses was calculated in order to further analyze the effect of continuous fuel flow pulsing. Figure 7.13 shows this average voltage efficiency difference for various feed concentrations as well as the previously analyzed hydraulic pulsing efficiency difference.

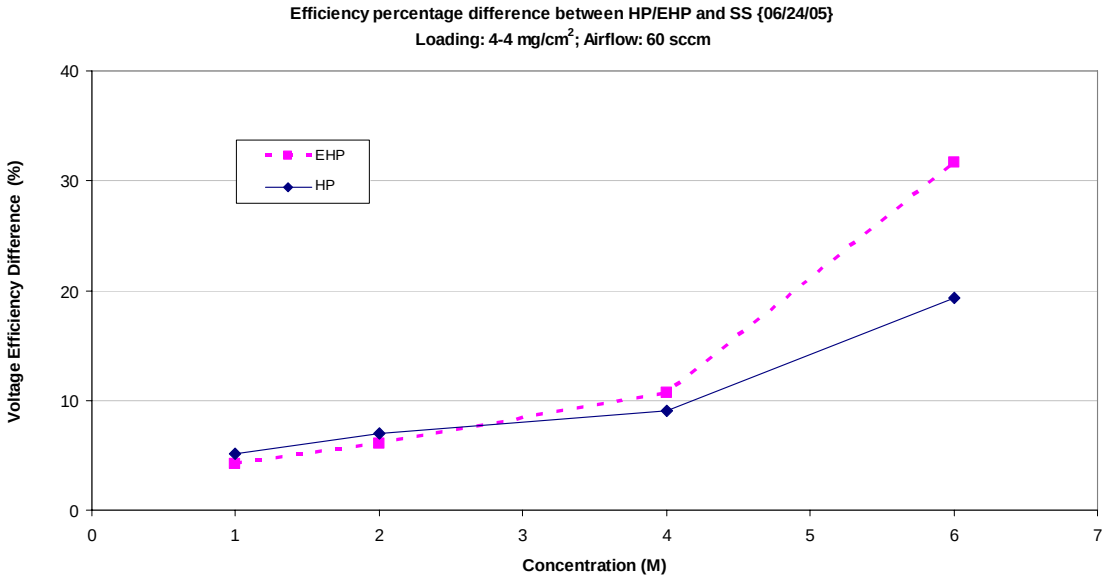

Figure 7.13: Voltage efficiency difference comparison between an electro-hydraulic (EHP) and hydraulic (HP) pulsing operation for various concentrations

As can be observed in Figure 7.13, the electro-hydraulic voltage efficiency difference was increased for higher concentrations. Again, this is indicative of the more significant performance enhancement attained at higher concentrations mainly due to greater methanol crossover depletion. The electro-hydraulic and hydraulic operation resulted in almost similar voltage enhancement at the lower concentrations (i.e., 1,2 and 4-molar). The relatively small difference could possibly be attributed to the steady flow rate variation between the two operations, which was affected by the period and duty cycle of each pulsing strategy. It is important to note that the hydraulic and electro-hydraulic pulsing operation utilized the same transient flow rate. Also, the electro-hydraulic period and duty cycle were lower and higher, respectively, due to the faster fuel

consumption at the higher current density. As a result, the steady flow rates were higher for the electro-hydraulic pulsing and thus possibly caused the observed efficiency variation. Interestingly, a more significant difference was observed at the higher concentration (i.e., 6-molar). This behavior once again supports the hypothesis that a more significant voltage enhancement can be attained during transient operation at higher concentrations.

7.5 Summary

A continuous hydraulic pulsing scheme was developed in order to enhance the average cell potential of a DMFC. Within one cycle of the pulsing scheme, three distinct regions were observed and were named reactant re-institution, methanol crossover restoration and methanol crossover depletion regions. In the reactant re-institution region, the fuel was reintroduced to the cell and caused a slight voltage enhancement. During the methanol crossover restoration region, methanol crossover started to rapidly increase, consequently causing a fast cell potential decay. The methanol crossover depletion region occurred due to the fuel discontinuation within the pulsing scheme, which caused a decrease in methanol crossover at the anode, and consequently increase in cell potential. However, it was found that for some duty cycles a cell potential enhancement was not observed simultaneous to fuel discontinuation. Therefore, it was hypothesized that the internal inertial of MEA permeation resulted in delayed benefits from fuel discontinuation.

Various duty cycles and methanol concentrations were tested in order to obtain the optimal pulsing schemes. It was observed that the lower duty cycle and higher

concentration resulted in a greater cell potential enhancement via pulsing. The pulsing at higher concentrations was more efficient primarily due to the associated high steady state methanol crossover. Finally, an electro-hydraulic pulsing scheme was developed wherein both the fuel flow and current density were pulsed. Again, it was observed that the higher concentration resulted in a greater cell potential enhancement. Therefore, it can be concluded that a greater benefit can be attained from a proactively transient operation, whether hydraulic or electro-hydraulic pulsing, at higher methanol concentrations.

8. Conclusions and Recommendations

8.1 Conclusions

In general, a transient flow operation can result in a significant methanol crossover reduction that consequently enhances the performance of the DMFC. This enhancement is more evident when operating at higher fuel concentrations wherein greater reactant permeation is mitigated. Furthermore, fuel is utilized more efficiently via this proactively transient operation. Therefore, hydraulic pulsing can also result in reduced fuel tank size by allowing effective operation at higher concentration fuel mixture conditions.

Steady flow polarization curves at various mixture concentrations showed some important trends that can be directly related to the methanol crossover phenomenon. Higher concentrations limit cell performance due to the associated significant amount of fuel permeation; meanwhile, lower concentrations hinder power density output due to significant concentration polarization at higher current densities. However, there is a steady flow optimal concentration range wherein both methanol crossover and concentration losses are effectively minimized resulting in a potential optimal cell performance under specific operating conditions. Nonetheless, operation at high fuel concentrations without significant methanol crossover is always desirable due to the resulting high power and energy densities and low concentration polarization.

During the study of transient phenomena in DMFCs, the fuel was first temporarily discontinued in order to analyze the corresponding cell response. It was found that a significant cell potential enhancement occurred due to anodic fuel concentration reduction and thus reduced reactant crossover. The percentage voltage increase during this transient is considerably greater at concentrations higher than one molar. An

interesting trend was observed when the fuel was discontinued at various current densities. Despite the different current rates, nearly the same absolute voltage rise was observed, which is indicative that a possible optimal power density output can be achieved by pulsing the fuel at higher current densities.

Numerous continuous fuel pulsing schemes were tested. When fuel is re-introduced, the cell potential rapidly increases mainly due to the sudden supply of electrochemical reactant. However, the methanol crossover "mixed potential" phenomenon soon becomes a dominant polarization that results in rapid voltage decay. During some transient schemes, ensuing fuel discontinuation did not result in an instantaneous cell potential enhancement due to the dynamic and capacitive inertial effects associated with methanol MEA permeation. Specific hydraulic pulsing schemes were found, however, that resulted in significantly greater fuel efficiencies and cell potential output. It is important to note that the feasibility of hydraulic pulsing in an application depends upon the necessary power electronics and system design characteristics. As an example, the strategic pulsing scheme(s) will be more effective if a proper selection of pumps and other necessary flow control equipment is utilized.

Finally, the electro-hydraulic pulsing shows that it is also possible to enhance power density while increasing the fuel efficiency. The effectiveness of this type of transient operation depends upon the particular application and its power and voltage requirements.

8.2 Recommendations

In this thesis, a detailed experimental analysis of the transient phenomena was performed. Therefore, an analytical model of a DMFC should be developed in order to accurately predict the transient response under various operation conditions. The model should take into account the secondary effects that were discussed in Chapter 6, such as carbon dioxide agglomeration at the cathode and cell degradation. Furthermore, it must account for the methanol concentration within the membrane that can potentially affect the transient response, especially at lower duty cycles.

Due to time constraints, a more detailed analysis of the fuel flow rate effect on a specific transient scheme was not performed. Thus, such analysis should be attempted, both experimentally and analytically, for a domain of operating conditions (fuel concentrations, current densities, etc.). It would provide more insights on the transient phenomena as well as the possibility of further optimizing the pulsing schemes.

A physical method of quantifying fuel permeation in DMFCs is needed to more effectively present the possible crossover depletion occurring in a transient operation. The technique introduced by Jiang, *et al* requires a significant amount of cathodic methanol reaction and also a good sample size that will more likely take a long time to collect depending on the size of the cell. Therefore, a more efficient method to test small DMFCs should be developed and used to further explain most of the steady and transient results that are presented in this work.

REFERENCES

Arico, A.S., A.K. Shukla, El-Khatib, P. Creti, V. Antonucci, 1999, "Effect of Carbon Supported and Unsupported Pt-Ru Anodes on the Performance of Solid-Polymer-Electrolyte Direct Methanol Fuel Cells", *Journal of Applied Electrochemistry*, 29, 671-676.

Department of Energy, 2002, *Fuel Cell Handbook (Sixth Edition)* November, Morgantown, WV

Fowler, A M., R. Mann, J. Amphlett, B. Peppley, P. Roberge, 2002, "Incorporation of Voltage Degradation into a Generalised Steady State Electrochemical Model for a PEM Fuel Cell", *Journal of Power Sources*, 106, pp. 274-283.

Ge, J., H. Liu, 2004, "Performance and Modelling of a Liquid-Fed Direct Methanol Fuel Cell", *IMECE Proceedings, November 13-19*, Anaheim, California, ASME.

Havranek, A., K. Klafki, K. Wippermann, 2001, "The Influence of the Catalyst Loading and the Ionomer Content on the Performance of DMFCs Anodes", *Advanced Batteries and Accumulators Conference*, Brno, Czech Republic.

Haynes, C., S Leahy, D Parekh, L Lay, L McCarthy, 2004, "Enhanced DMFC Performance via Electro-Hydraulic Pulsing", *IMECE-04: Proceedings of the ASME International Mechanical Engineering Congress and RD&D Expo, November 16-19,* Anaheim, California, ASME.

Heinzel, A. and V.M. Barragan, 1999, "A Review of the State-of-the-Art of the Methanol Crossover in Direct Methanol Fuel Cells", *Journal of Power Sources*, 84, 70-74.

Jiang, R. and D. Chu, 2004, "Comparative Studies of Methanol Crossover and Cell Performance for a DMFC", *Journal of Electrochemical Society*, 151, A69-A76.

Leahy, S., 2004, *Active Flow Control of Lab-Scale Solid Polymer Electrolyte Fuel Cells,* Master's Thesis, The Georgia Institute of Technology, Atlanta, GA.

Mench, M., 2005, Correspondence from the Pennsylvania State University

Neergat, M., K.A. Friedrich, U. Stimming, 2003, "New Materials for DMFC MEAs", *Handbook of Fuel Cells-Fundamentals, Technology and Applications,* 4, 856-877.

Scott, K., W.M. Taama, P. Argyropoulos, 1999, "Engineering Aspects of the Direct Methanol Fuel Cell System", *Journal of Power Sources*, 79, 43-59.

Shukla, A., C.L. Jackson, K. Scott, R.K. Raman, 2002, "An Improved-Performance Liquid-Feed Solid-Polymer-Electrolyte Direct Methanol Fuel Cell Operating at Near Ambient Conditions", *Electrochimica Acta*, 47, 3401-3407.

Sundmacher, K., T. Schultz, S. Zhou, M. Ginkel, E.D. Gilles, 2001, "Dynamics of the Direct Methanol Fuel Cell (DMFC): Experiments and Model-Based Analysis", *Chemical Engineering Science*, 56, 333-341.

Wang, Z.H. and C.Y. Wang, 2003, "Mathematical Modeling of Liquid-Feed Direct Methanol Fuel Cells", *Journal of The Electrochemical Society*, 150, A508-A519.